THE UNIVERSITY OF MICHIGAN

College of Engineering
Department of Nuclear Engineering
Laboratory for Fluid Flow and Heat Transport Phenomena

Technical Report No. 19

GAS CONTENT EFFECTS ON CAVITATION NUMBER IN WATER IN A CAVITATING VENTURI

Frederick G. Hammitt
M. John Robinson
Ronald P. Koopman
David M. Ericson, Jr.

August, 1966

Under contract with:

National Aeronautics and Space Administration

Grant NsG-39-60
Washington 25, D. C.

ABSTRACT

The effects of entrained and/or dissolved gases in a venturi with water as test fluid on the observed cavitation number for inception were investigated. Tests were conducted for air contents from ∿ 0.5% to 4.0% by volume in water over a temperature range of 50 to 150°F, a velocity range of 65 to 200 ft./sec., and a venturi throat diameter range from 1/8" to 3/4", including intermediate sizes of 1/4" and 1/2".

Since it is quite difficult to differentiate between the amount of gas that is in solution and that which is entrained, the results are presented in terms of total gas content. The facilities used for the investigation are briefly described and the experimental techniques presented.

Computerized least mean square regression analyses have been made in order to develop equations relating the dependent variable of observed cavitation number to the independent variables, which include: gas content, temperature, loss coefficient, and throat velocity. The last two variables were then combined in the form of a throat Reynolds' Number.

It was found as a result of this investigation that:

a) There is a significant effect of gas content on cavitation number for inception (incipient cavitation number). In general it increases with increasing gas content.

b) No very significant temperature correlations were possible due to the limited temperature range permitted with the existing equipment.

c) There is a significant effect of velocity on incipient cavitation number. In general, it decreases with increasing velocity.

d) The general trend for size effects is an increase of incipient cavitation number with increasing venturi throat diameter.

e) There is a decrease of incipient cavitation number with increasing Reynold's Number, although the correlations seem to be restricted in their application to the various venturi throat sizes so that no good fit was obtained across the whole range of venturi sizes.

ACKNOWLEDGMENTS

The authors would like to acknowledge the assistance of Dr. Willy Smith, Michael P. Rothstein, O.S.M. Ahmed, R. A Robinson, and Ramon Garcia for their contribution to the early stages of this work, particularly in connection with the computer correlations.

TABLE OF CONTENTS

NOMENCLATURE

Symbol	Description
σ_c	Cavitation number
P_{min}	Minimum observed static pressure
P_v	Vapor pressure of working fluid
ρ	Density of working fluid
V_t, Vel., V.	Free stream velocity in venturi throat
L.C., l.c.	Loss Coefficient
Vol%, G.C.	Gas content in volume percent
Temp., T	Temperature of fluid

LIST OF TABLES

LIST OF FIGURES

Figure | Page

CHAPTER I

INTRODUCTION

To the present there have been only a very few attempts at delineating the effect of gas content on cavitation performance of fluid-handling machinery such as centrifugal pumps, hydraulic turbines, etc. It is expected that there are significant effects both upon cavitation damage and fluid-dynamic performance. The damage effects of entrained gas have been touched upon slightly in the literature and some slight indications of the probable effects have been gathered by tests of this laboratory. The present state of affairs regarding gas content effects upon cavitation damage are covered in another report from this laboratory.[1] The present report is concerned only with the effects upon fluid-dynamic performance.

No clear-cut understanding of these performance effects has yet evolved. It is evident that the relationships are very complex and are also bound up with the general group of phenomena labelled "scale effects" in the cavitation literature, ie, the observed departures from classical scaling relations due to changes in velocity, size, temperature, gas content, etc. In past reports from this laboratory[2,3,etc.] considerable data regarding these effects in cavitating venturi systems using both water and mercury as test fluids has been presented. The effects of gas content in particular have been covered in ref. 4 and 5 for mercury. The present report presents comparable information for the water tests, and in the same form so that eventually the behavior of these two fluids in similar flow configurations can be compared.

It is expected on theoretical grounds that entrained gas will be much more important in influencing cavitation inception than dissolved gas. Since the lifetime of a cavitation bubble in a flowing system is very short (order of millisec.), substantially only that dissolved gas which is within the liquid volume which actually vaporizes to form the bubble can be involved. This will then be only an extremely small fraction of the bubble contents since the saturation content of air in water is only a few ppm by mass. Entrained gas, however, is of very great importance in bubble nucleation, since, per se it provides an interface or nucleus necessary to start a rupture of the liquid. In the absense of even traces of entrained gas, substantial liquid tensions would be possible so that for all practical engineering purposes, cavitation would not exist. There is some indication that in some liquid metal systems the quantity of entrained and/or dissolved gas is so low that this condition may be approached.[6] From the view point of boiling systems this means that inconveniently large superheats are required to nucleate boiling.

In water tests, the entrained portion of the gas is usually only a very small portion of the total gas. Since only the total can be conveniently measured, it is difficult to separate out that portion which is thought to be important, ie, the small entrained portion. Since the solubility of gasses varies with pressure, temperature, etc., so that at any given position in a rapidly flowing system equilibrium solubility conditions probably cannot be expected. For this reason, tests to measure the effect of gas content upon cavitation inception number, for example, may be subject to great lack of precision if only the total gas content is measured. Unfortunately this is the case with most existing studies including the present tests. It is thus indicated that the development of an instrument capable of measuring only the entrained gas (or the "nuclei content" as it is sometimes called) is of great importance. Possible techniques for such an instrument utilize either the absorption of acoustic energy in appropriate frequencies by bubbles[7] or high-magnification visual techniques.

As indicated, results with mercury have already been reported from this laboratory.[4,5] This mercury data has an inherent advantage as compared with the present water data, in that only entrained gas is involved, since, as for most liquid metals, gas solubilities are essentially nil.

Considerable data in water of application to this general approach has been gathered for a doctoral thesis,[3] and has been reduced and correlated in the same manner as the above mentioned mercury data in order that comparisons of this data can be made between the two fluids in the same geometries. A systematic variation of the many variables in the systems has been made in a controlled manner in order to explore the effects of each variable individually. These variables include venturi size, fluid velocity and temperature, degree of cavitation, and gas and impurity content.

CHAPTER II

MAJOR EXPERIMENTAL FACILITIES

The main facility used in the current investigation has been thoroughly described in the literature[8], and will be briefly presented in this section. The water system consists of a centrifugal pump, stainless steel piping, and four cavitation test loops (Fig. 1 and 2). These four loops are all fed from a main high pressure tank. They discharge into a low pressure tank (or manifold). Flow is returned by a centrifugal pump driven by a variable speed drive. For the current tests, only one loop was used. A bypass loop exists to vary the gas and impurity content of the fluid, and a cooling system allows some degree of temperature variation. The maximum temperature is limited by the plexiglas venturis to about 150°F. Velocities between 65 and 200 ft./sec. can be attained in 1/2" diameter throat venturis for cavitation inception conditions.

Flow control on this system is achieved by variation of venturi back pressure (through gas loading of a surge tank) and pump RPM, so that no control valves are required. Flow measurement is obtained by suitable orifice plates of three sizes, to obtain precise measurement over the entire range of velocities used.

The measurement of total gas content of the water was accomplished with the use of a Van Slyke apparatus, (Fig. 3), which was originally designed for use in the medical profession

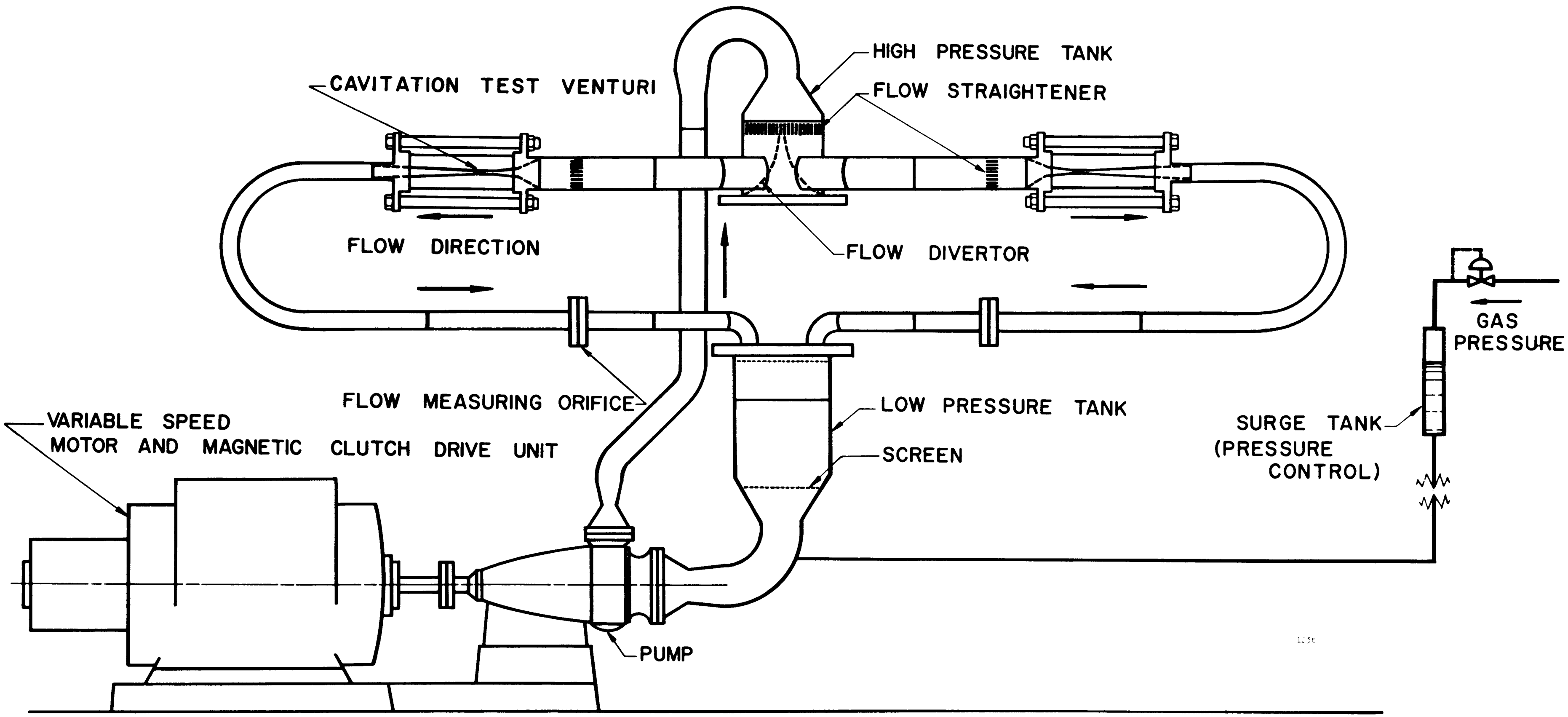

Fig. 1.--Schematic of water cavitation facility (only two of the four loops are shown).

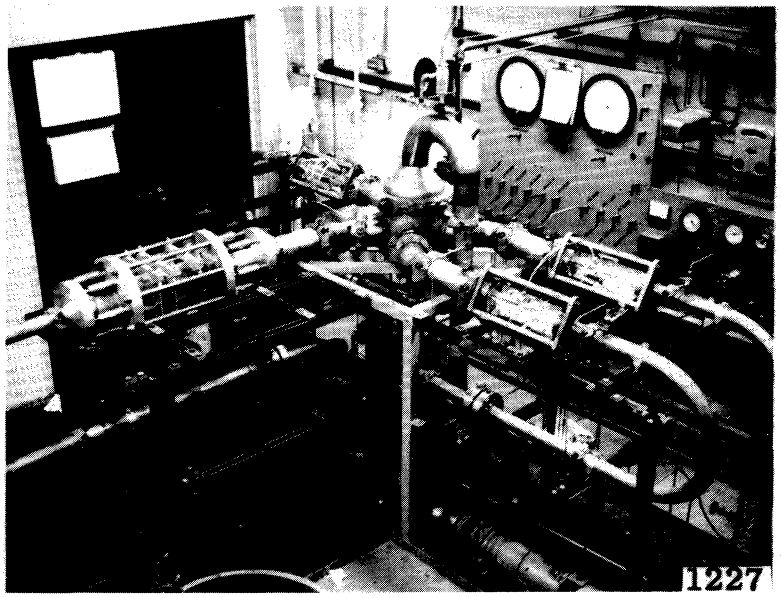

Fig. 2.--Photograph of water cavitation, closed loop, venturi facility.

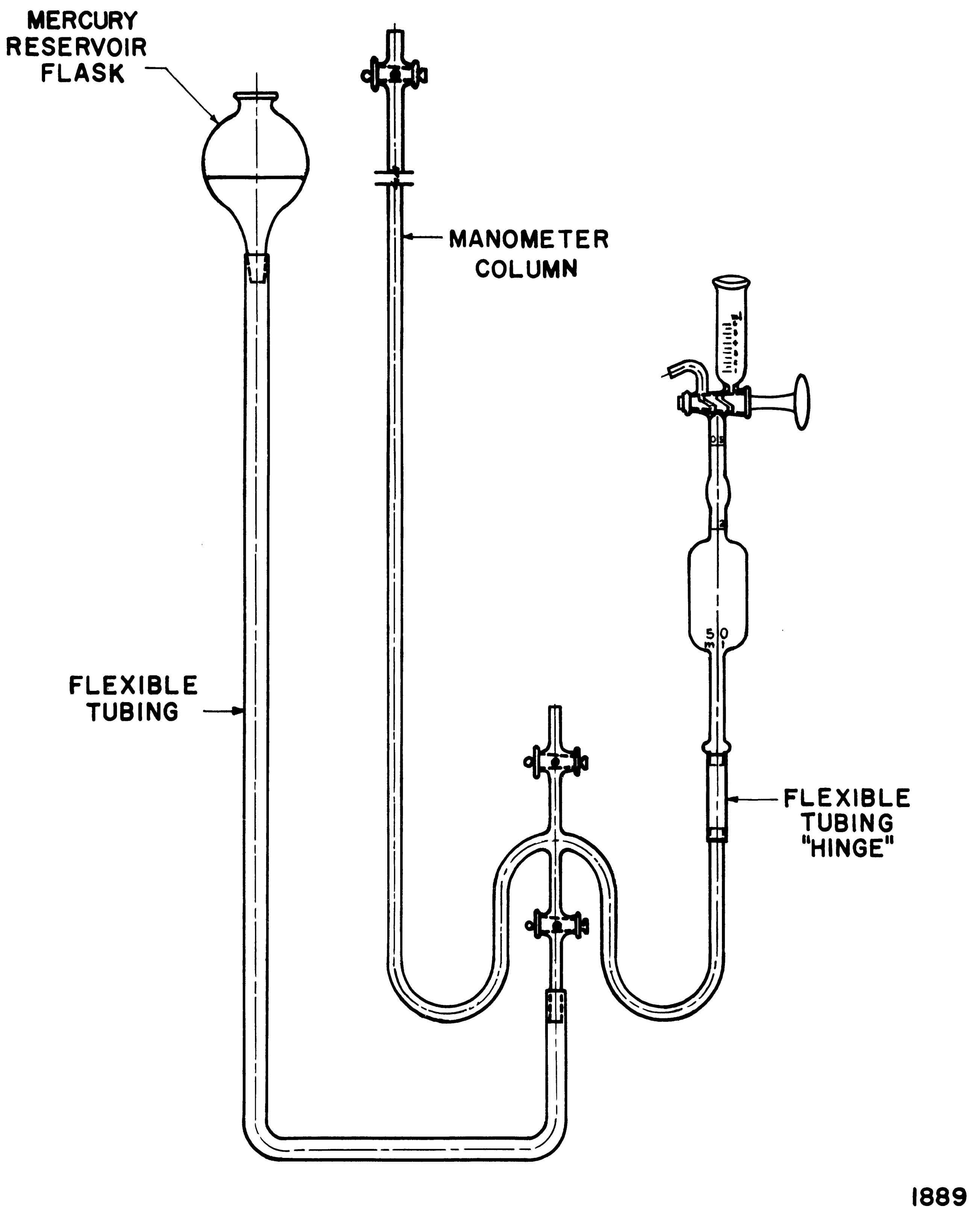

Fig. 3.--Schematic of conventional Van Slyke apparatus

for "blood gas" analysis. To accomplish the measurement in the present system, a sample of the water-gas mixture is removed from the venturi outlet and immediately put into the Van Slyke. The sample is put under a torricellion vacuum and agitated to separate all gas from the water. This gas is then quickly compressed into a known volume at known temperature, and the pressure is measured with a manometer. With the temperature, volume and pressure known the mass of the gas sample can be determined and related to the original mass of the known sample size in order to compute the percent volume gas content of the fluid.

The pressures that are required from the system are measured with high-precision Heise gages selected to suitably cover the full pressure range, reading from a manifold which can be quickly connected to various tap positions along the entire length of the venturi. These are spaced more closely in the regions where the minimum pressures are known to exist from previous experience. Vapor pressure is subtracted from the measured pressures. The result is then normalized by dividing through by the kinetic pressure, so that all pressures are reported in the form of a cavitation number. The minimum such number along the venturi for a given flow condition is then the classical cavitation number for that condition. The reduction and subsequent plotting of this raw data is accomplished with the aid of a digital computer program.

There are several important effects to be considered during the planning of a test program, one of which is the effect of the past history of the water to be cavitated. There has been previous reference to the importance of this effect[9,10], in that when the water has been held under high pressure for some time before the test is initiated, the cavitation number is affected. This is presumably due to the fact that the gas solubility of the fluid is higher at higher pressures and thus less entrained gas is present at the onset of the test for bubble nucleation, ie, the gas nuclei are reduced both in number and size. Succeeding exposure to low pressure and turbulence in the cavitating region drives some of the gas from solution back into the entrained form. Thus the water is returned to its normal state and can no longer sustain a high degree of tension. This has been clearly demonstrated in recent tests in this laboratory[3], Fig. 4.

Other parameters as roughness, pressure pulses in the flow due to pumping effects, etc. may influence the magnitude of the measured cavitation number. Currently tests to determine the transient pressure behaviour and detailed structure of the flow in a cavitating venturi are being conducted in this laboratory.[11] It is hoped to relate these effects to the measured cavitation number.

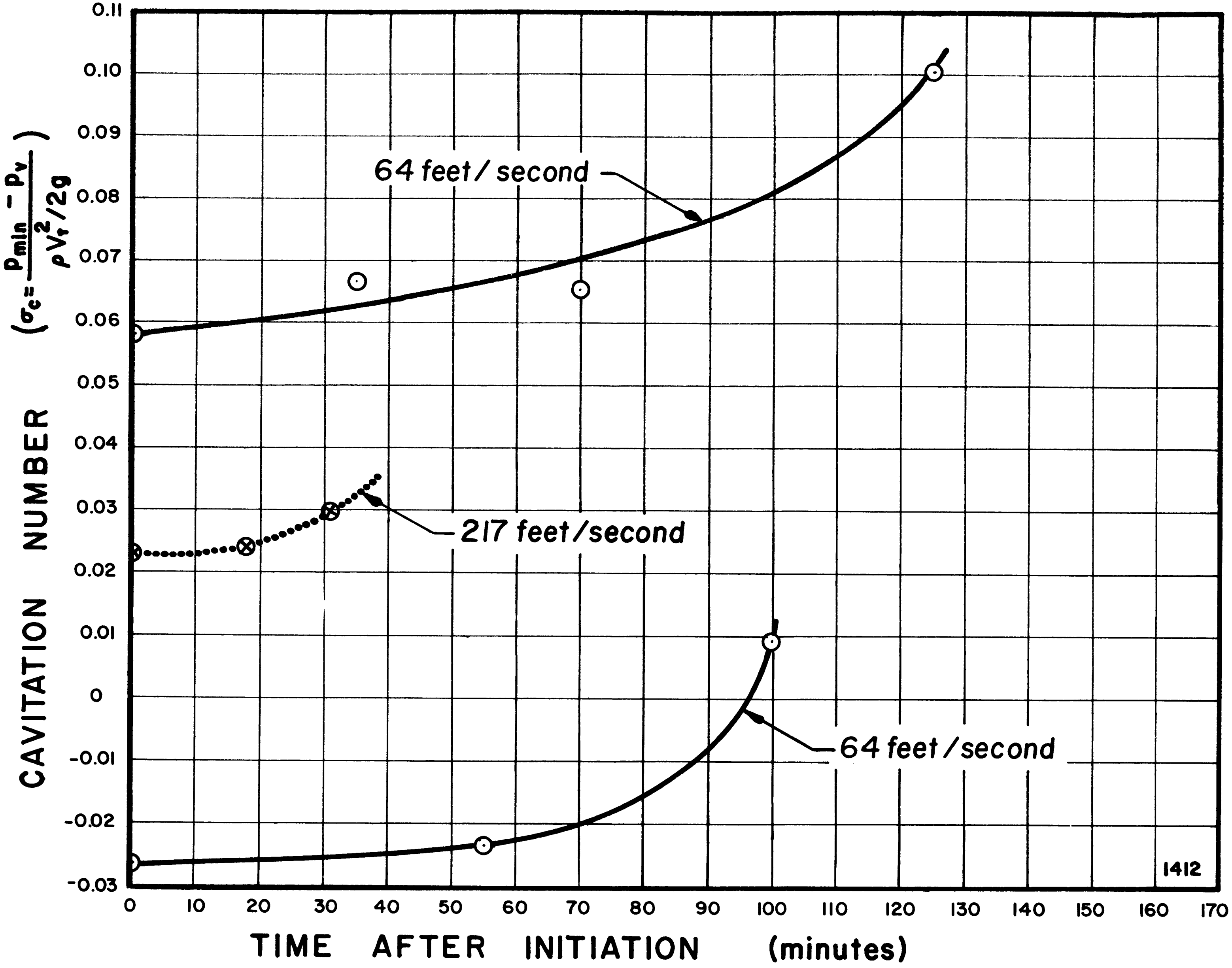

Fig. 4.--Cavitation inception number vs. time after initiation for visible initiation in water.

CHAPTER III

SCOPE OF THE EXPERIMENTAL DATA

The venturis used in the facility were all geometrically similar plexiglas venturis (Fig. 5) with throat diameters of 3/4", 1/2", 1/4", and 1/8". These venturis correspond to the venturi numbers of 534, 412, 614, and 818, respectively, and are shown in Figs. 6, 7, 8, and 9, with the water loop connections shown. The experimental data was all taken within the temperature range of 50°F to 140°F.

In the water system it was not possible to visually detect any gas (using strobe light illumination), when the measured content was below the saturation level of about 2% by volume, so that it was assumed that substantially all the gas was either in solution or in the form of microbubbles of a size below the visual limit under the stated conditions of observation. Above the saturation level, gas was admitted to the system through a small valve and mixed in the loop until homogenous conditions were attained. A previous report[12] summarizes this work. The total gas content for the data under consideration all varies between 0.68% and 2.60% of saturation by volume at STP.

The flow velocities vary between 60 ft./sec. and 220 ft./sec., with the majority of the data points distributed around the velocities of 70 ft./sec., 100 ft./sec., and 200 ft./sec.

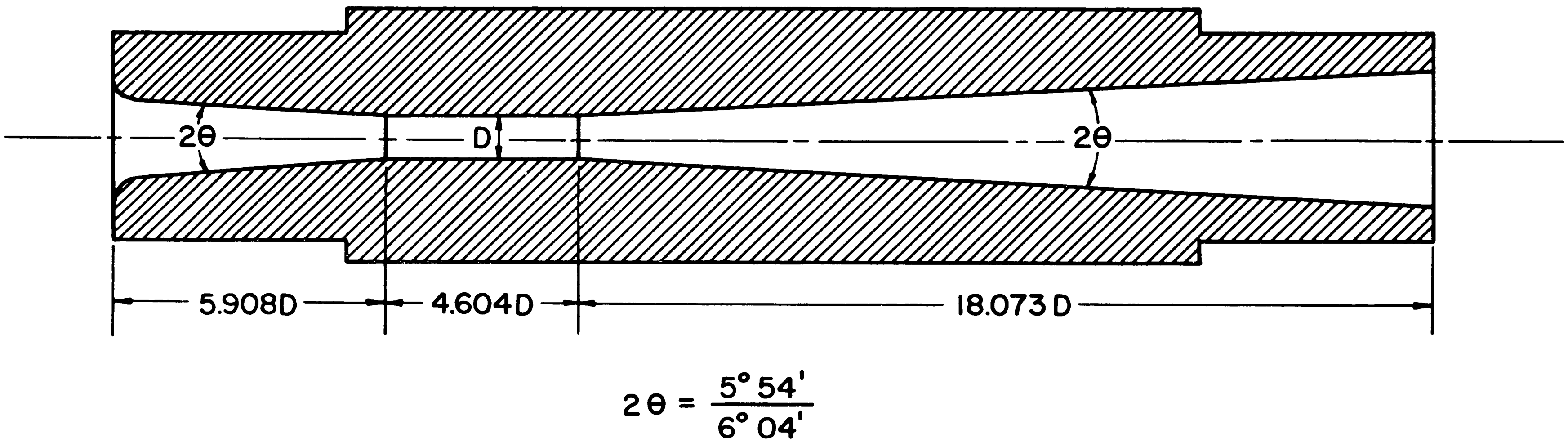

1849

Fig. 5.--Basic venturi flow path dimensions.

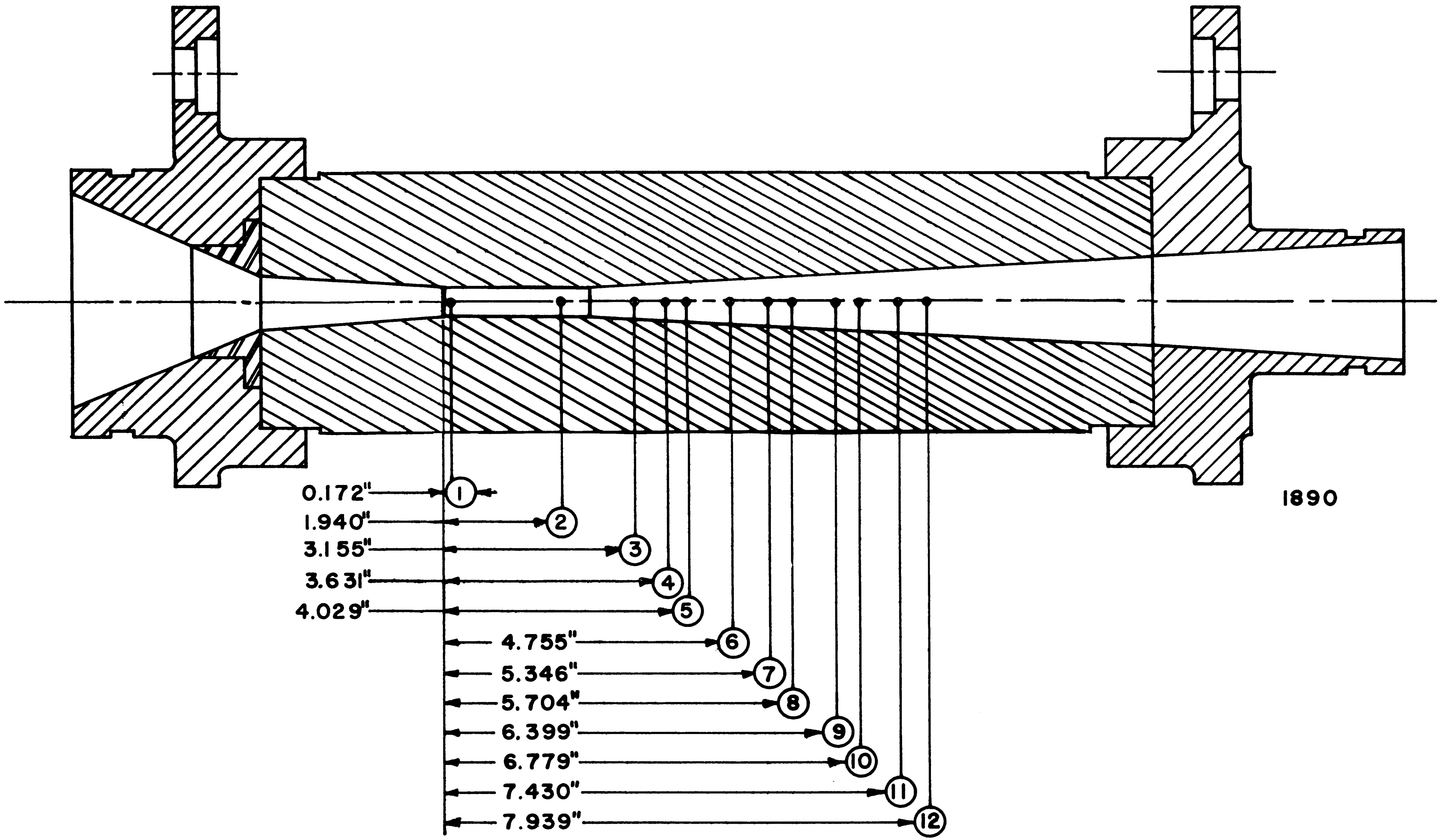

Fig. 6.--Pressure tap locations and water loop installation geometry for 3/4" plexiglas venturi.

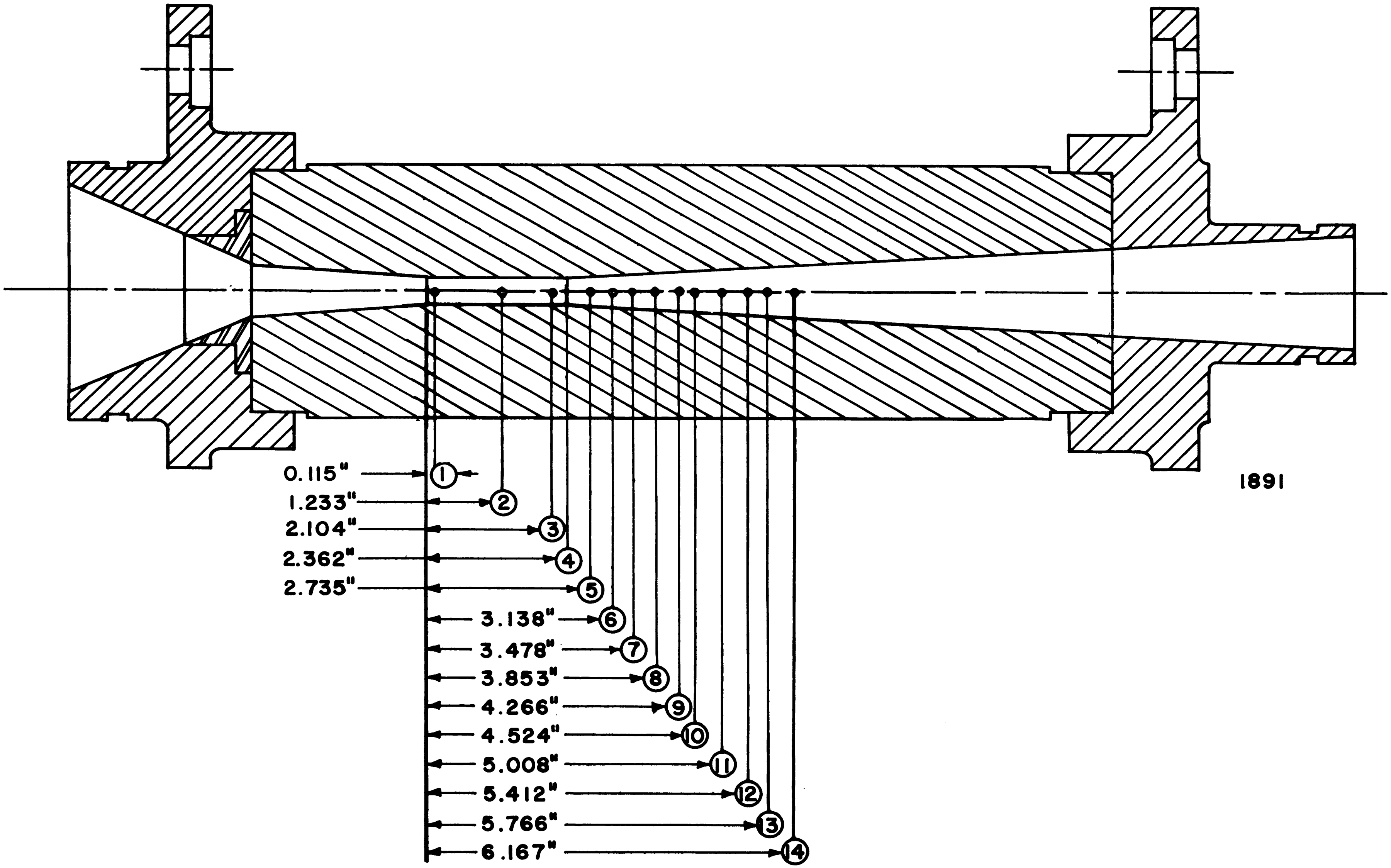

Fig. 7.--Pressure tap locations and water loop installation geometry for 1/2" plexiglas venturi.

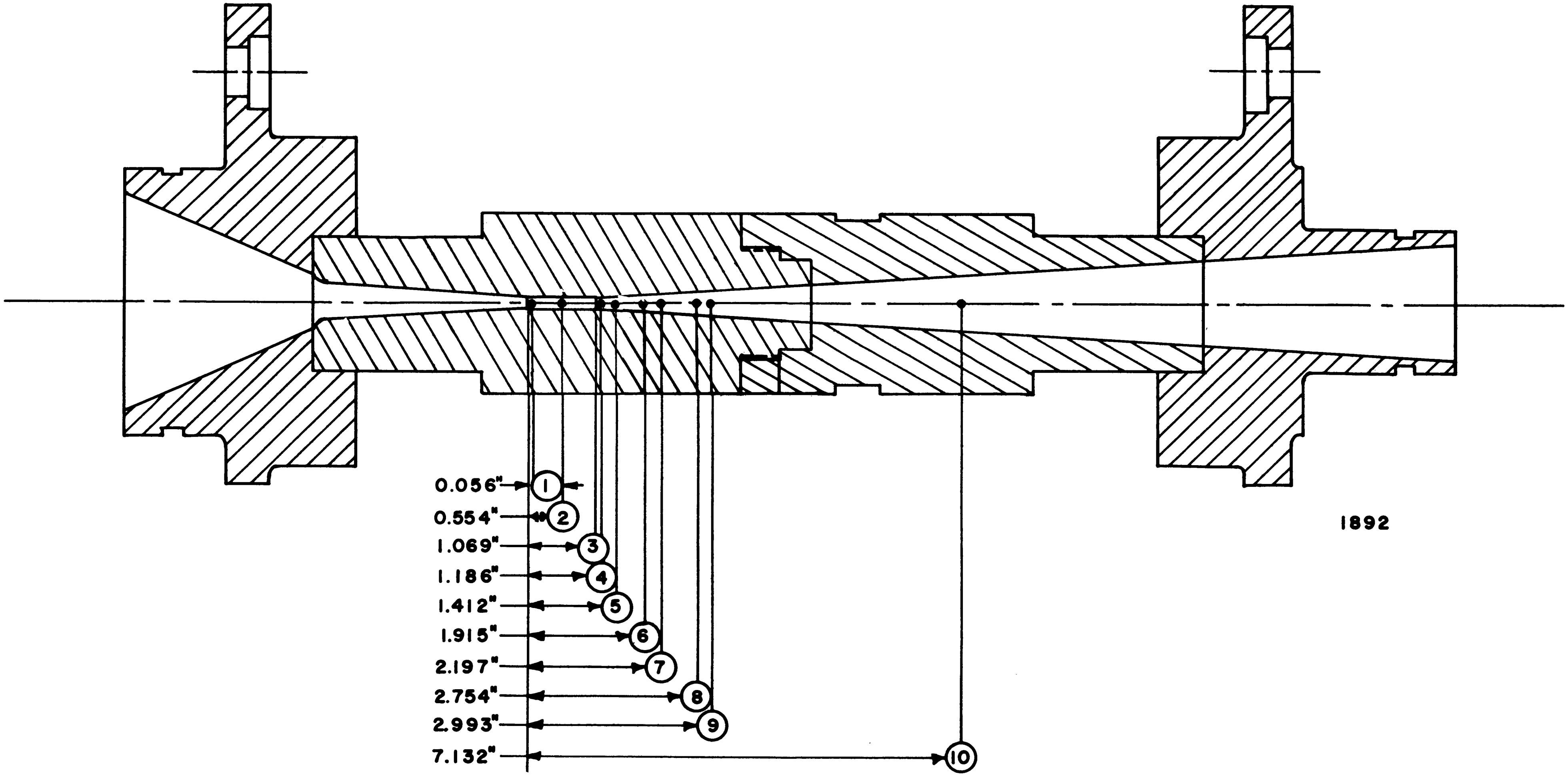

Fig. 8.--Pressure tap locations and water loop installation geometry for 1/4" plexiglas venturi.

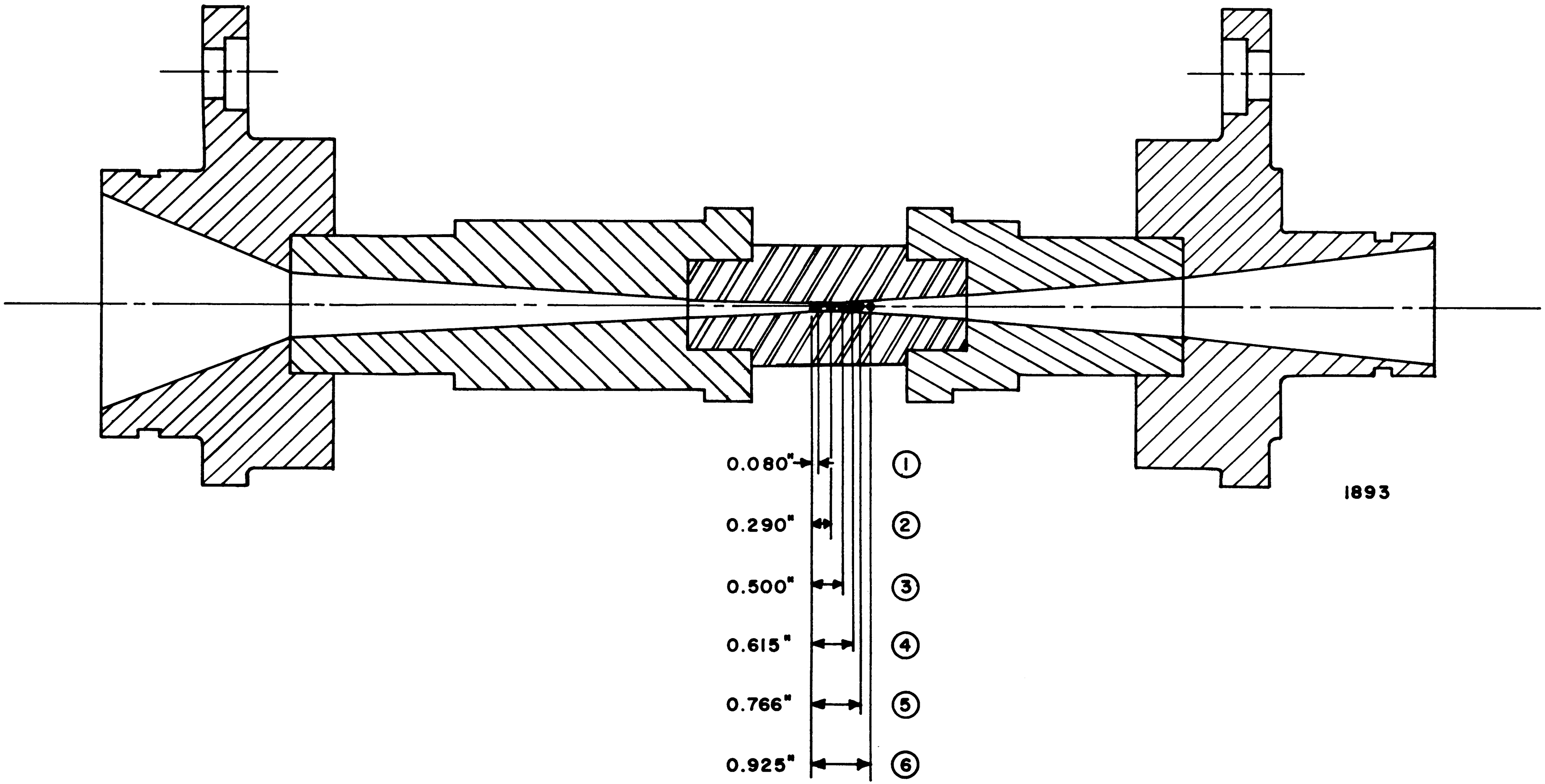

Fig. 9--Pressure tap locations and water loop installation geometry for 1/8" plexiglas venturi.

Approximately 64 runs were made using the 3/4" diameter venturi. Similar runs were lumped together for the computer analysis yielding a total of 32 data sets. These runs include data at the following cavitation conditions (defined in the appendix): zero cavitation, initiation* (including sonic and visible which were equivalent for these tests**), standard cavitation, and first mark cavitation. Approximately 132 runs were made using the 1/2" diameter venturi. These were lumped into a total of 44 data sets, including data for the same four cavitation conditions. Approximately 80 runs were made with the 1/4" venturi, yielding a total of 39 data sets in the same four cavitation conditions. Approximately 60 runs were made using the 1/8" venturi, yielding a total of 30 data sets, again in the same four cavitation conditions.

---

*Called "sonic" in Tables, Appendix, and text.

**No difference was detected in these tests, except for those using prepressurized water, as has been reported elsewhere[9,14] between the inception cavitation condition as approached alternately from the non-cavitating or fully cavitating side. However, no very detailed attempt to investigate the possibility of such a difference was made.

CHAPTER IV

REDUCTION OF THE DATA

Since there were many variables to be considered in this investigation, it was necessary to group the data into several sets according to three cavitation conditions (initiation, standard, and first mark, zero cavitation being of no interest) and four venturi sizes (3/4", 1/2", 1/4", and 1/8"). This results in twelve groups of data. The parameters of velocity, gas content, temperature, and loss coefficient were then allowed as variables, and a correlation made with a regression analysis computer program[4] between these variables and the measured cavitation numbers. This was deemed to be the only practical way of handling the data in view of the large number of variables so that a meaningful correlation could be determined. The range of the experimental variations in the variable parameters is shown in Table 1 with the problem numbers indicated where the data sets were used for the computer correlations as shown in the appendix.

TABLE 1

Venturi Number	Cavitation Condition	Temperature °F	Velocity ft./sec.	Problem Vol%	Number L. C.
534	Sonic	80	70	1	4,5,6
		80	100	2	
		80	180	3	
534	Standard	60	100		
		80	70		
		80	100		
		80	182		
534	1st Mark	80	70	35	
		80	100	35	
		90	180	35	
412	Sonic	50	63		
		50	100	7	
		80	220		
		120	63	9	
		120	100	8	11,12,13
		120	220	10	
412	Standard	55	65		
		80	210		
		113	65		
		100	55	23	24,25,26
		100	120		
		140	212		
412	1st Mark	55	65		
		55	100	36	
		77	200		
		105	65		
		120	100		
		135	200		
614	Sonic	70	68	14	
		70	96	15	
		82	195	16	
614	Standard	65	70		
		65	100	27	29,30,31
		85	200		
		100	100		29,30,31
614	1st Mark	70	67		
		70	100		
		85	200		

TABLE 1 (Continued)

Venturi Number	Cavitation Condition	Temperature °F	Velocity ft./sec.	Problem Vol%	Number L. C.
818	Sonic	65	75	17	
		65	100	18	20,21,22
		65	150		
		80	200	19	
		100	80		
		100	100		
818	Standard	60	76	32	
		65	100	33	
		75	200	34	
		100	80	32	
		100	100	33	
818	1st Mark	65	75		
		65	100		
		70	200		

The computer analysis employed is a simple linear regression. Basically the analysis involves taking a set of experimental data which includes a series of independent variables (the program can handle 100 such variables) and a single dependent variable and deriving a linear combination of the independent variables which best describes the distribution of the dependent variable data over a certain range according to the criterion of least mean square error in the approximation.

The independent variables being considered here are:

1. Venturi throat diameter: 3/4", 1/2", 1/4", 1/8"
2. Temperature: 50°F to 140°F
3. Throat velocity: 70 ft./sec., 100 ft./sec., 200 ft./sec.
4. Cavitation condition: sonic, standard, first mark
5. Gas content: 0.68% to 2.60% by volume

For any fixed combination of the above independent variables of the experiment, there presumably exists a definite wall pressure profile and flow rate. These constitute the basic dependent variable measurements which were made. From the wall pressures, the minimum wall pressure is determined, and considering the vapor pressure at the set temperature, the cavitation number is computed, utilizing the throat velocity derived from the flow rate measurement and the observed cavitation condition:

$$\sigma_c = \frac{p_{min} - p_v}{\rho V_t^2 / 2g_o} \qquad \text{--- (1)}$$

In addition, the loss coefficient for the venturi,

$$L.C. = \sigma_L = \frac{p_{in} - p_{OUT}}{\rho_L V_t^2 / 2g_o} \qquad \text{--- (2)}$$

is computed. This is a measure of the disturbance to the single phase flow caused by the cavitation. It increases rapidly for more developed cavitation conditions, since the diffuser efficiency decreases rapidly for increased cavitation.

For the purposes of this investigation it is assumed that a relation of the following type exists:

$$\sigma_c = \sigma_c(\text{L.C., Vol.\%, V, T, Cavitation Condition}) \quad \text{--- (3)}$$

In view of this relation, single plots of cavitation number vs. gas content, or any other single parameter, are not meaningful unless the variation in all other parameters listed has only negligible effect. Difficulties were encountered in actually conducting the tests at selected values of some of the independent variables and a sometimes substantial variation in loss coefficient was noted when the cavitation condition was set. Thus the data generally could not be considered as applying for all conditions except a single variable fixed. Hence it was decided to correlate the data assuming variation in all independent variables. The program could then be utilized to generate a power series summation utilizing only a small number of terms, wherein the effects of the different parameter variations could be assumed to act independently. Thus relations of the form exhibited below are to be generated:

$$\sigma_c = C_0 + \sum_{i=0}^{3} C_i(\text{L.C.})^i + \sum_{i=0}^{3} C_i(\text{Vol\%})^i + \sum_{i=0}^{3} C_i(V)^i + \sum_{i=0}^{3} C_i(T)^i + \cdots \quad (4)$$

A more detailed explanation of the program was given in a previous report.[4]

To derive any meaningful information from the computer developed correlations, it is necessary to examine the behavior of the cavitation number under the influence of individual parameters with the remaining variables held constant. Thus the data sets under each group were lumped into problems with the cavitation number as a function of the independent variable of interest and the remaining variables held constant by using their average values in the computer developed group equations. Only data containing a small range of other than the variable of primary interest were lumped to obtain the average values for these other variables which were then used as constants in the equations from which the two-variable plots were made.

For example, suppose that it is desired to consider the cavitation number as a function of gas content for venturi 534 at the sonic cavitation condition with constant temperature, velocity, and loss coefficient (group equation No. 1). The data selected to give the average temperature, velocity, and loss coefficient to be used as constants in the group equation must cover only a small range. Thus runs with temperatures of 80°F ± 10°F and velocities of 70 ft./sec.±10 ft./sec. were considered suitable, and an average loss coefficient for this data was found, since the loss coefficient is a function of these variables. Using these averages, curves were generated for cavitation number versus gas content for venturi 534 at the sonic cavitation condition for an average loss coefficient of 0.2698 by the computer plotting routine described earlier.[5] A similar procedure was followed for other independent variables of interest for other venturies and other cavitation conditions resulting in a total of 36 computer plotted single variable correlations which are all included for the sake of completeness in the appendix. These were combined into several multiple plots for comparison and evaluation of the effect of varying different parameters.

A least mean square curve following the form of eq.(4) was generated to fit the data with the aid of a computer for each data group using the regression analysis developed previously. The resulting group equations from which the two-variable plots were generated by holding all variables but one constant by using averaged values applicable to a given run set for the others, are:

1. Venturi 534, sonic (including sonic, visible, and visible +*) cavitation condition.

$$\sigma_c = 0.107984 - 0.19342(\text{vol\%})^2 + 0.0817994(\text{vol\%})^3 - 0.0000011593(\text{vel})^2 + 0.0012874(\text{temp}) - 2.0668583(\text{l.c})^3$$

2. Venturi 412, sonic (including sonic, visible, and visible +) cavitation condition.

$$\sigma_c = 0.230813 - 0.02924(\text{vol\%}) + 0.00609217(\text{vol\%})^3 - 0.001398201(\text{vel}) + 0.000000017214(\text{vel})^3 + 0.0011736(\text{temp}) - 0.000000040486(\text{temp})^3 - 0.876878(\text{l.c.}) + 6.6044644(\text{l.c.})^3$$

3. Venturi 614, sonic (including sonic, visible, and visible +) cavitation condition.

$$\sigma_c = 0.13561814 - 0.03736142(\text{vol\%})^2 + 0.021944314(\text{vol\%})^3 - 0.0013994318(\text{vel}) + 0.00000519484(\text{vel})^2 - 0.000000086895(\text{temp})^3$$

---

*Cavitation condition slightly greater than visible inertia.

4. Venturi 818, sonic (including sonic, visible, and visible +) cavitation condition.

$$\sigma_c = 0.53389034 + 0.0010037953(vol\%)^3 + 0.0000066279l\ (vel)^2 - 0.000000033542(vel)^3 - 2.3543948(l.c) + 6.4742613(l.c.)^3$$

5. Venturi 534, standard cavitation condition.

$$\sigma_c = 0.018438258 - 0.0000000220666(temp)^3$$

6. Venturi 412, standard cavitation condition.

$$\sigma_c = 0.28363498 + 0.016803564(vol\%) - 0.00030307242(vel) + 0.000000001889(vel)^3 - 0.0000000l036023(temp)^3 - 10.679294(l.c.)^2 + 26.997634(l.c.)^3$$

7. Venturi 614, standard cavitation condition

$$\sigma_c = 0.04827969 - 0.0014004958(vol\%)^3 - 0.00045697679(vel) + 0.0000000050095(vel)^3 + 0.043272207(l.c.)$$

8. Venturi 818, standard cavitation condition.

$$\sigma_c = 0.026887401 - 0.00055891578(vol\%)^3 - 0.000095049423(vel)$$

9. Venturi 534, first mark cavitation condition.

$$\sigma_c = -0.0204071892 + 0.015932593(vol\%) + 0.00041013340(vol\%)^3$$

10. Venturi 412, first mark cavitation condition.

$$\sigma_c = 0.013075832 - 0.039778393\ (vol\%)^2 + 0.017262038(vol\%)^3 - 0.000016933835(vel) + 0.000003961l217(temp)^2 - 0.000000027824(temp)^3 + 0.057207588(l.c.)$$

11. Venturi 614, first mark cavitation condition. Insufficient data was taken in this area for the regression analysis to occur.

12. Venturi 818, first mark cavitation condition.

$$\sigma_c = 0.020174654 - 0.000077390731(vel)$$

CHAPTER V

RESULTS

The results presented here represent approximately 300 test runs and approximately 150 distinct data sets, taken for all the various conditions described above. Multiple correlations and cross correlations are presented in hand plots which in most cases have been taken from a combination of several computer plots.

A. Gas Content Effects

Cavitation number versus gas content is plotted as a function of various other parameters for cavitation inception in Figs. 10 through 15. The general trend observed from these plots is that the observed cavitation number increases as the gas content of the water increases. Fig. 10 is a plot of the inception cavitation number versus gas content for three velocities, 64 ft./sec., 100 ft./sec., and 215 ft./sec. This plot was obtained from preliminary data[3] and shows the theoretically anticipated trends more closely than do some of the computer developed plots using all the data. Many of the curves show cavitation number decreasing with increasing gas content in the

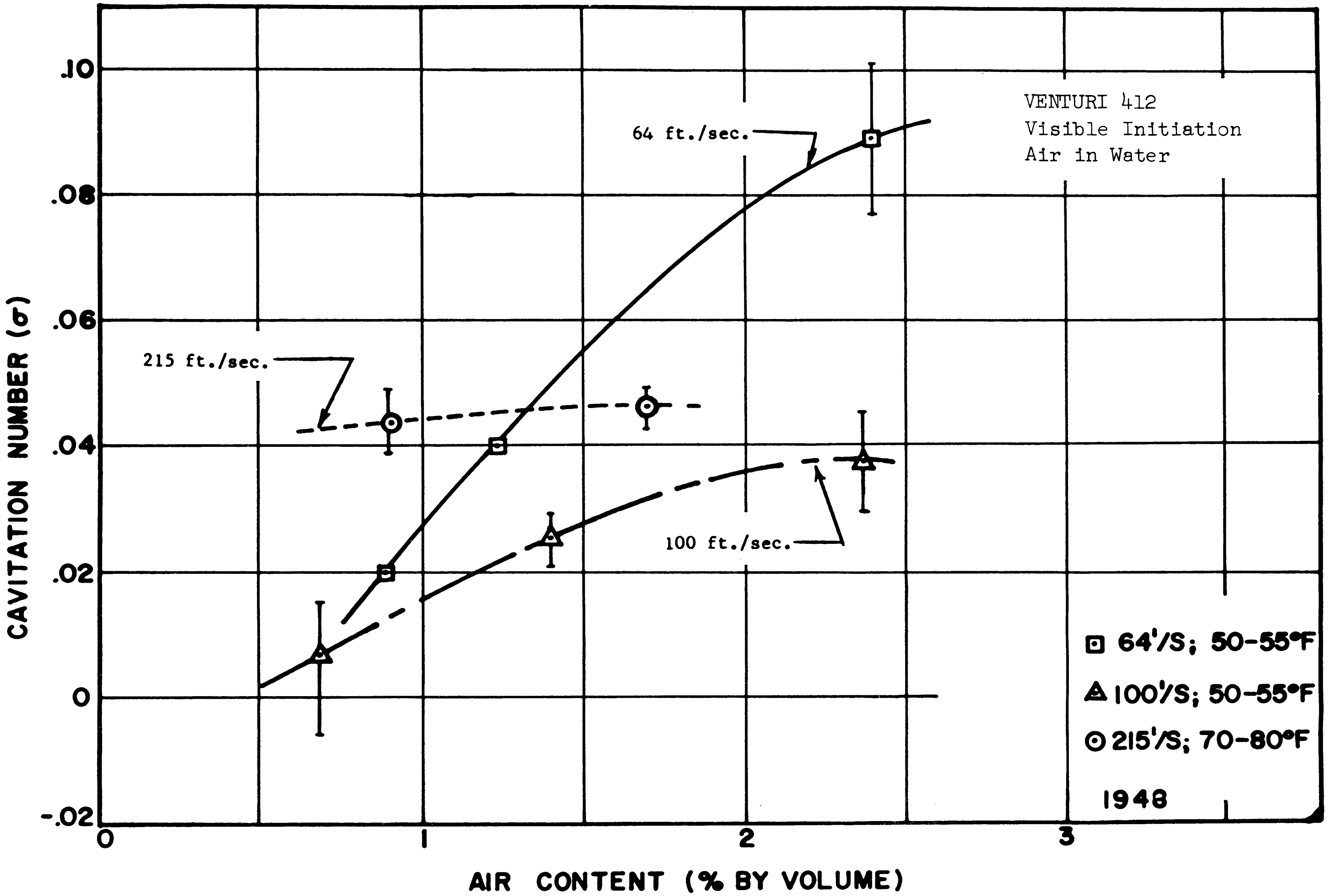

Fig. 10.--Cavitation inception number vs. air content for 1/2" plexiglas venturi at three velocities in water.

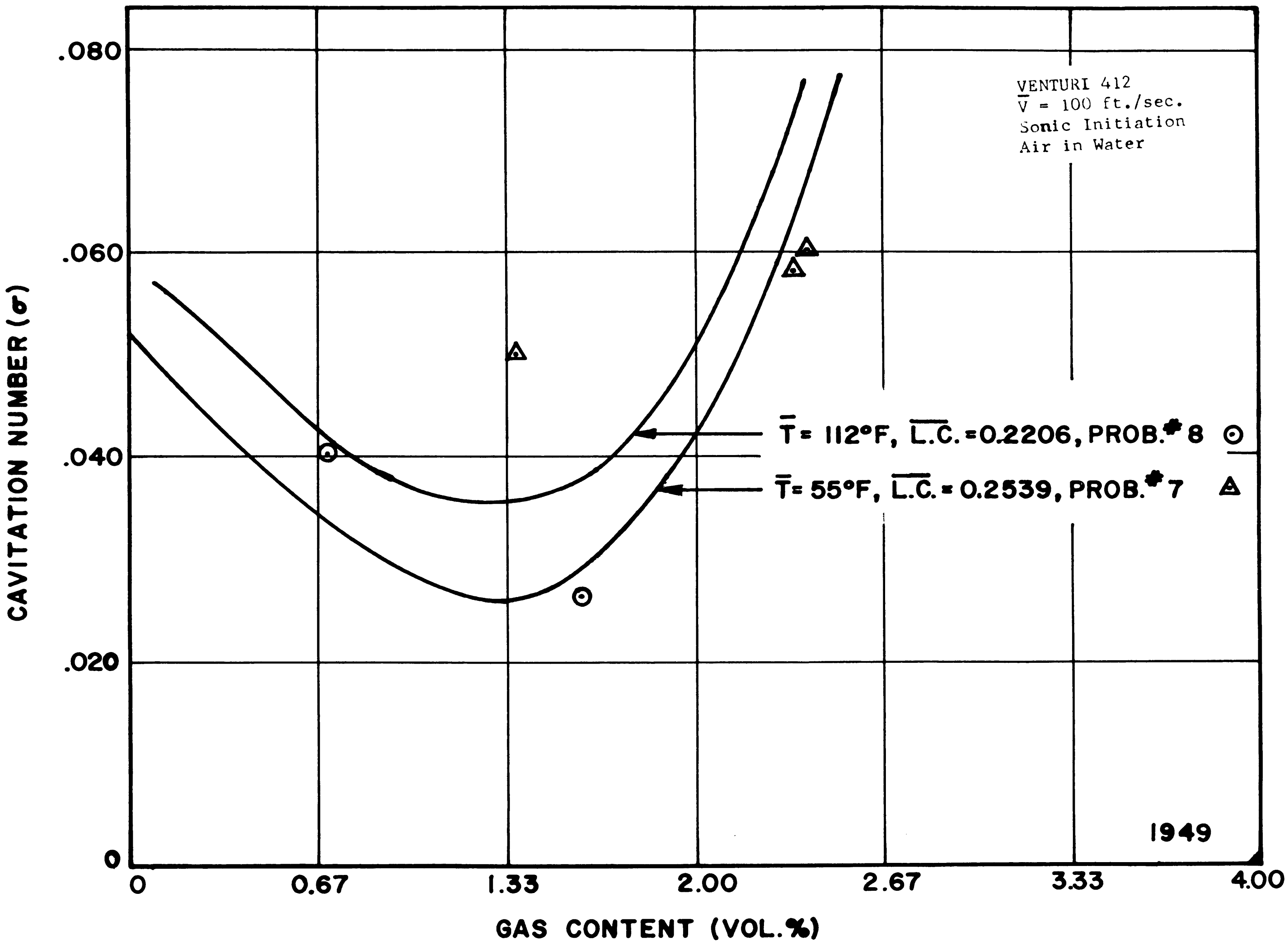

Fig. 11.--Cavitation inception number vs. air content for 1/2" plexiglas venturi at 100 ft./sec. and two temperatures in water.

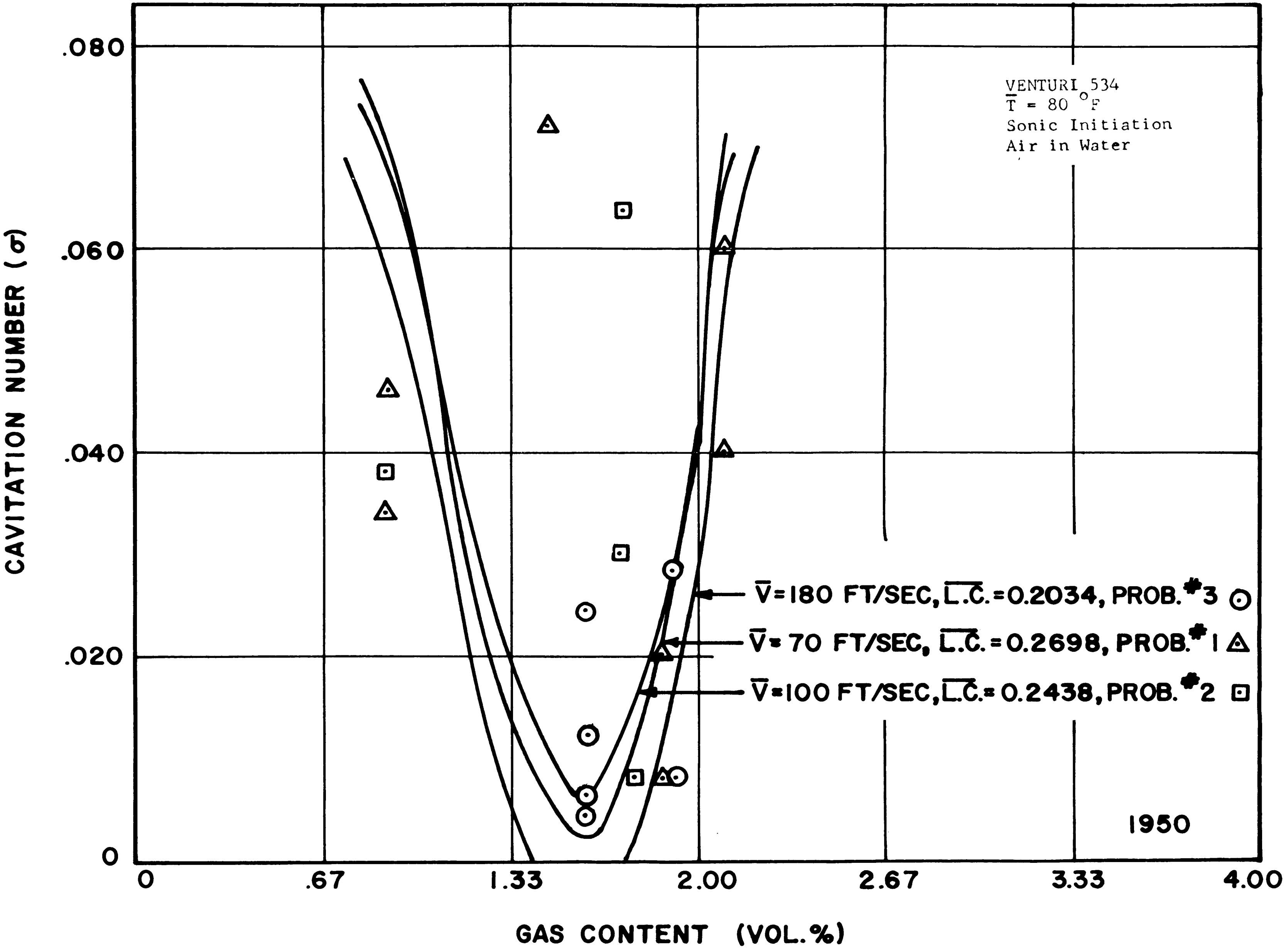

Fig. 12.--Cavitation inception number vs. air content for 3/4" plexiglas venturi at 80°F and three velocities in water.

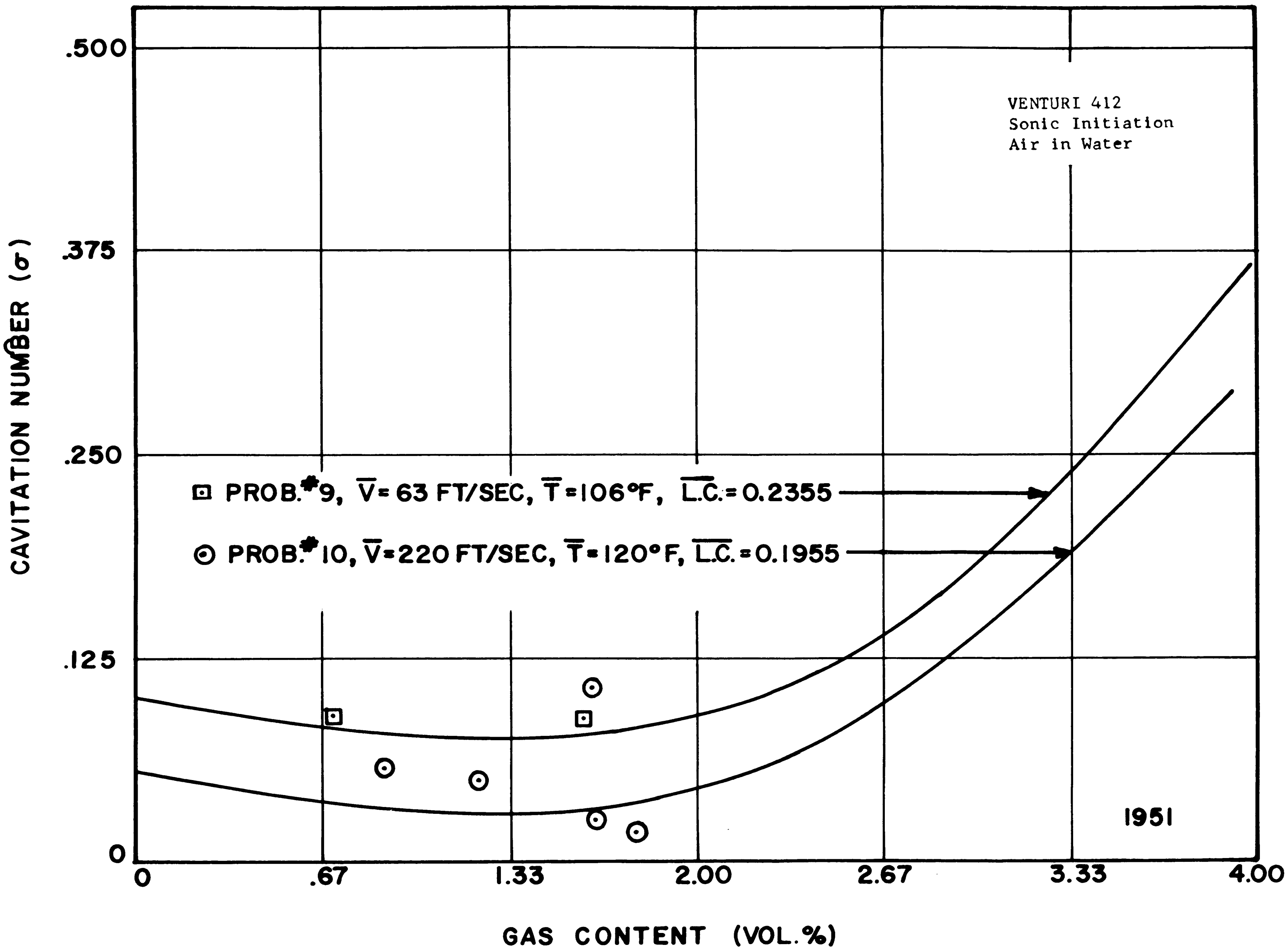

Fig. 13.--Cavitation inception number vs. air content for 1/2" plexiglas venturi at two temperatures and two velocities in water.

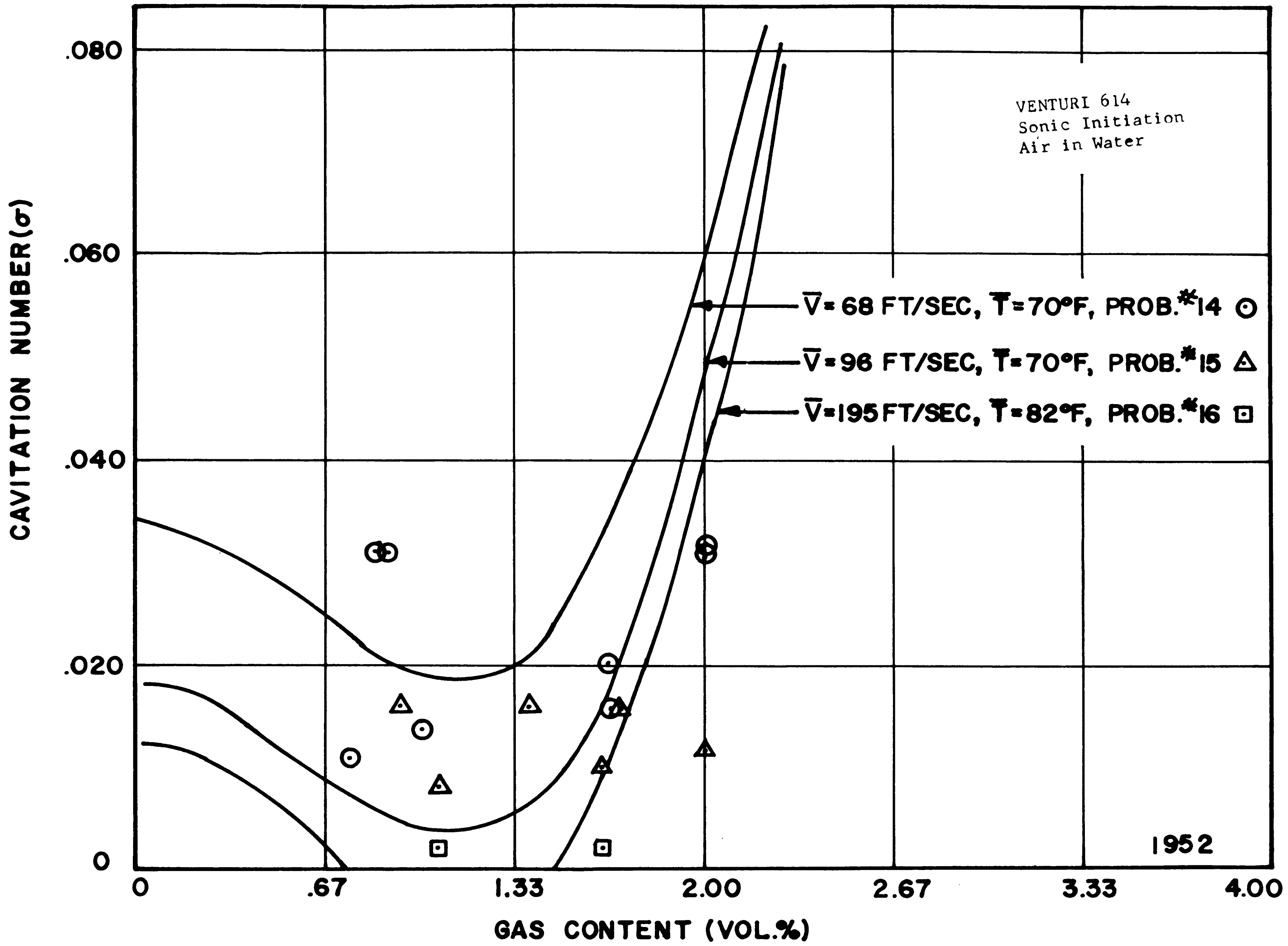

Fig. 14.--Cavitation inception number vs. air content for 1/4" plexiglas venturi at room temperature and three velocities in water.

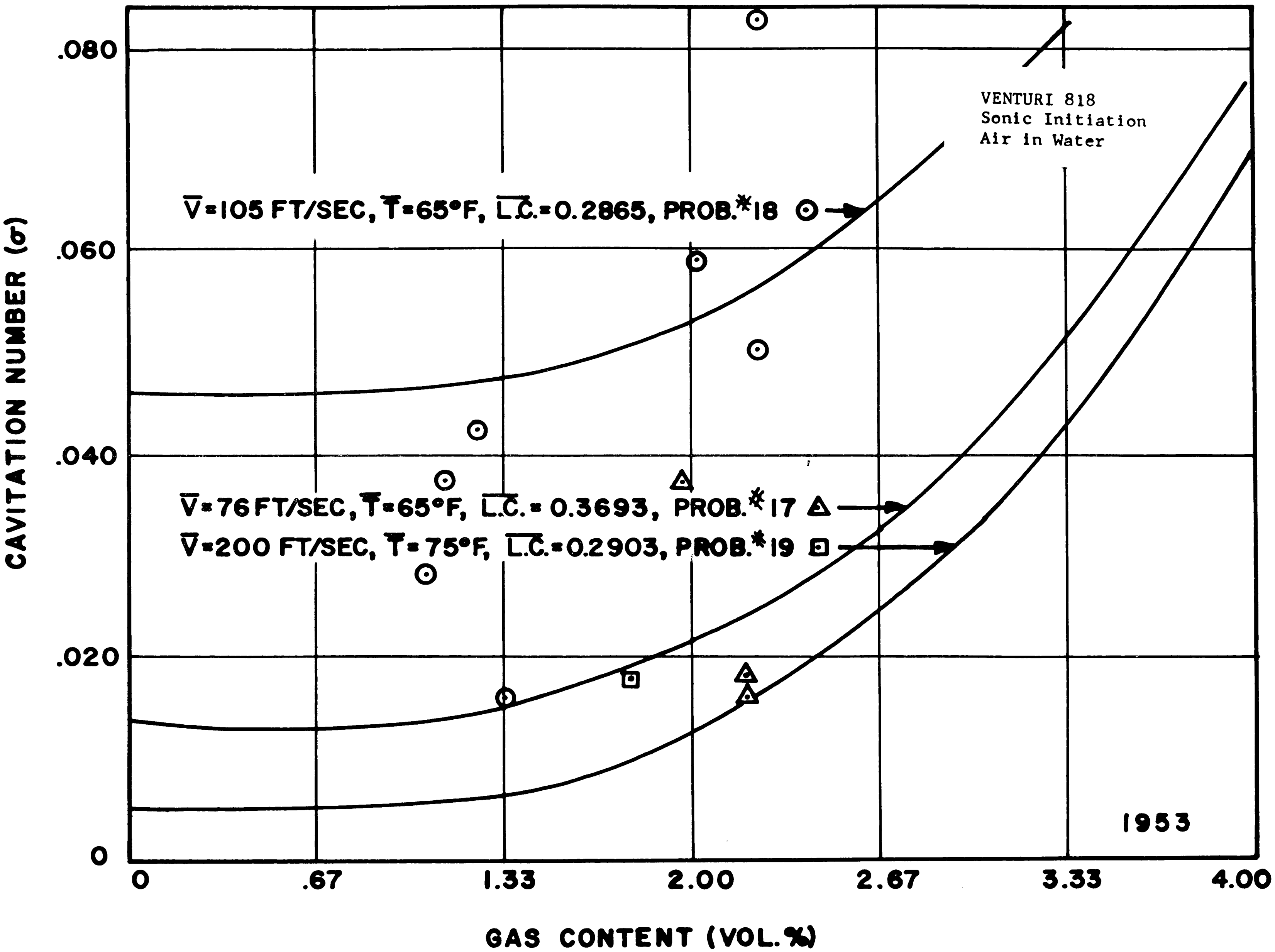

Fig. 15.--Cavitation inception number vs. air content for 1/8" plexiglas venturi at room temperature and three velocities in water.

low gas content range ($\leq$1.5%) and increasing thereafter. It is believed that the curve fitting techniques have generated the rising curve toward the low pressure end, which is the "tail" of the polynomial generated to fit the data primarily in the higher gas content range where most of the data was taken. Thus it seemed reasonable to disregard the very low gas content region. Thus in general, as the gas content of the water increases so does the inception cavitation number. This is of course to be expected on theoretical grounds.

Figs. 16 and 17 show the effect of gas content upon cavitation number for a more fully developed cavitation condition, "standard cavitation". For this cavitation condition the cavitation number definitely decreases as gas content increases, ie, the pressure in the cavitation is apparently less when some air is present. No explanation for this rather unexpected result is presently available.

B. Temperature Effects

Due to test apparatus limitations, it was not possible to make very significant changes in the operating temperature. The plexiglas venturis could not be operated at temperatures $>$ 150°F, and the minimum possible temperature was about room temperature, so that only a small temperature differential was possible. The data reflects this limitation showing no very consistent or significant temperature correlations.

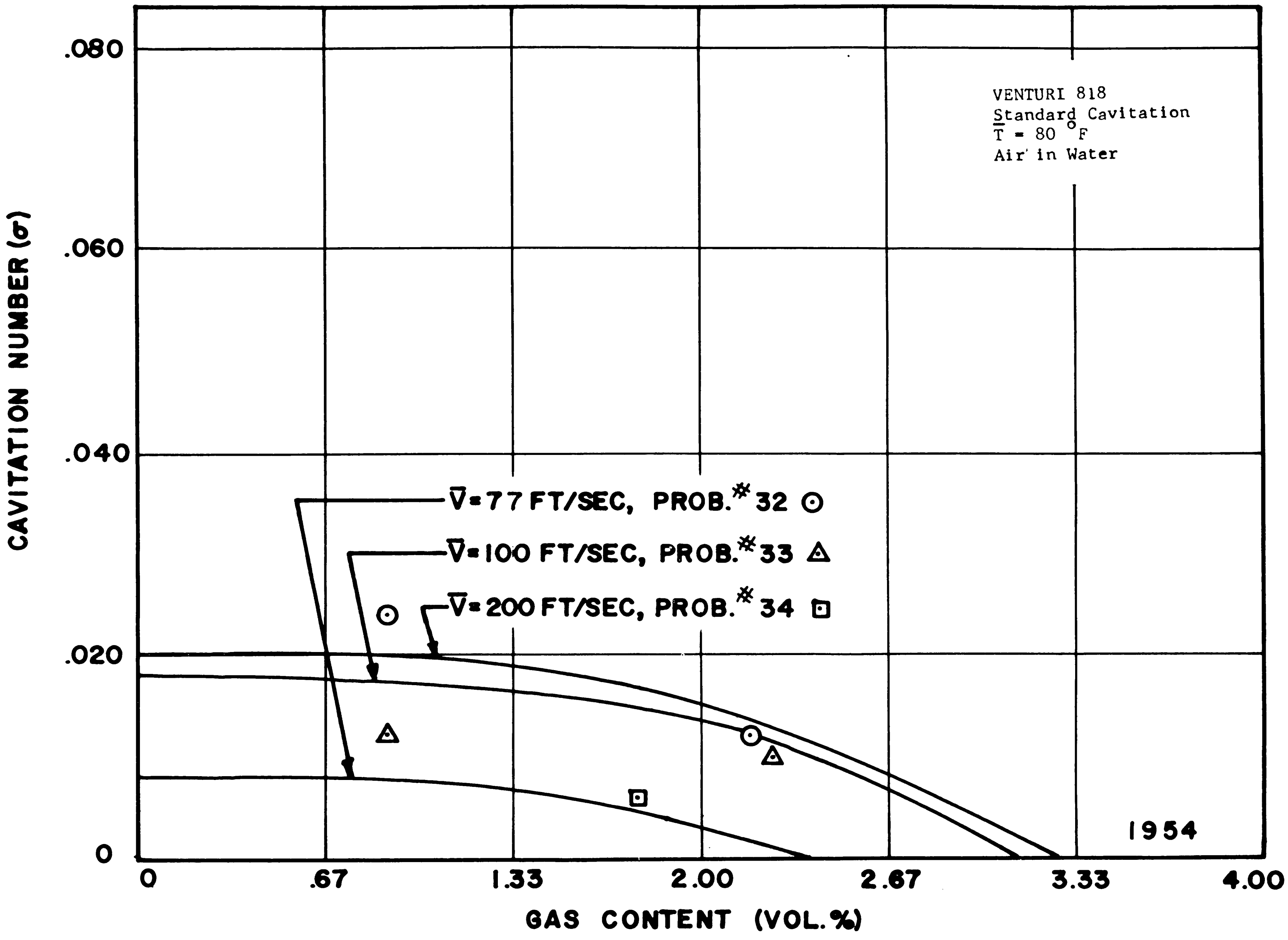

Fig. 16.--Cavitation number vs. air content for 1/8" venturi for "standard cavitation" at room temperature at three velocities in water.

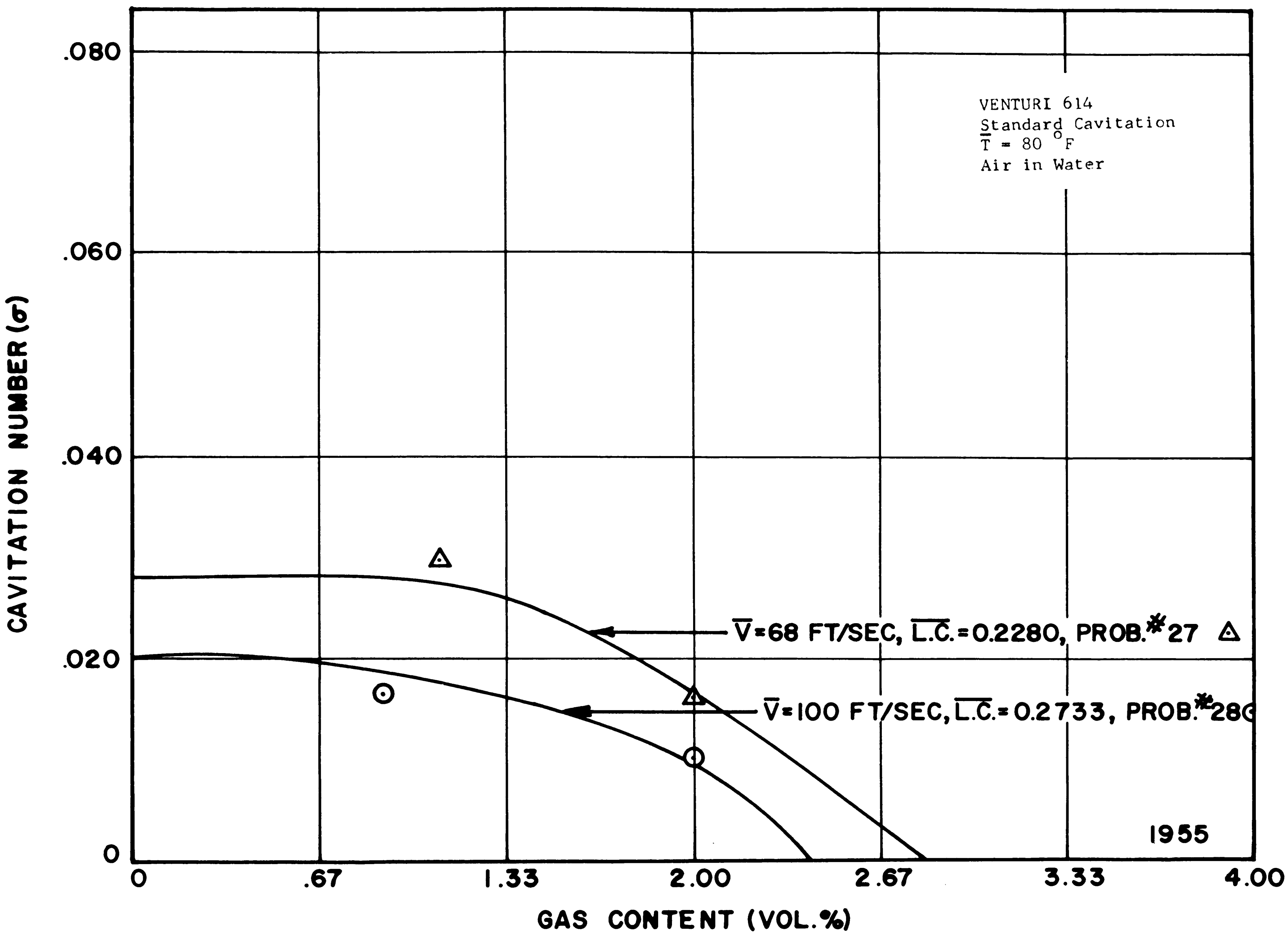

Fig. 17.--Cavitation number vs. air content for 1/4" venturi for "standard cavitation" at room temperature at two velocities in water.

C. Velocity Effects

In general, as the velocity of the water through the venturi increases, within the range of the experiment, the cavitation number decreases. Fig. 11 includes only one velocity and hence presents no information for a velocity correlation. While Fig. 12 shows no correlation with velocity, the data scatter is great and the curves are not widely spread. Figs. 13 and 14 do verify the velocity effect stated above for cavitation inception. Fig. 15 shows the same effect if the curve for 76 ft./sec. is neglected, since its loss coefficient differs significantly from that of the others. A correction to the loss coefficient to the lower value exhibited by the other curves on this figure would raise the curve, ie, move it in the direction required for consistent results. Fig. 16, for "standard cavitation" shows a reverse effect, perhaps due to the fact that only five data points were available for this correlation. Thus the conclusion that an increase in velocity, all other parameters being held constant, results in a decrease in the inception cavitation number (in the range tested) is verified by the data.

Fig. 18 (reproduced from a previous study[3]) shows that a decrease in the inception cavitation number occurs until a velocity of approximately 150 ft./sec. is reached. There is then a slight increase for higher velocities. Other factors seem to come into play after a certain velocity is reached which nullify or overshadow the pure velocity effects. This data (Fig. 18) comes from earlier tests conducted expressly

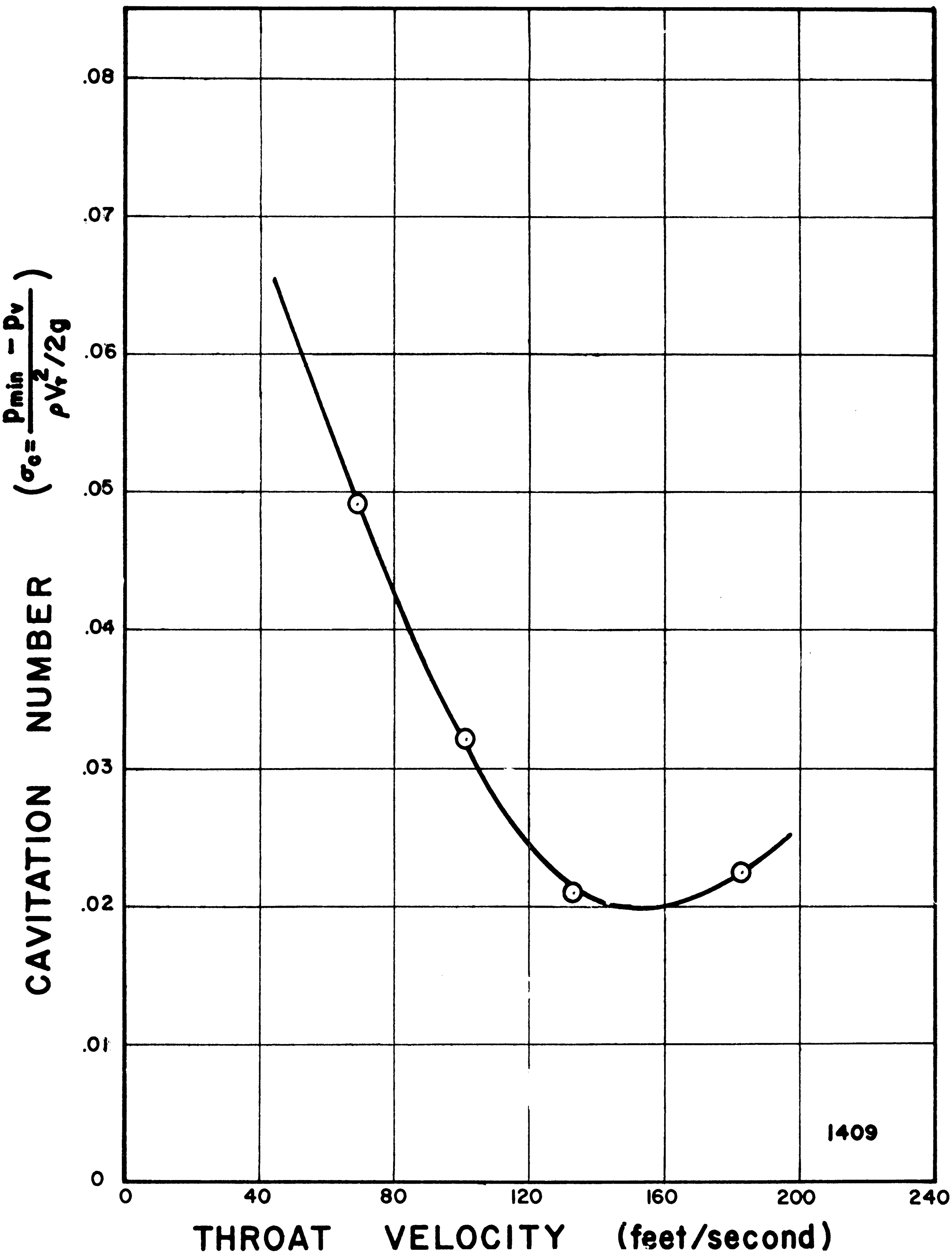

Fig. 18.--Cavitation inception number vs. throat velocity for 3/4" plexiglas venturi at 80°F in water.

to observe the effects of velocity variation. The present data, correlated by the regression analysis, is not in sufficient detail to detect the increase in cavitation number at very high velocity. Fig. 19 is a cross plot of the preliminary data which was presented in Fig. 10. Again this is much closer to the predicted trends than any of the computer developed correlations using all of the data. It is shown (Fig. 19) that:

a) Gas content effects upon cavitation number are much more pronounced at low velocity than at high velocity, perhaps because more time is afforded for the emergence of gas from solution.

b) For near saturation air content (STP) cavitation number decreases with increasing velocity for low velocities and then increases at high velocity, giving an "optimum" velocity from the viewpoint of attempting to avoid cavitation.

c) For low air content, cavitation number increases continuously with increasing velocity. However, the extreme low air content curves shown are merely extrapolated and hence must be considered relatively unreliable.

It appears that the water data is extremely sensitive to environmental parameters such as the amount of gas entrained versus that dissolved and to temperature variations. This was shown to be the case by the prepressurization runs (Fig. 4). Thus problems of repeatability arise when the water in the loop is changed and when the data is taken on different days when slight changes in the environment may have occurred. For this reason the "preliminary data" already discussed (Figs. 10, 18,

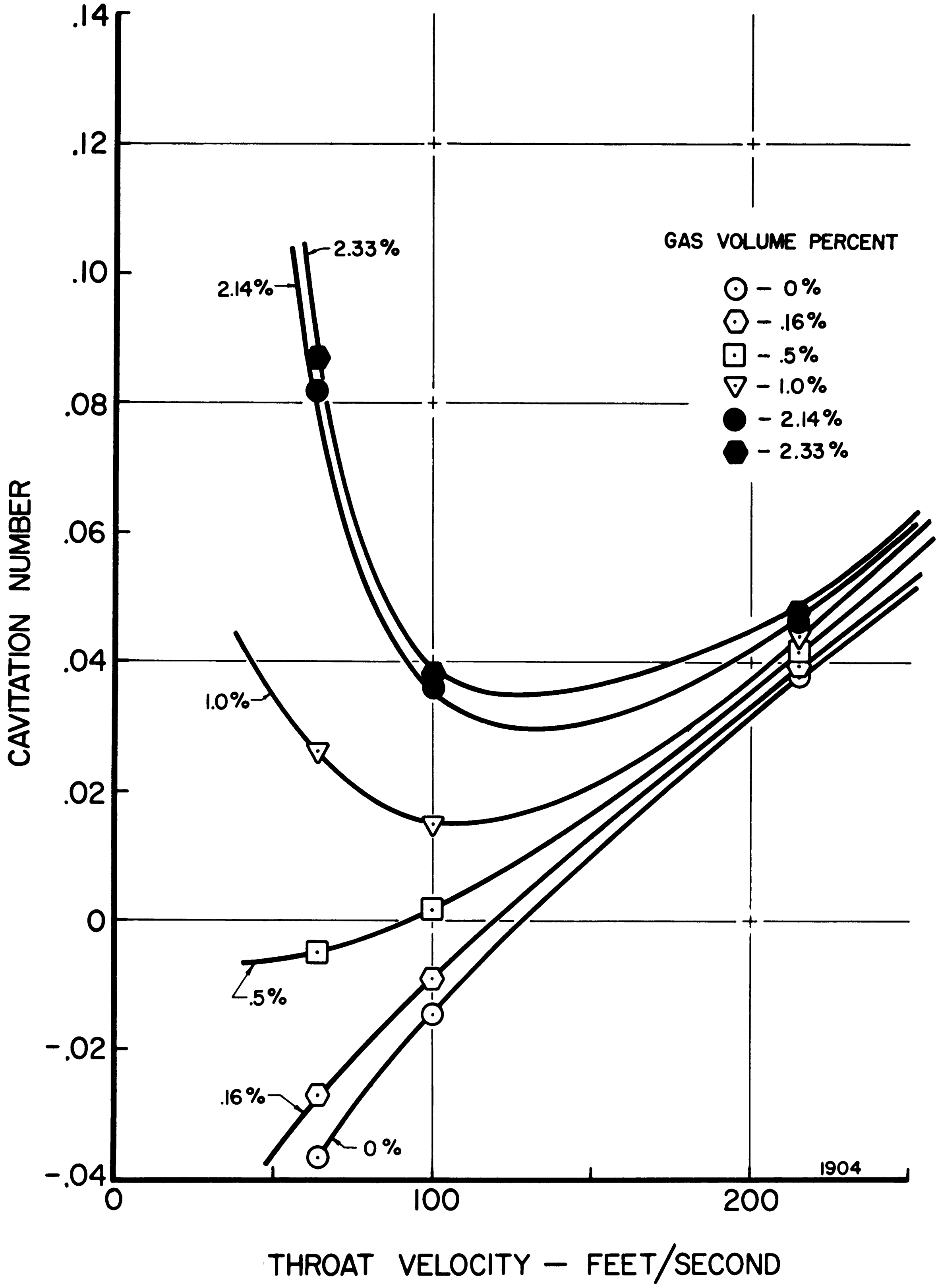

Fig. 19.--Cavitation inception number vs. throat velocity for 1/2" plexiglas venturi at room temperature and several air contents in water.

and 19) which was taken in runs of relatively short duration on the same day with the same water in the loop are much more consistent than the computer correlations of numerous data sets taken on many different occasions, since these also contain all variables of water condition other than as expressed by the total gas content, surface roughness changes as the venturi is exposed to cavitation, etc.

D. Venturi Size Effects

In general cavitation number increases with increasing venturi throat diameter. This trend is just opposite to that which was observed in this laboratory when mercury was used as the cavitating fluid in a stainless steel venturi, but relatively similar to that observed when mercury was used in a plexiglas venturi. This may indicate a significant effect due to the difference in roughness between the stainless steel and the plexiglas venturis. Figures 20, 21, and 22 are plots of cavitation number versus venturi throat diameter for plexiglas venturis, for inception and "standard cavitation" conditions, with water as the cavitating fluid. In slightly more than half of the cases the minimum cavitation number occurs for a venturi throat diameter of approximately 1/4" with an increase in the cavitation number for both the 1/8" and the 1/2" venturis. The increase generally continues on to the 3/4" size. A similar trend was also observed when mercury was used as the cavitating fluid in a plexiglas venturi in this laboratory. The increase of cavitation number for the very small diameter (1/8") may be due to what was termed a "blocking effect" for increasing gas

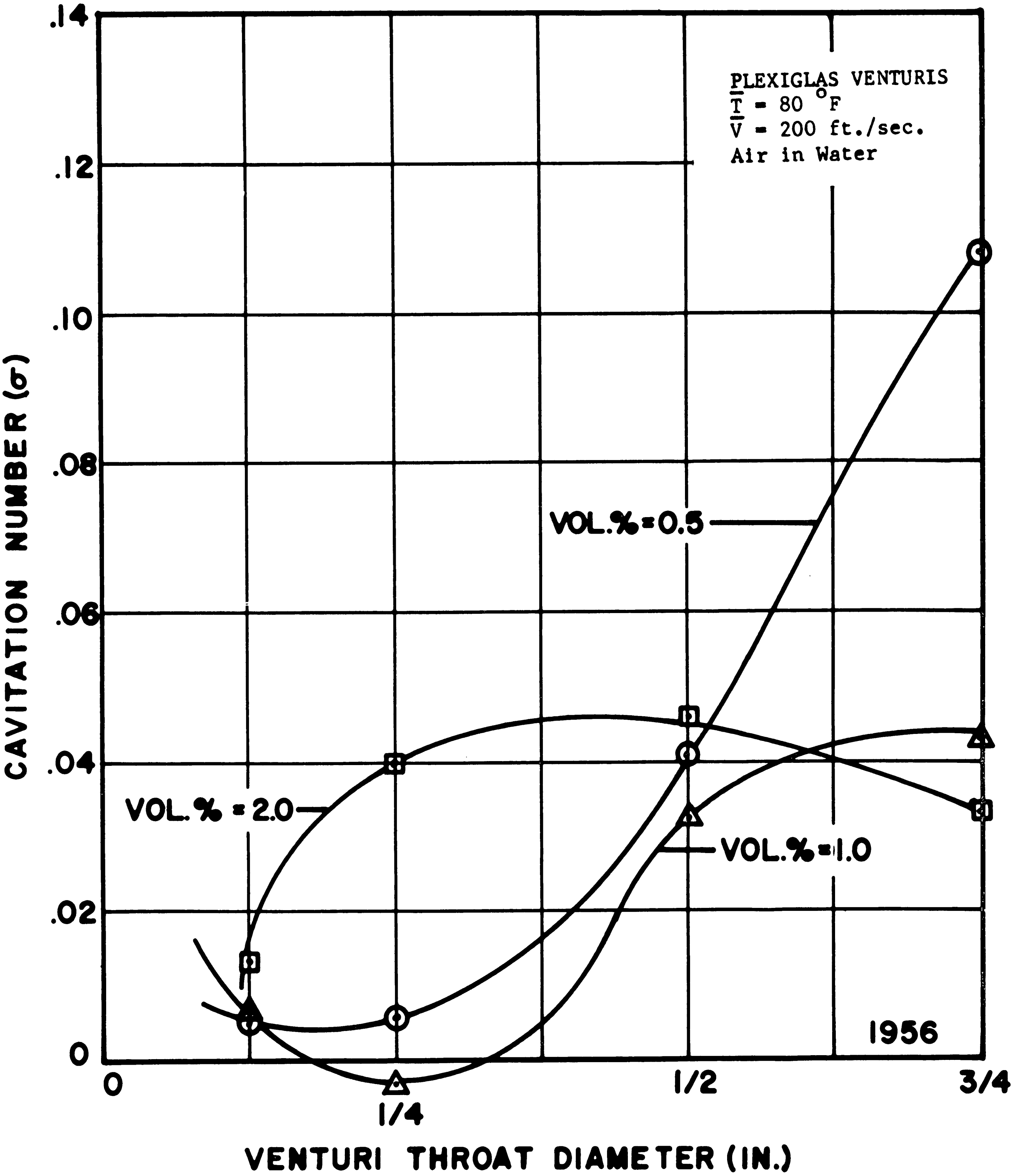

Fig. 20.--Cavitation inception number vs. throat diameter for plexiglas venturis at 80°F, 200 ft./sec. and several air contents in water.

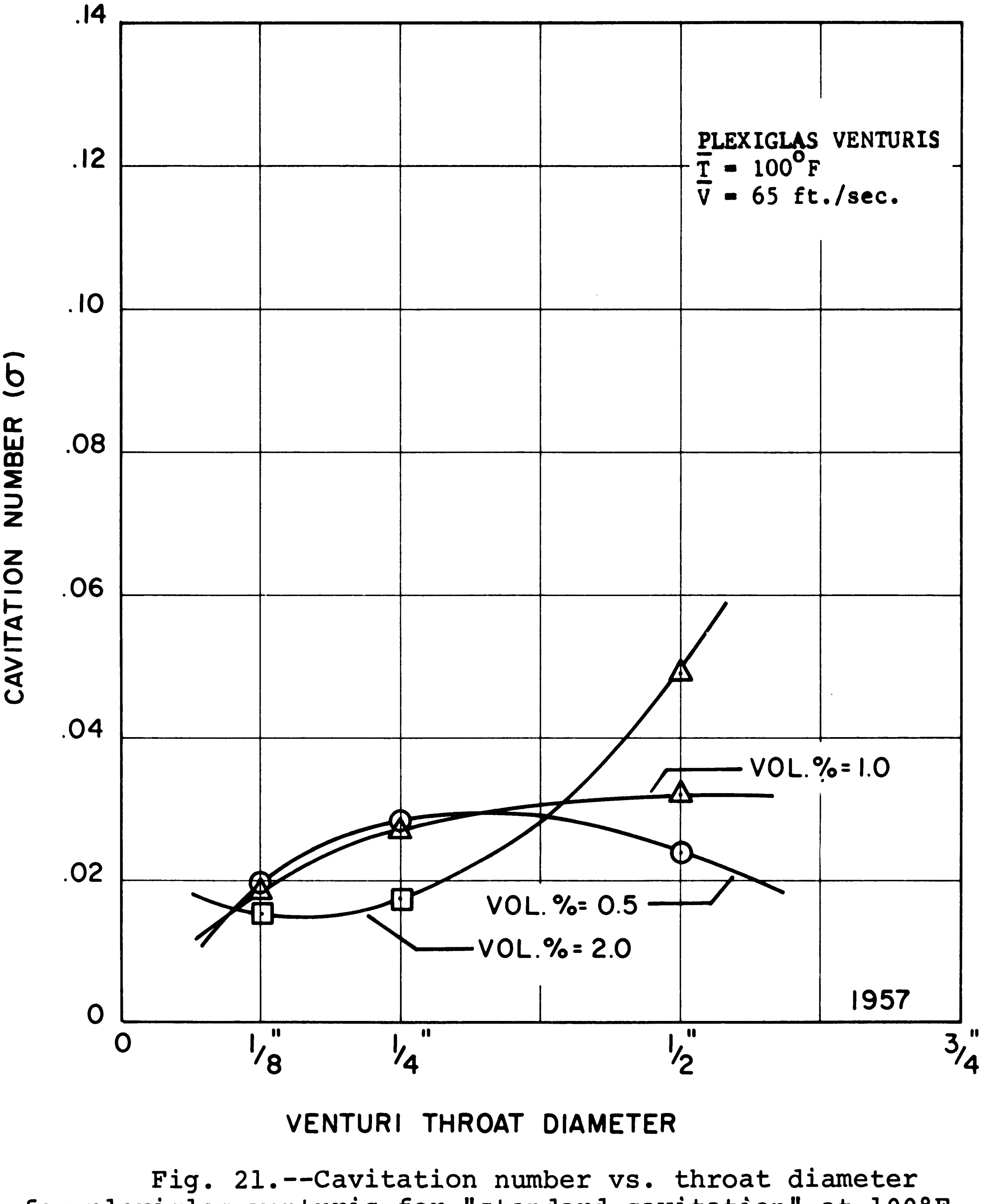

Fig. 21.--Cavitation number vs. throat diameter for plexiglas venturis for "standard cavitation" at 100°F, 65 ft./sec. and several air contents in water.

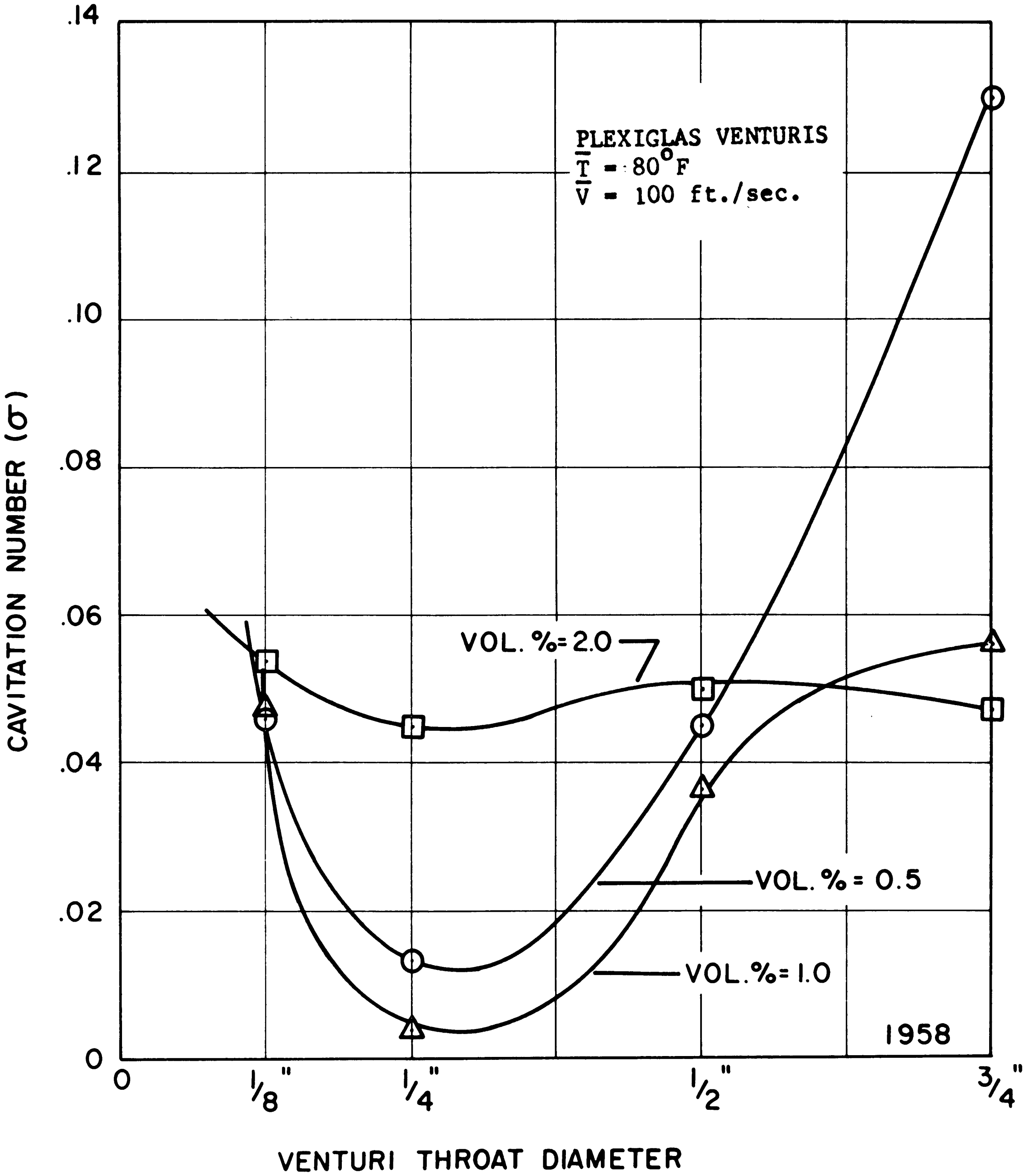

Fig. 22.--Cavitation inception number vs. throat diameter for plexiglas venturis at 80°F, 100 ft./sec., and several air contents in water.

content, since the gas and vapor bubbles become of large dimension compared to the throat opening and are thus capable of momentarily completely filling the passage. This is not the case when the venturi throat diameter is increased beyond 1/4". Thus this two-phase flow does not scale properly even though the flow passages used are geometrically similar.

E. Reynolds Number Effects

Figs. 23 and 24 are plots of cavitation inception number versus Reynolds number for the 3/4", 1/2", 1/4", and 1/8" diameter venturis at gas contents of 1%, 1.5%, and 2%. Fig. 23 shows the actual data points and Fig. 24 shows the points calculated from the computer developed curves. The curves are generally similar, although minor differences exist. The trend of decreasing cavitation number with increasing Reynolds number is shown in both cases. The curves are quite similar to those obtained in earlier investigations[2], showing a decreasing cavitation number with increasing Reynolds number for relatively low Reynolds number and relatively little change in cavitation number above a Reynolds number of 10^6. However, in the very high range there is a tendency for cavitation number to increase as Reynolds number is further increased. This minimum in the cavitation number versus Reynolds number curve is consistent with recent tests on a cavitating inducer.[13] This lower range indicates that the cavitation number increases with decreasing Reynolds number, Fig. 24, and then decreases sharply for the 1/8" venturi. Again this peculiar behavior may be due to the

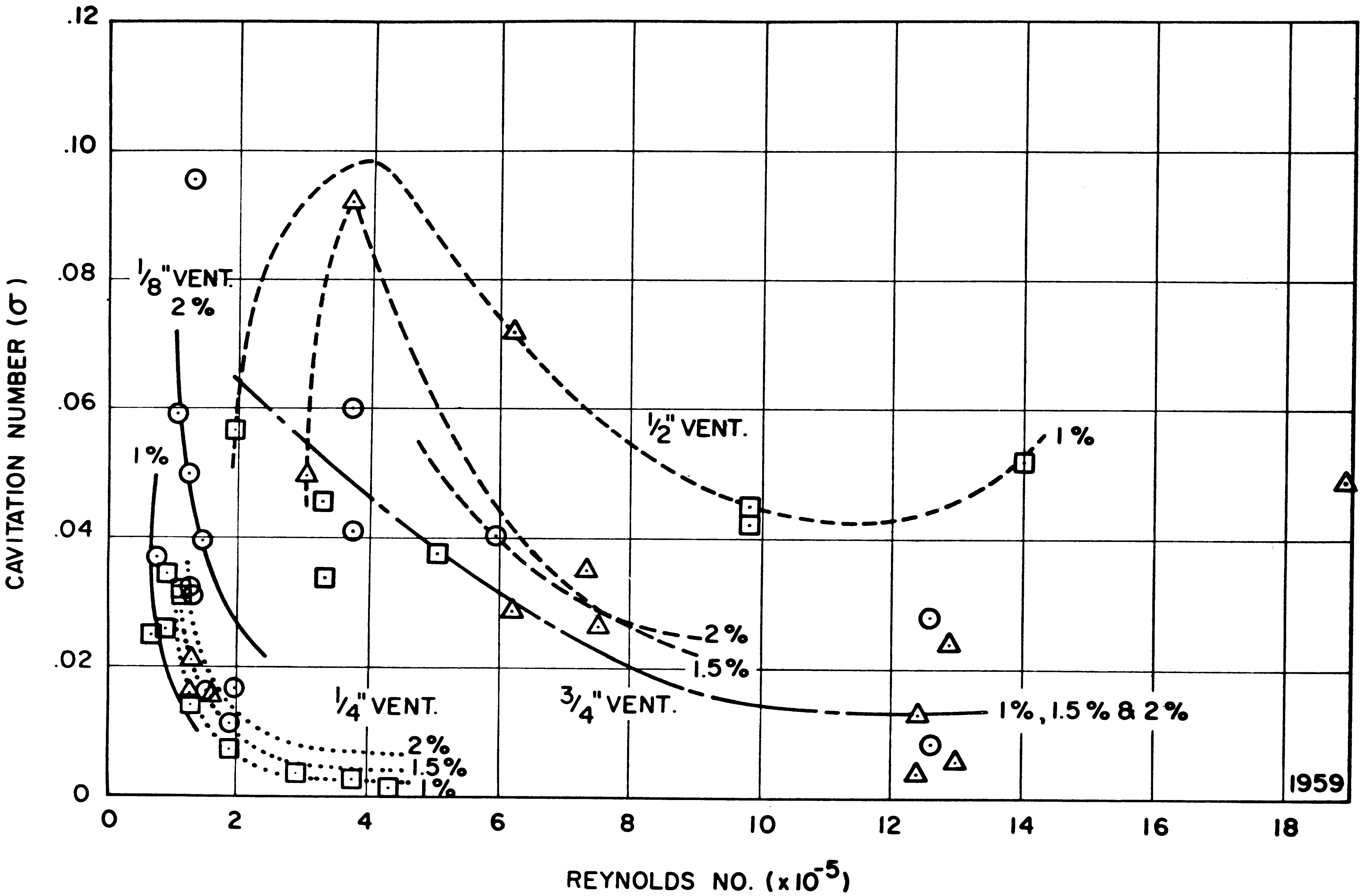

Fig. 23.--Cavitation inception number vs. Reynolds number for plexiglas venturis at several air contents in water (raw data points).

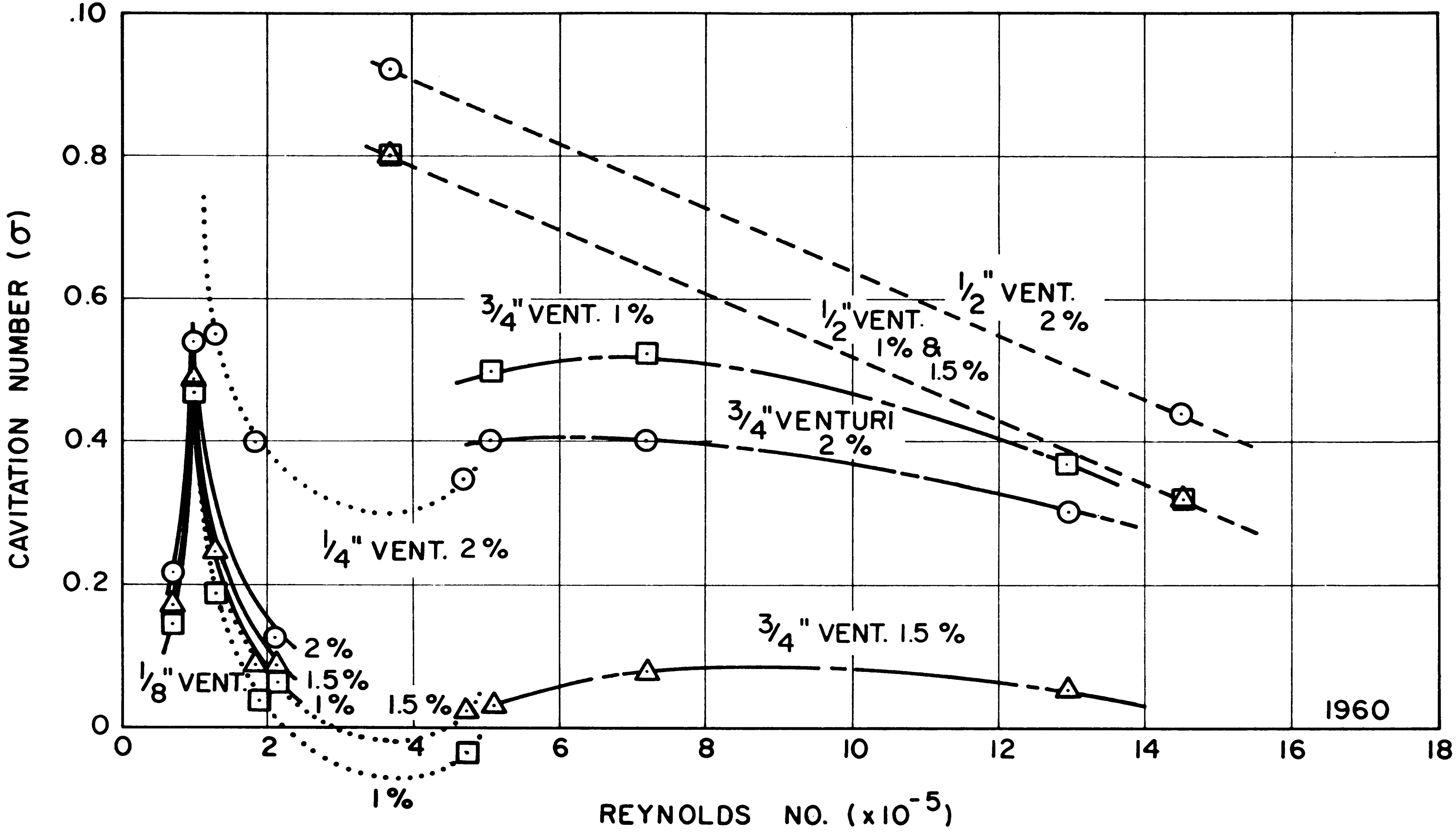

Fig. 24.--Cavitation inception number vs. Reynolds number for plexiglas venturis at several air contents in water (computer smoothed curves).

smallness of the passage size, and the lack of flow scaling previously mentioned. The general trend is that cavitation number decreases with increasing Reynolds number. However, the data does not plot on a single curve, but tends to be grouped according to the venturi throat diameter size. A previous comparison of venturi cavitation data in this laboratory (Fig. 25), showed that water and mercury data from the same venturi did not plot together. Hence it must be concluded that Reynolds number is not an all inclusive cavitation correlating parameter.

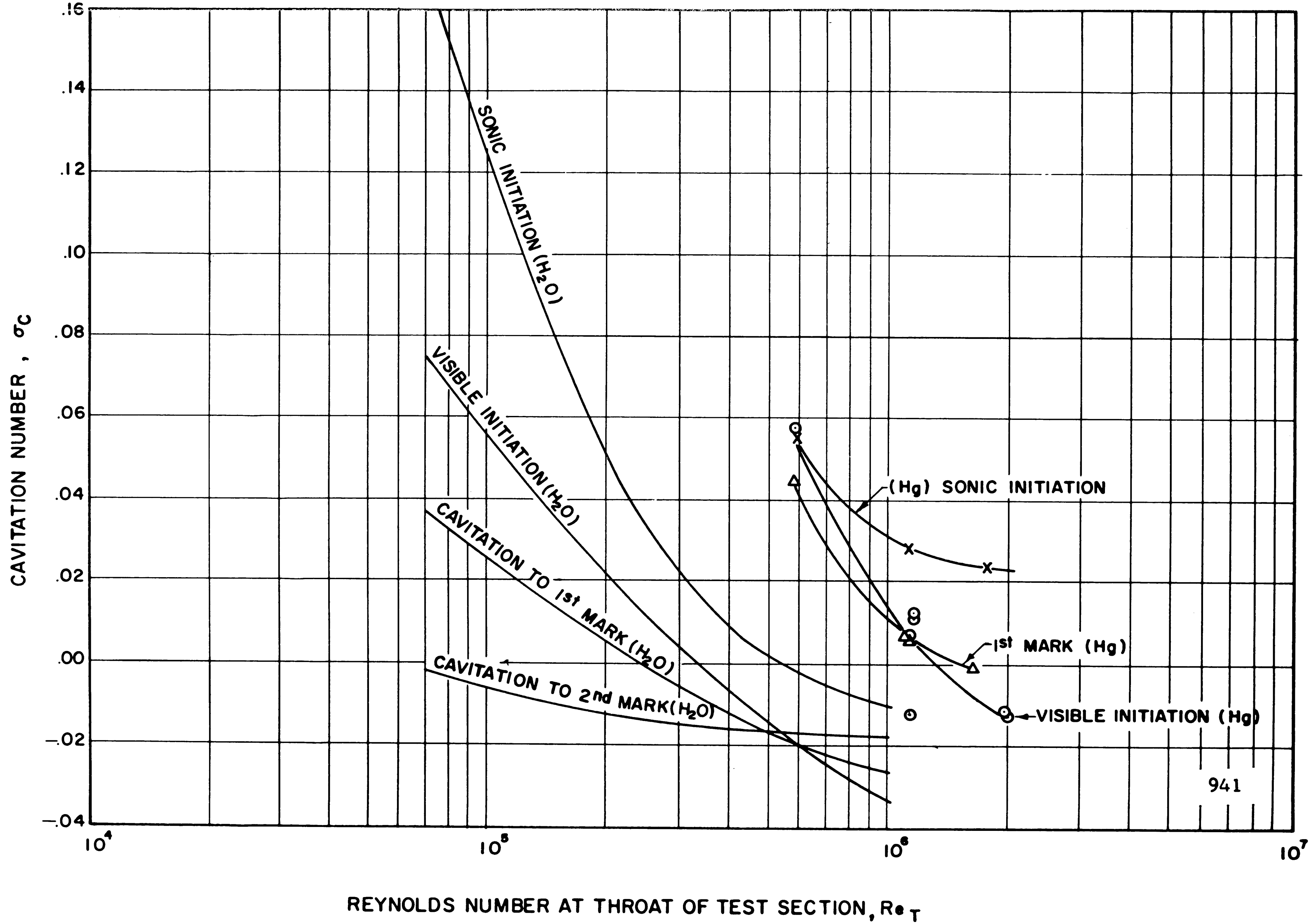

Fig. 25.--Cavitation number vs. Reynolds number for several cavitation conditions with mercury and water (1/2" venturi -- No. II).

CHAPTER VI

CONCLUSIONS

The general conclusions that can be drawn from this investigation are as follows.

1) There is a significant effect of gas content on cavitation number for all four venturi sizes tested. This effect is such that cavitation number generally increases with gas content increase. The effect is greatest for low velocity.

2) No significant temperature effects on the cavitation number were noted, as the temperature range covered was inadequate in this respect.

3) Cavitation number tends to steadily increase with increasing throat velocity for the low gas content values and tends to decrease and then increase with the higher gas contents, with the minimum in the latter plots falling at a velocity of approximately 150 ft./sec. for the 3/4" and 1/2" venturis.

4) Cavitation number generally increases with increasing throat diameter for the lower gas contents and remains relatively constant for gas contents around the saturation level at STP.

5) Cavitation number generally decreases with increasing Reynolds number above a value of $\sim 2 \times 10^5$ with a lessening rate of

decrease above a value of $\sim 10^6$. An increase is observed for still higher Reynolds numbers. The Reynolds number data plots best when grouped according to venturi throat size, and this is consistent with previous data from water and mercury tests in the same venturi where the two fluids did not plot together. Thus Reynolds number is apparently not an all inclusive correlating parameter for cavitating venturis.

APPENDIX

A. Definition of Cavitation Conditions

The following are the definitions of the degrees of cavitation as used in this investigation:

Sonic Initiation* --- first visible or sonic manifestation of cavitation in the venturi.

Visible Initiation*-- continuous ring of cavitation at the throat outlet, about 1/8" long.

Standard Cavitation - cavitation cloud extends from throat outlet to termination at 1.520(D) inches downstream.

First Mark Cavitation-cavitation cloud extends from throat outlet to termination at 3.440(D) inches downstream.

*The flow conditions corresponding to these two inception conditions are the same for this set of tests so that both conditions are called "cavitation inception" in the report.

B. Computer Plots and Correlations of Data

The following plots are the direct output from the computer plotting program and list the correlating equations that resulted from the data fitting, with plots of both the experimental data(*) and the generated correlation curve(+) from the listed equation. In general, more experimental data was used to generate the correlation equation than appears to be the case looking at the small number of experimental data points presented on some of the plots. The equations were generated using all applicable data, which may have included several gas contents, temperatures, velocities, and loss coefficients, all for the same venturi and cavitation condition. However, once the equation was in hand, it was necessary to fix all independent variables but one in order to obtain a two-variable plot. Then only that data which had direct correspondence with the actual values of the fixed independent variables that were inserted into the correlation equation was plotted.

PLOTTING OF EXPERIMENTAL AND CALCULATED VALUES FOR PROBLEM NO 1

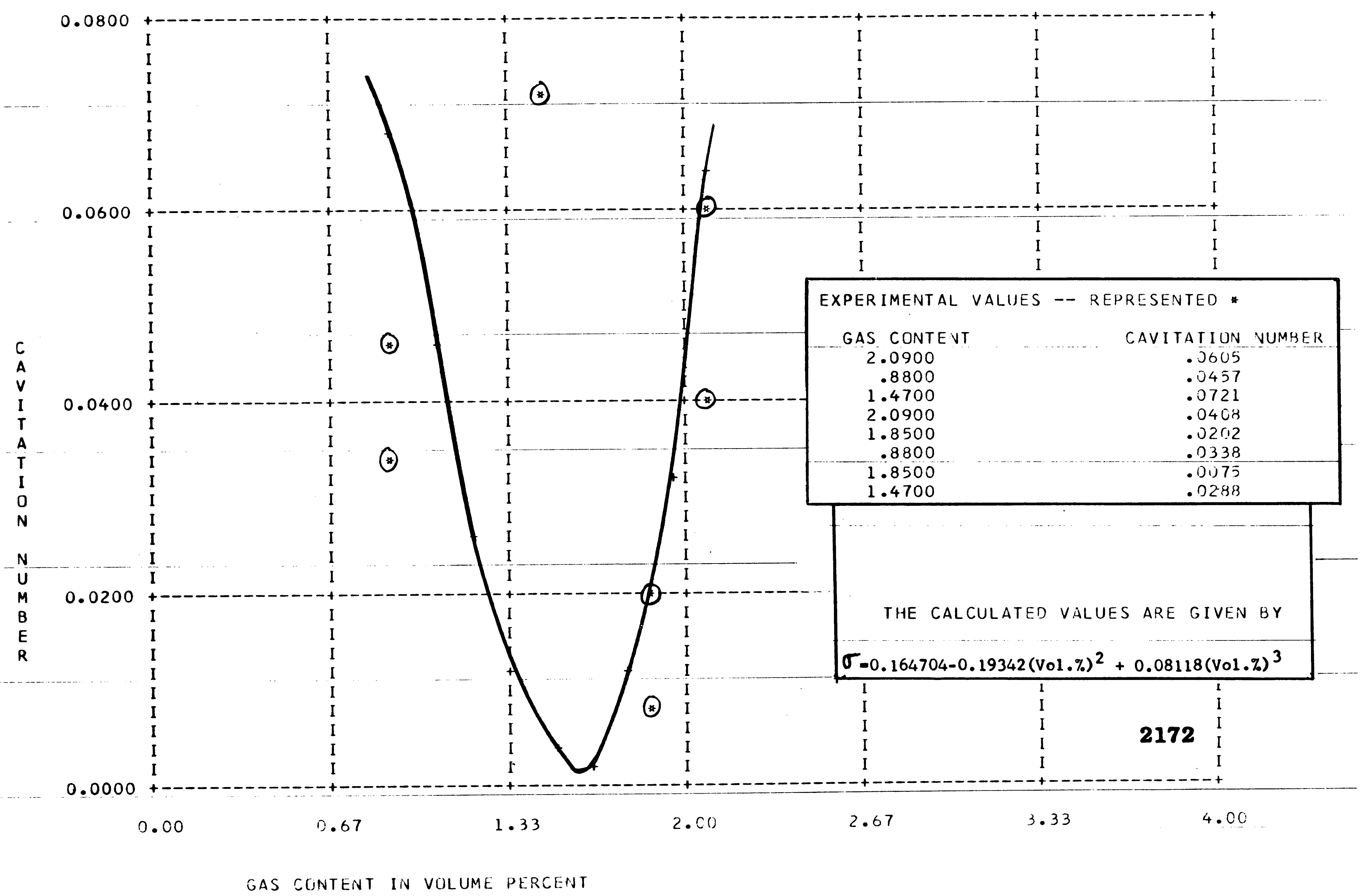

EXPERIMENTAL VALUES -- REPRESENTED *

GAS CONTENT	CAVITATION NUMBER
2.0900	.0605
.8800	.0457
1.4700	.0721
2.0900	.0408
1.8500	.0202
.8800	.0338
1.8500	.0075
1.4700	.0288

THE CALCULATED VALUES ARE GIVEN BY

$\sigma = 0.164704 - 0.19342(\text{Vol.\%})^2 + 0.08118(\text{Vol.\%})^3$

PLOTTING OF EXPERIMENTAL AND CALCULATED VALUES FOR PROBLEM NO 2

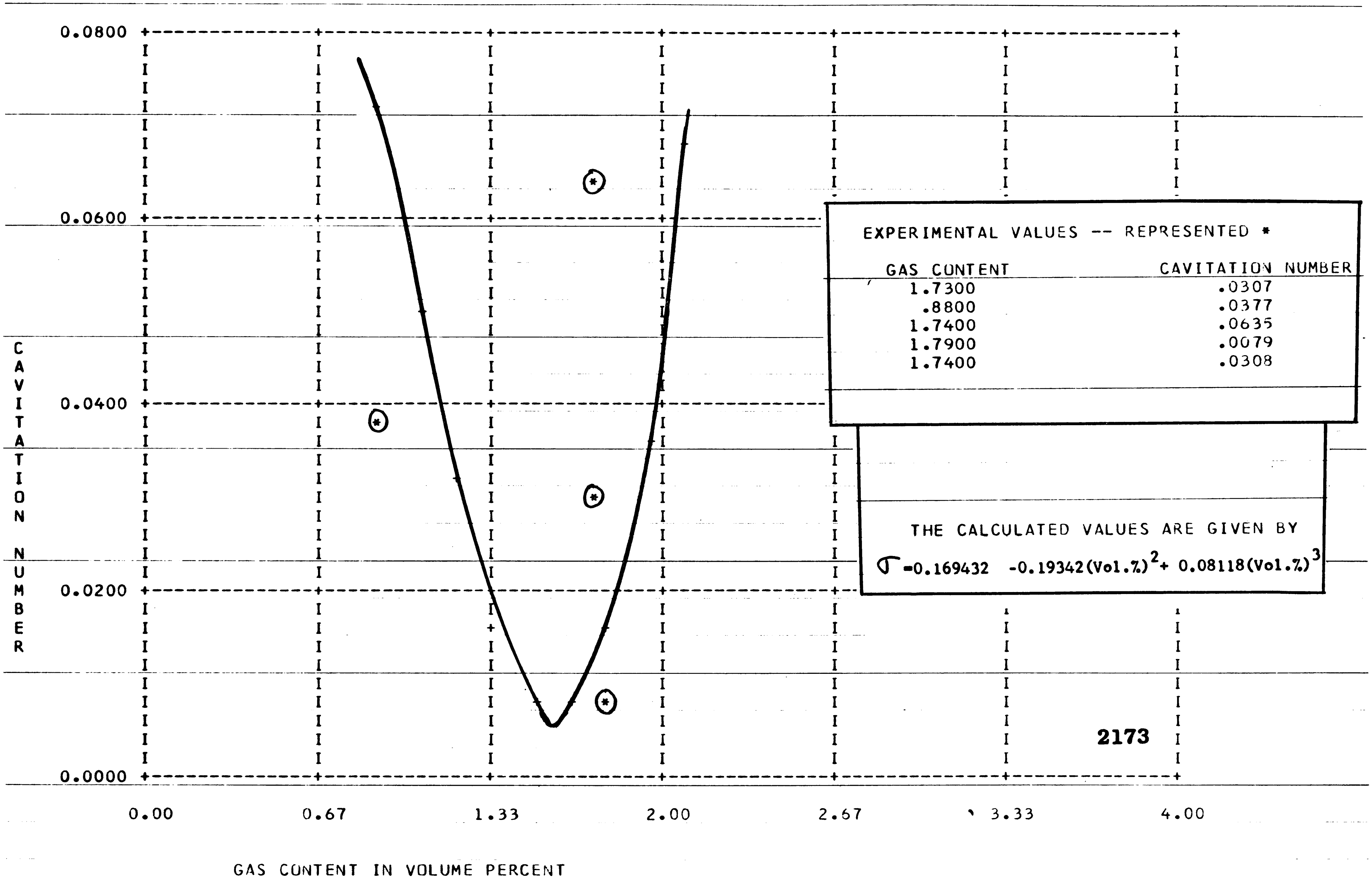

EXPERIMENTAL VALUES -- REPRESENTED *

GAS CONTENT	CAVITATION NUMBER
1.7300	.0307
.8800	.0377
1.7400	.0635
1.7900	.0079
1.7400	.0308

THE CALCULATED VALUES ARE GIVEN BY

$$\sigma = 0.169432 - 0.19342(\text{Vol.\%})^2 + 0.08118(\text{Vol.\%})^3$$

PLOTTING OF EXPERIMENTAL AND CALCULATED VALUES FOR PROBLEM NO 3

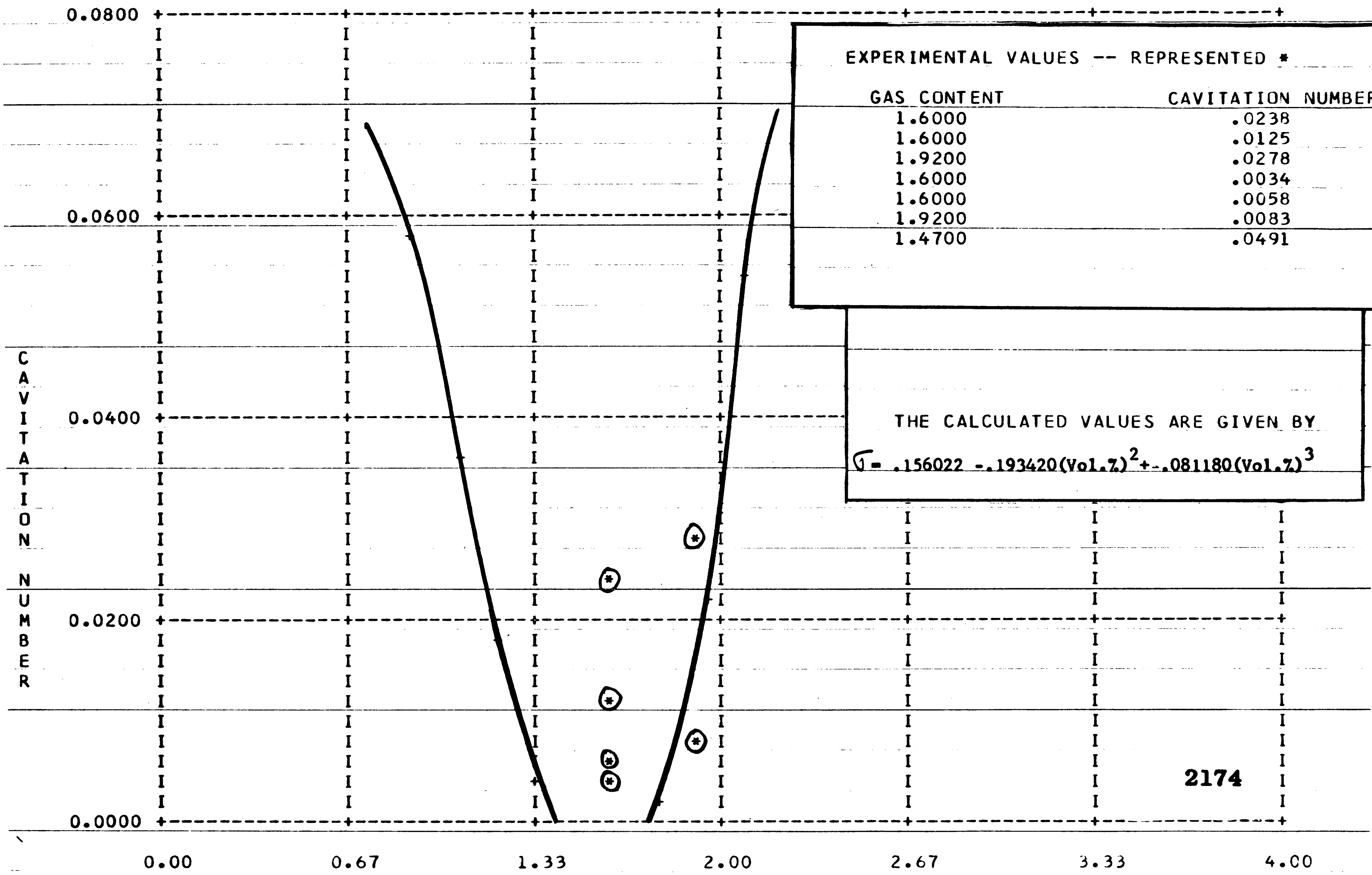

EXPERIMENTAL VALUES -- REPRESENTED *

GAS CONTENT	CAVITATION NUMBER
1.6000	.0238
1.6000	.0125
1.9200	.0278
1.6000	.0034
1.6000	.0058
1.9200	.0083
1.4700	.0491

THE CALCULATED VALUES ARE GIVEN BY

$\sigma = .156022 - .193420(\text{Vol.\%})^2 + -.081180(\text{Vol.\%})^3$

GAS CONTENT IN VOLUME PERCENT

PLOTTING OF EXPERIMENTAL AND CALCULATED VALUES FOR PROBLEM NO 4

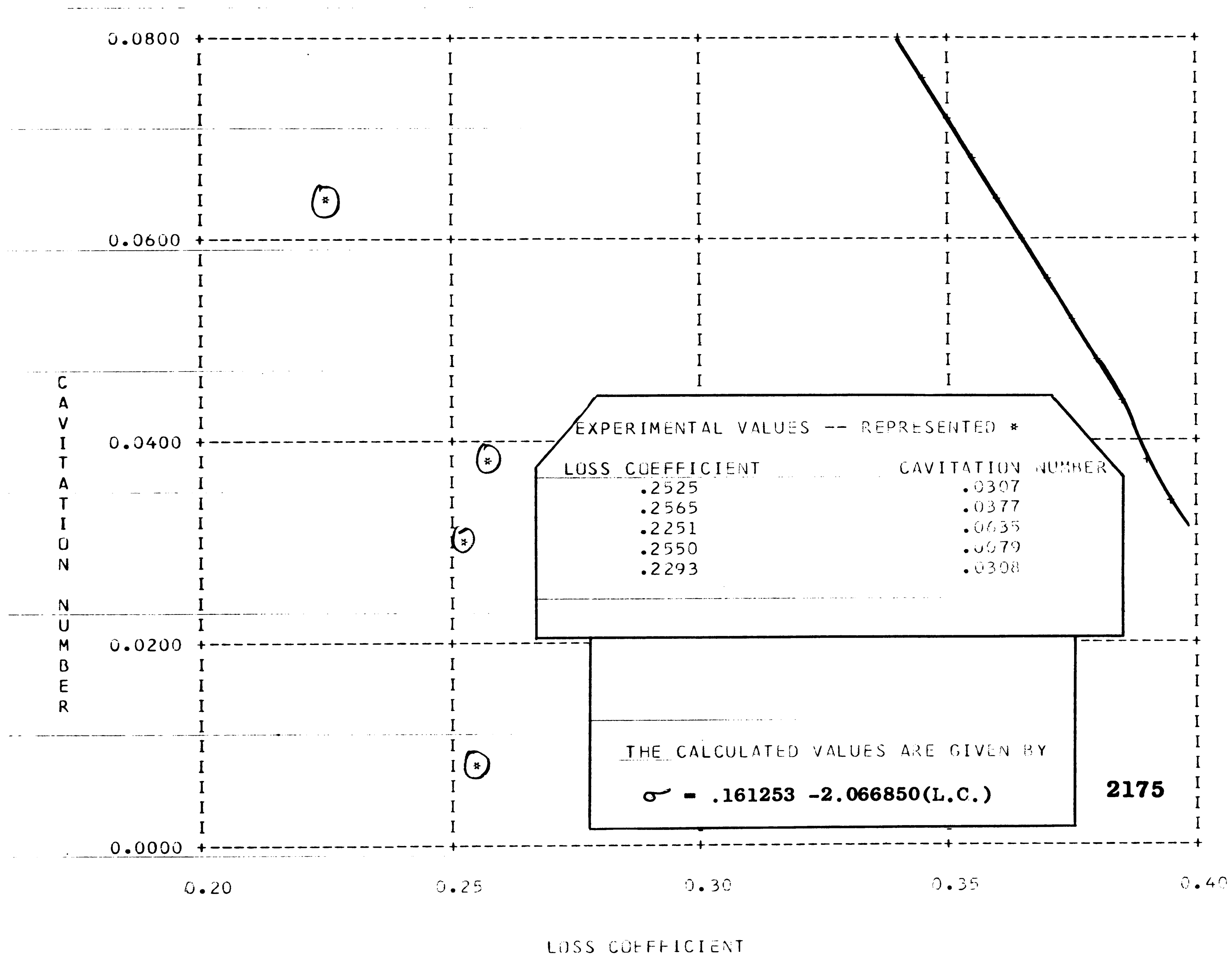

EXPERIMENTAL VALUES -- REPRESENTED *

LOSS COEFFICIENT	CAVITATION NUMBER
.2525	.0307
.2565	.0377
.2251	.0635
.2550	.0079
.2293	.0308

THE CALCULATED VALUES ARE GIVEN BY

σ = .161253 -2.066850(L.C.)

2175

PLOTTING OF EXPERIMENTAL AND CALCULATED VALUES FOR PROBLEM NO 5

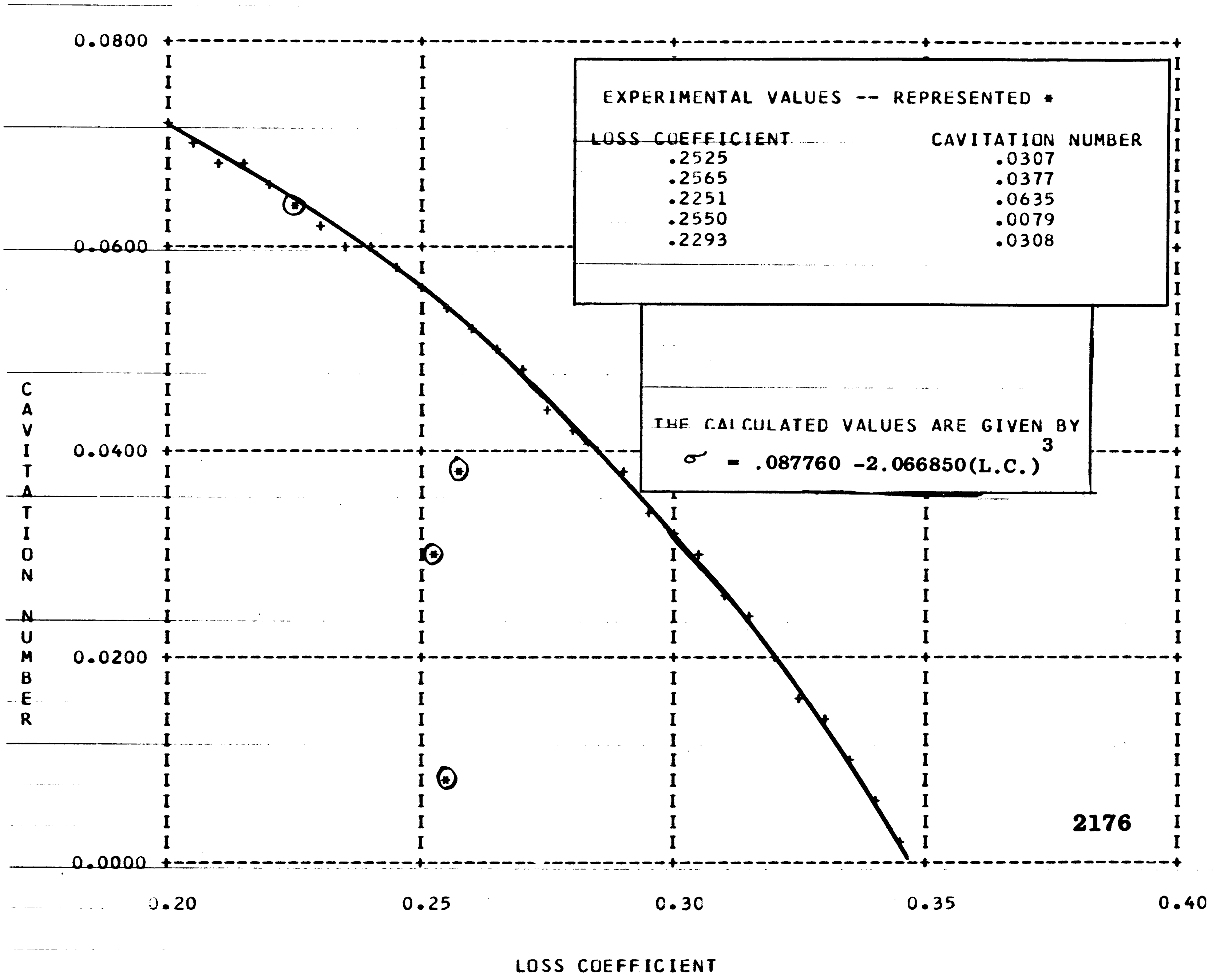

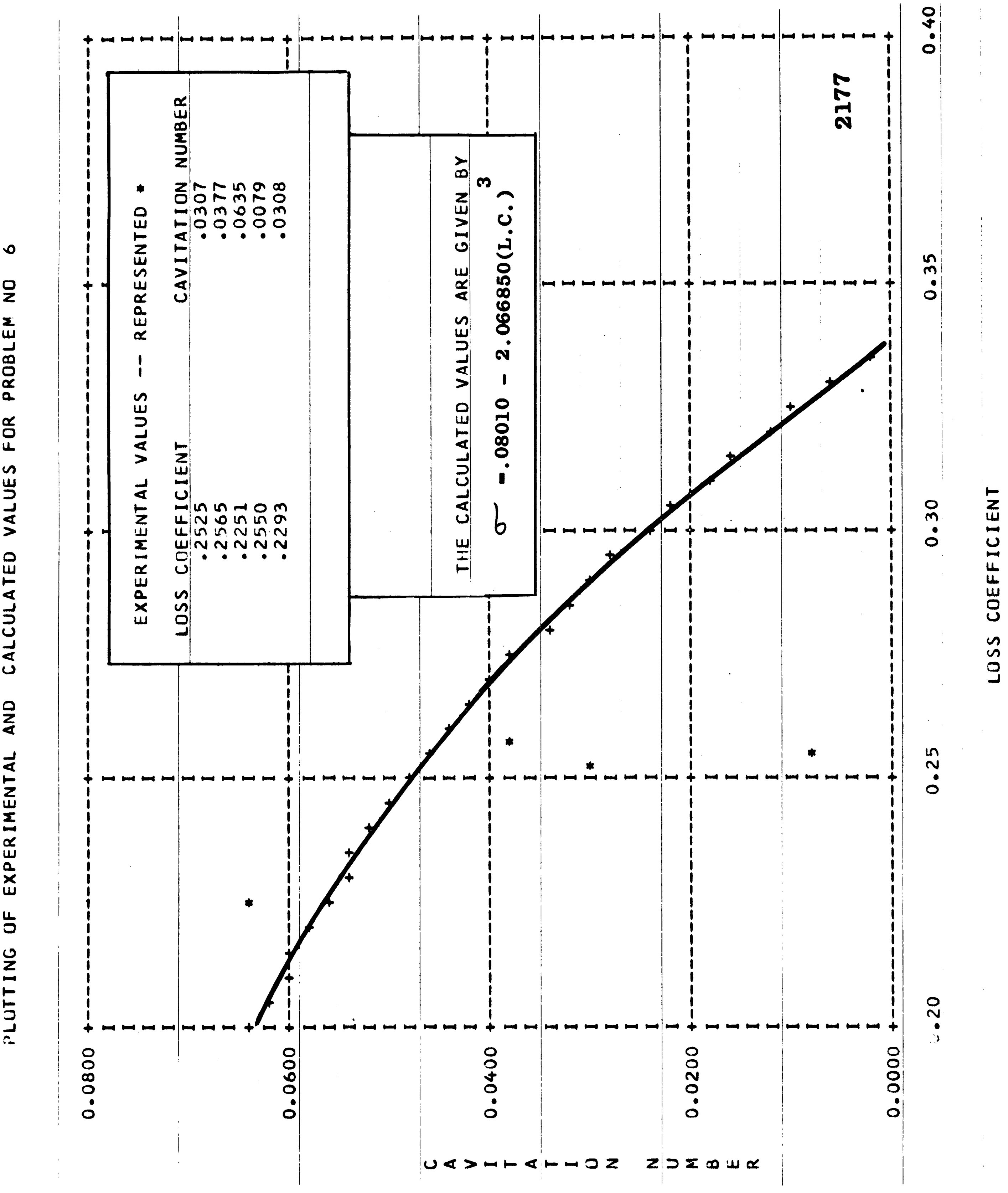
PLOTTING OF EXPERIMENTAL AND CALCULATED VALUES FOR PROBLEM NO 6
EXPERIMENTAL VALUES -- REPRESENTED *
LOSS COEFFICIENT CAVITATION NUMBER
.2525 .0307
.2565 .0377
.2251 .0635
.2550 .0079
.2293 .0308
THE CALCULATED VALUES ARE GIVEN BY
σ =.08010 - 2.066850(L.C.)^3
2177
0.0800
0.0600
0.0400
0.0200
0.0000
CAVITATION NUMBER
0.20
0.25
0.30
0.35
0.40
LOSS COEFFICIENT

PLOTTING OF EXPERIMENTAL AND CALCULATED VALUES FOR PROBLEM NO 7

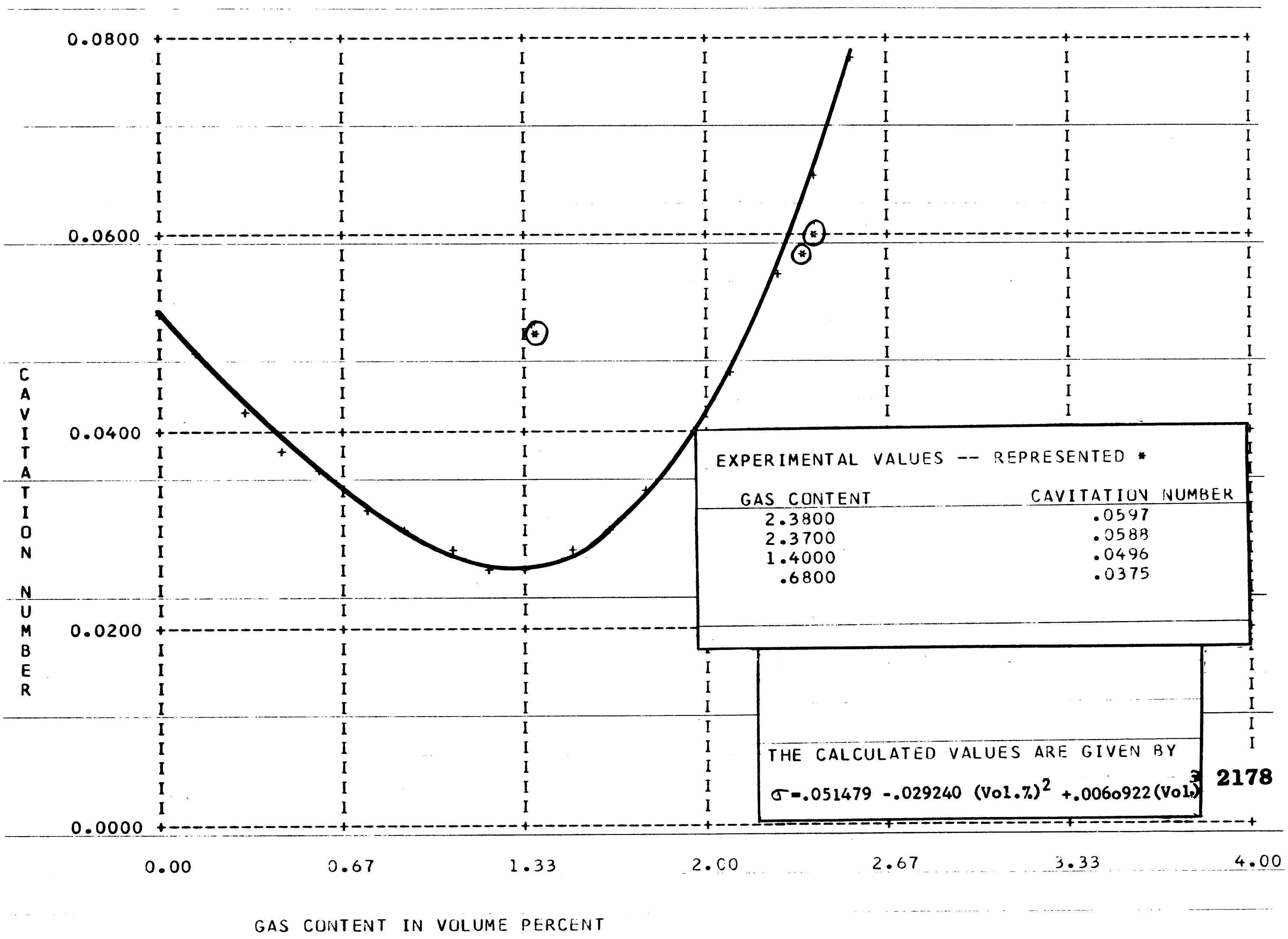

PLOTTING OF EXPERIMENTAL AND CALCULATED VALUES FOR PROBLEM NO 8

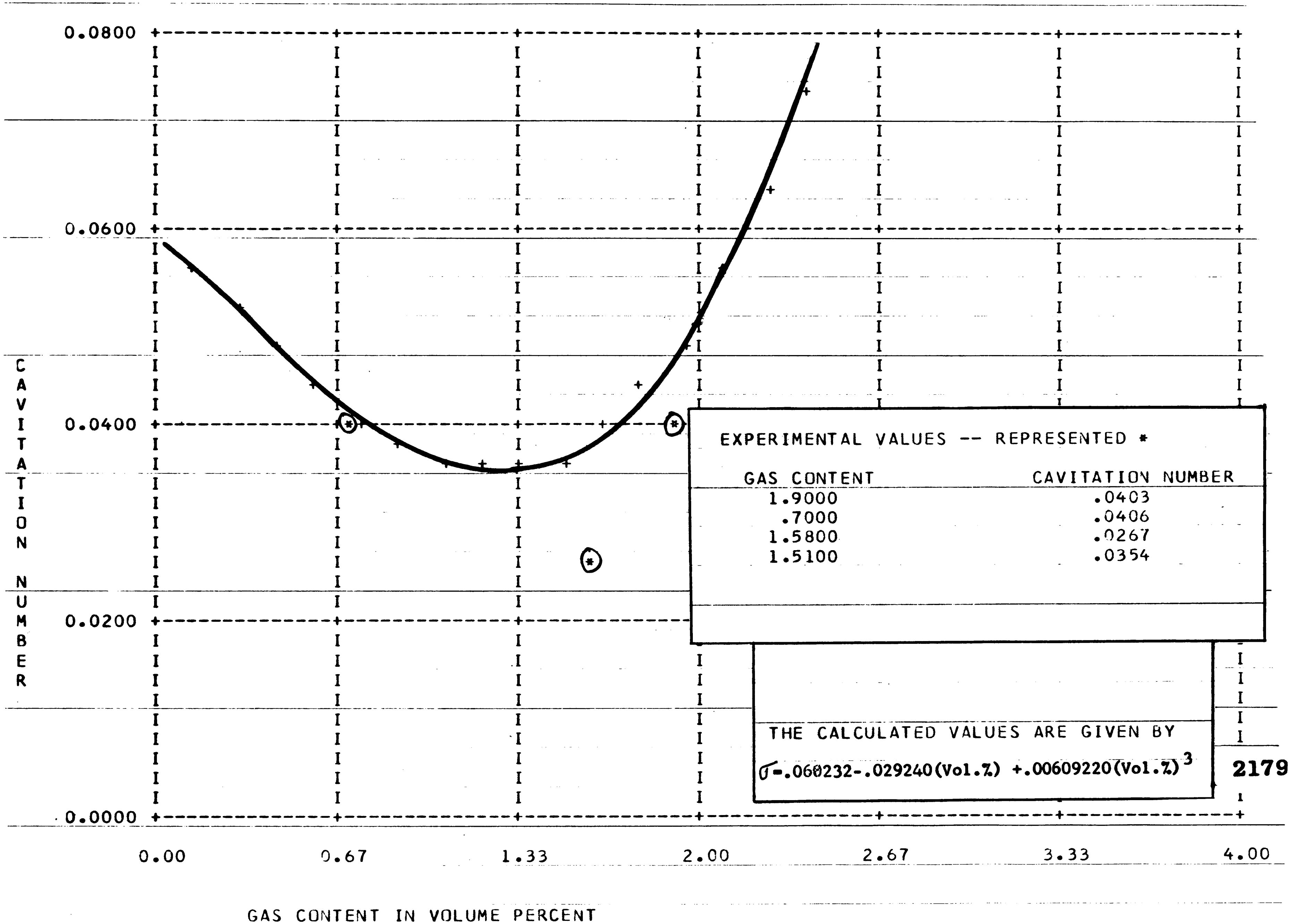

EXPERIMENTAL VALUES -- REPRESENTED *

GAS CONTENT	CAVITATION NUMBER
1.9000	.0403
.7000	.0406
1.5800	.0267
1.5100	.0354

THE CALCULATED VALUES ARE GIVEN BY

$\sigma = .060232 - .029240(\text{Vol.\%}) + .00609220(\text{Vol.\%})^3$

2179

PLOTTING OF EXPERIMENTAL AND CALCULATED VALUES FOR PROBLEM NO 9

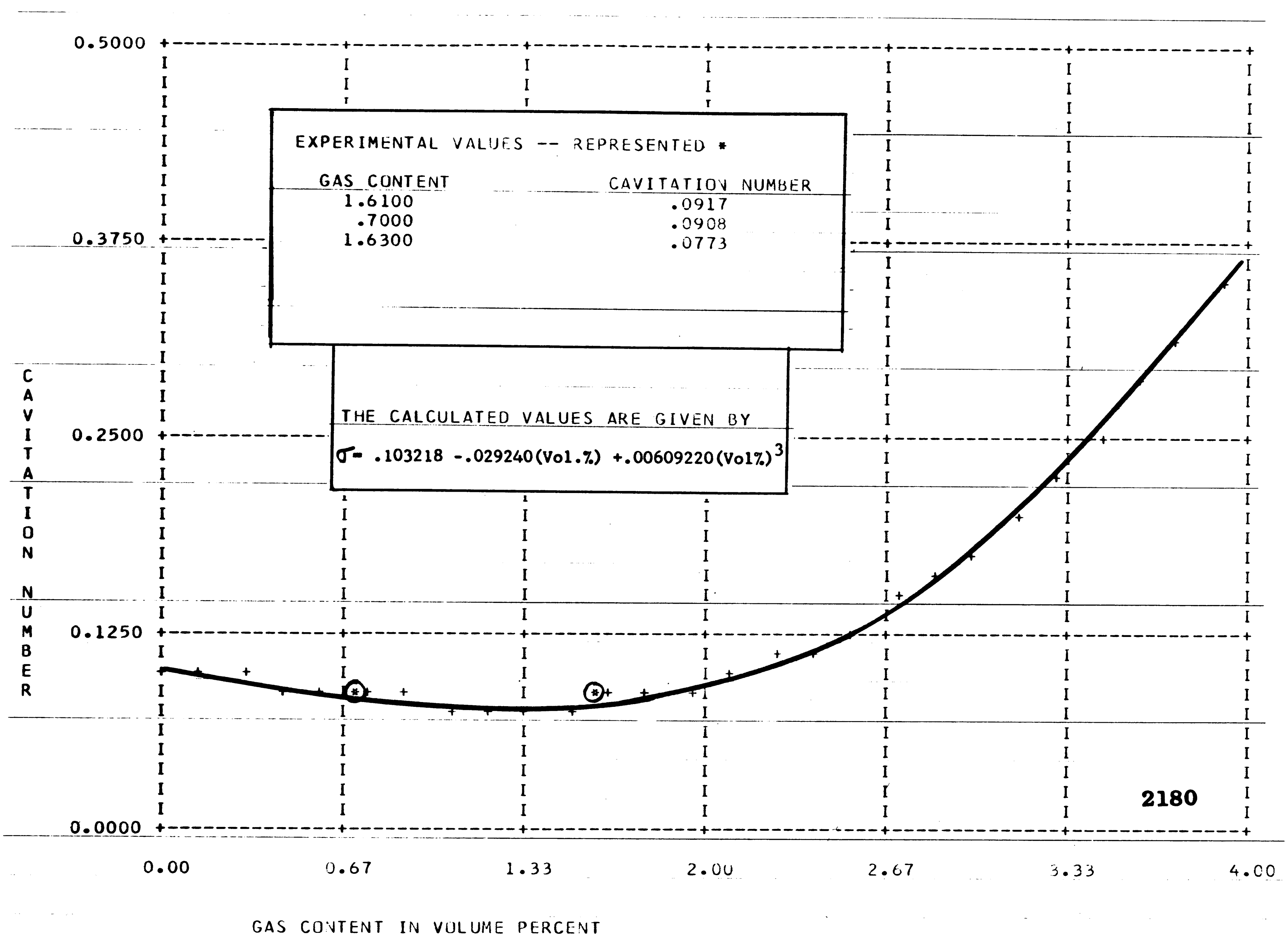

PLOTTING OF EXPERIMENTAL AND CALCULATED VALUES FOR PROBLEM NO 10

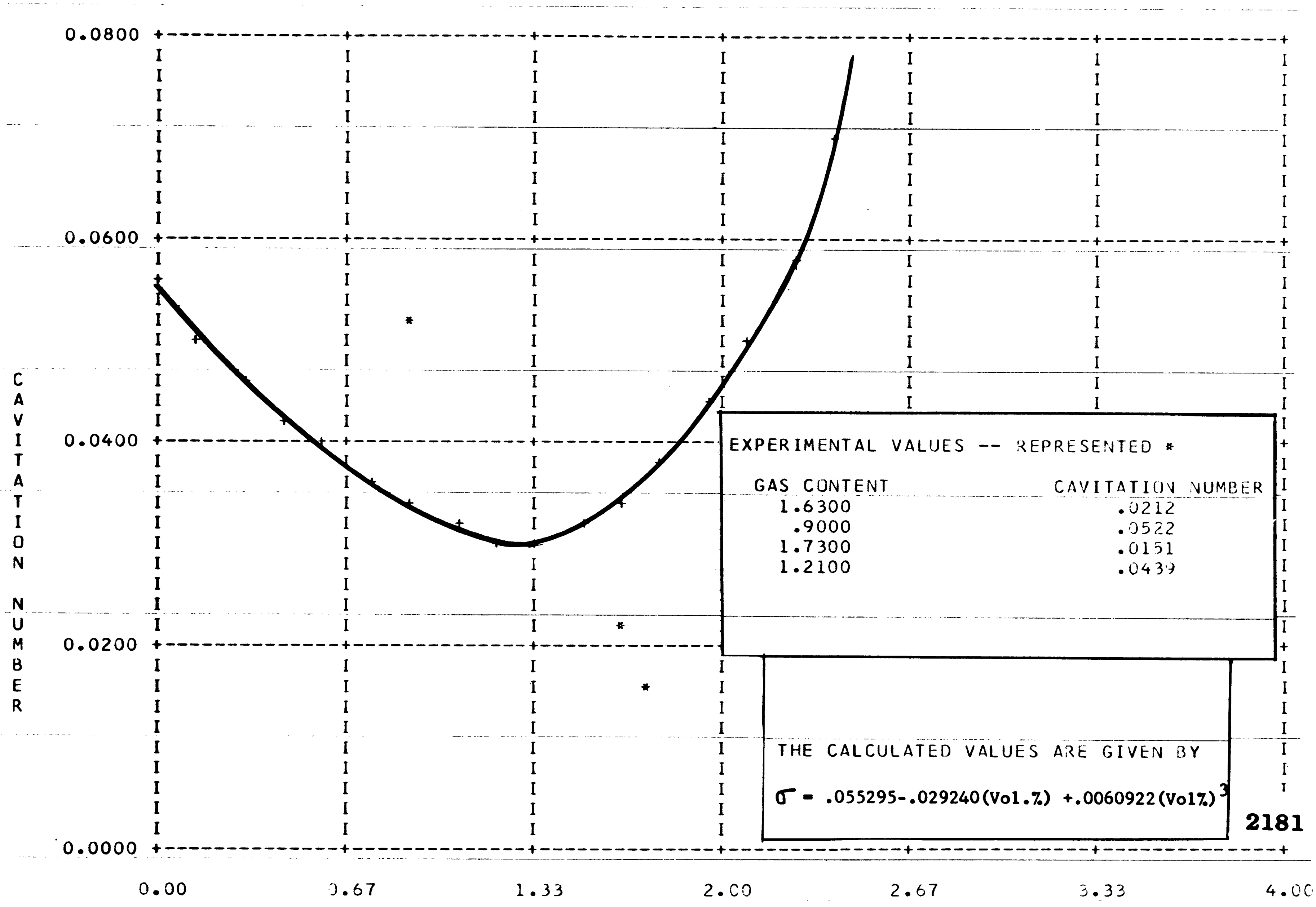

GAS CONTENT IN VOLUME PERCENT

PLOTTING OF EXPERIMENTAL AND CALCULATED VALUES FOR PROBLEM NO 11

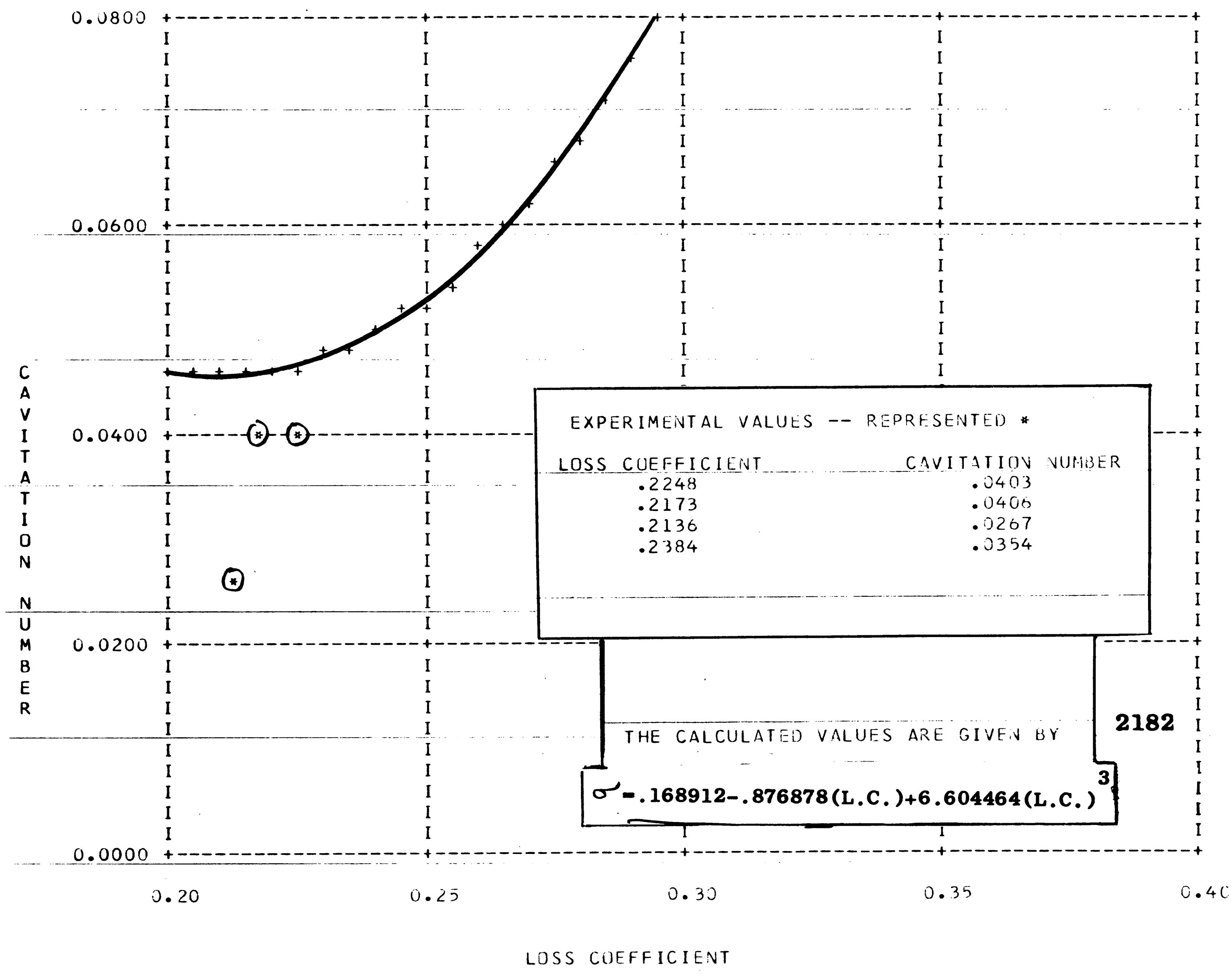

EXPERIMENTAL VALUES -- REPRESENTED *

LOSS COEFFICIENT	CAVITATION NUMBER
.2248	.0403
.2173	.0406
.2136	.0267
.2384	.0354

THE CALCULATED VALUES ARE GIVEN BY

$$\sigma = .168912 - .876878(L.C.) + 6.604464(L.C.)^3$$

2182

PLOTTING OF EXPERIMENTAL AND CALCULATED VALUES FOR PROBLEM NC 12

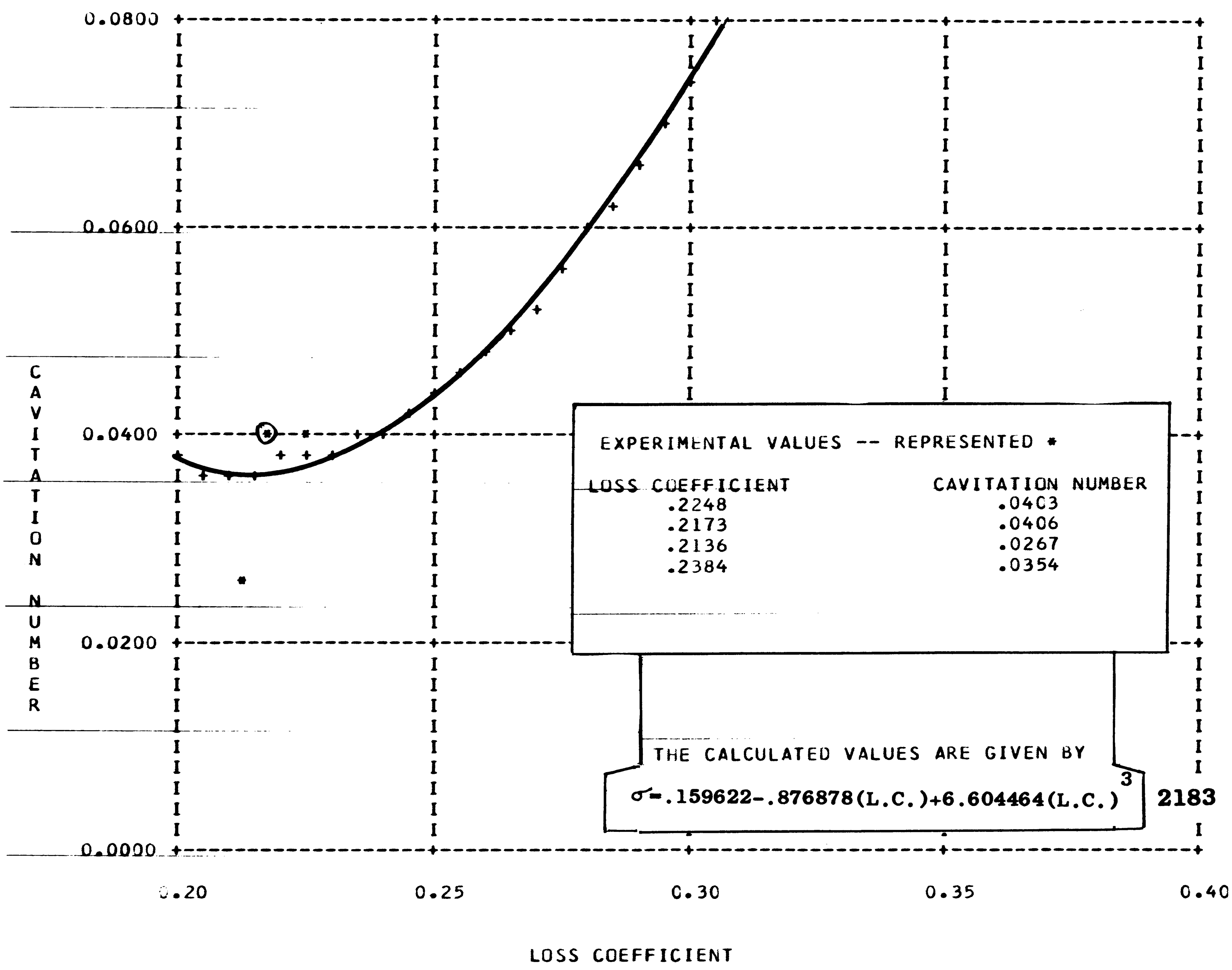

PLOTTING OF EXPERIMENTAL AND CALCULATED VALUES FOR PROBLEM NO 13

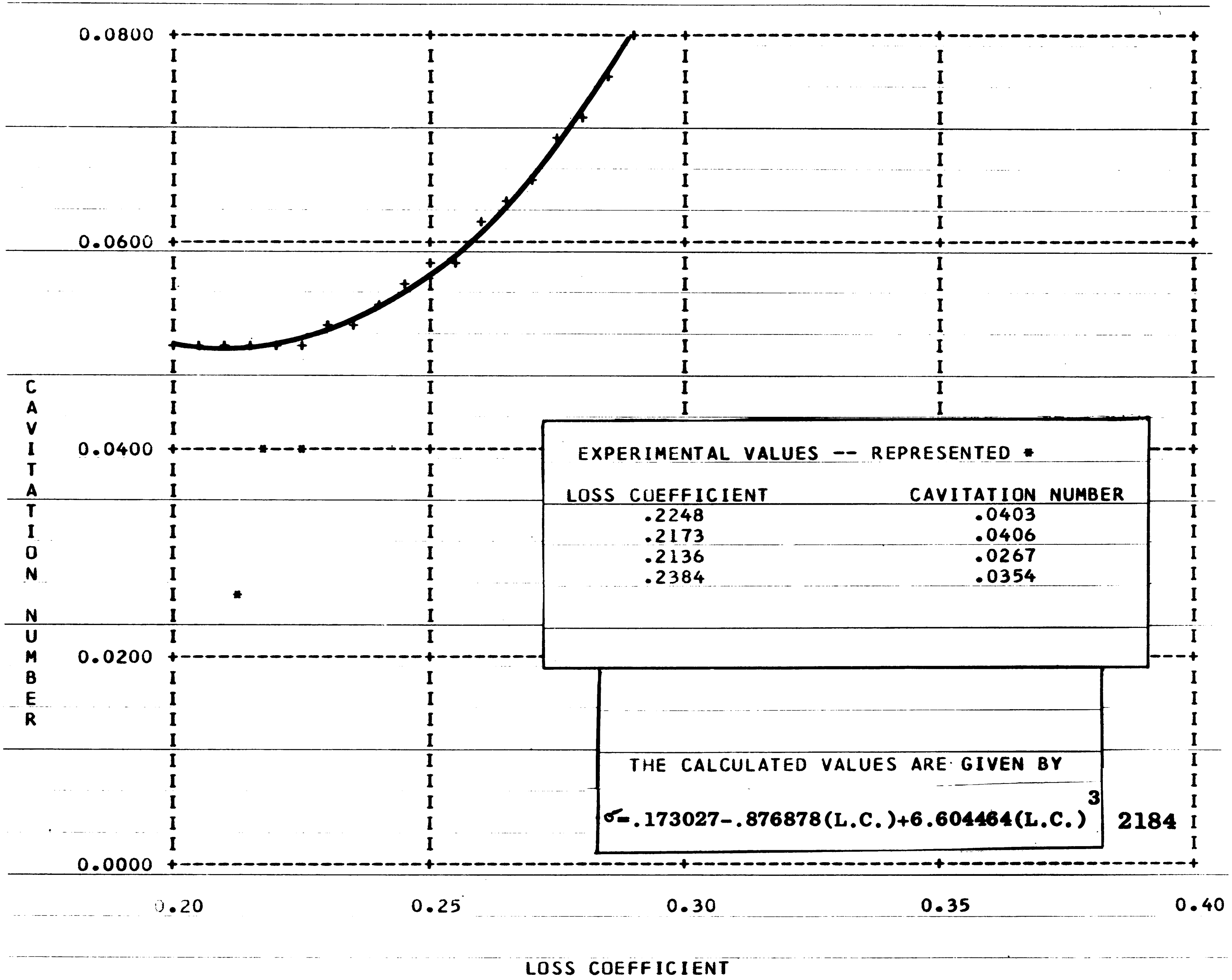

PLOTTING OF EXPERIMENTAL AND CALCULATED VALUES FOR PROBLEM NO 14

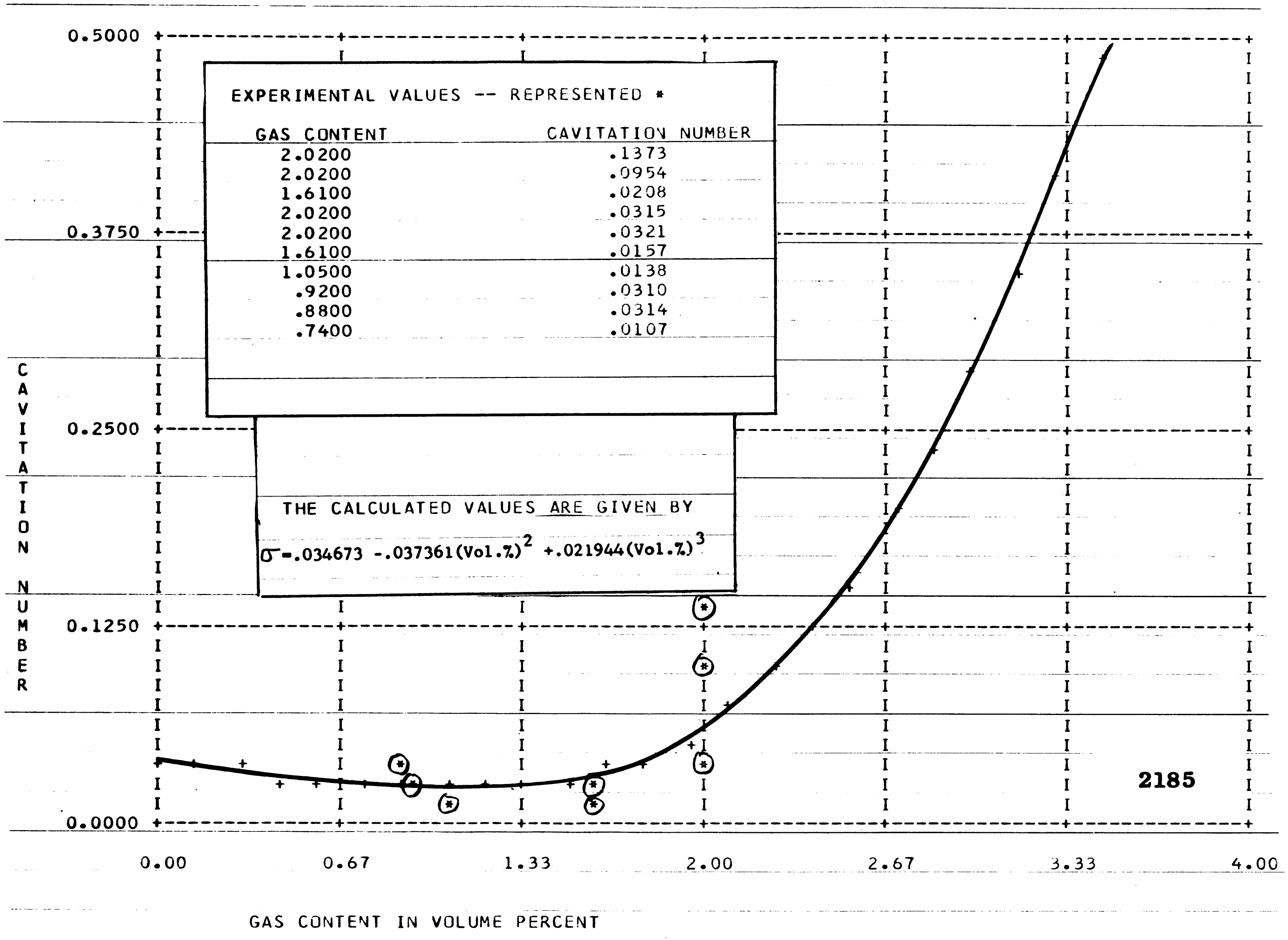

EXPERIMENTAL VALUES -- REPRESENTED *

GAS CONTENT	CAVITATION NUMBER
2.0200	.1373
2.0200	.0954
1.6100	.0208
2.0200	.0315
2.0200	.0321
1.6100	.0157
1.0500	.0138
.9200	.0310
.8800	.0314
.7400	.0107

THE CALCULATED VALUES ARE GIVEN BY

$$\sigma = .034673 - .037361(\text{Vol.\%})^2 + .021944(\text{Vol.\%})^3$$

PLOTTING OF EXPERIMENTAL AND CALCULATED VALUES FOR PROBLEM NO 15

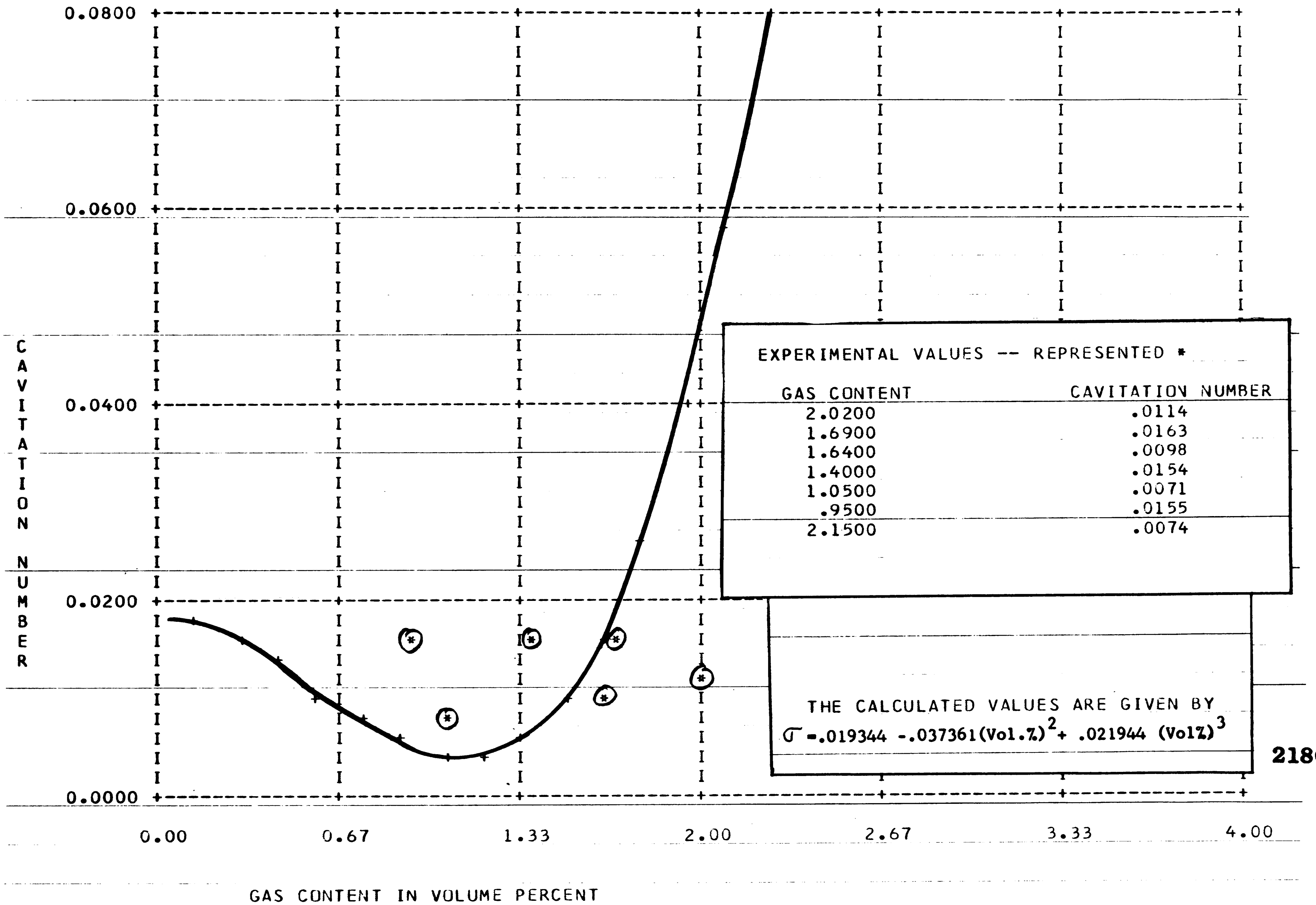

EXPERIMENTAL VALUES -- REPRESENTED *

GAS CONTENT	CAVITATION NUMBER
2.0200	.0114
1.6900	.0163
1.6400	.0098
1.4000	.0154
1.0500	.0071
.9500	.0155
2.1500	.0074

THE CALCULATED VALUES ARE GIVEN BY

$\sigma = .019344 - .037361(Vol.\%)^2 + .021944\ (Vol\%)^3$

2186

PLOTTING OF EXPERIMENTAL AND CALCULATED VALUES FOR PROBLEM NO 16

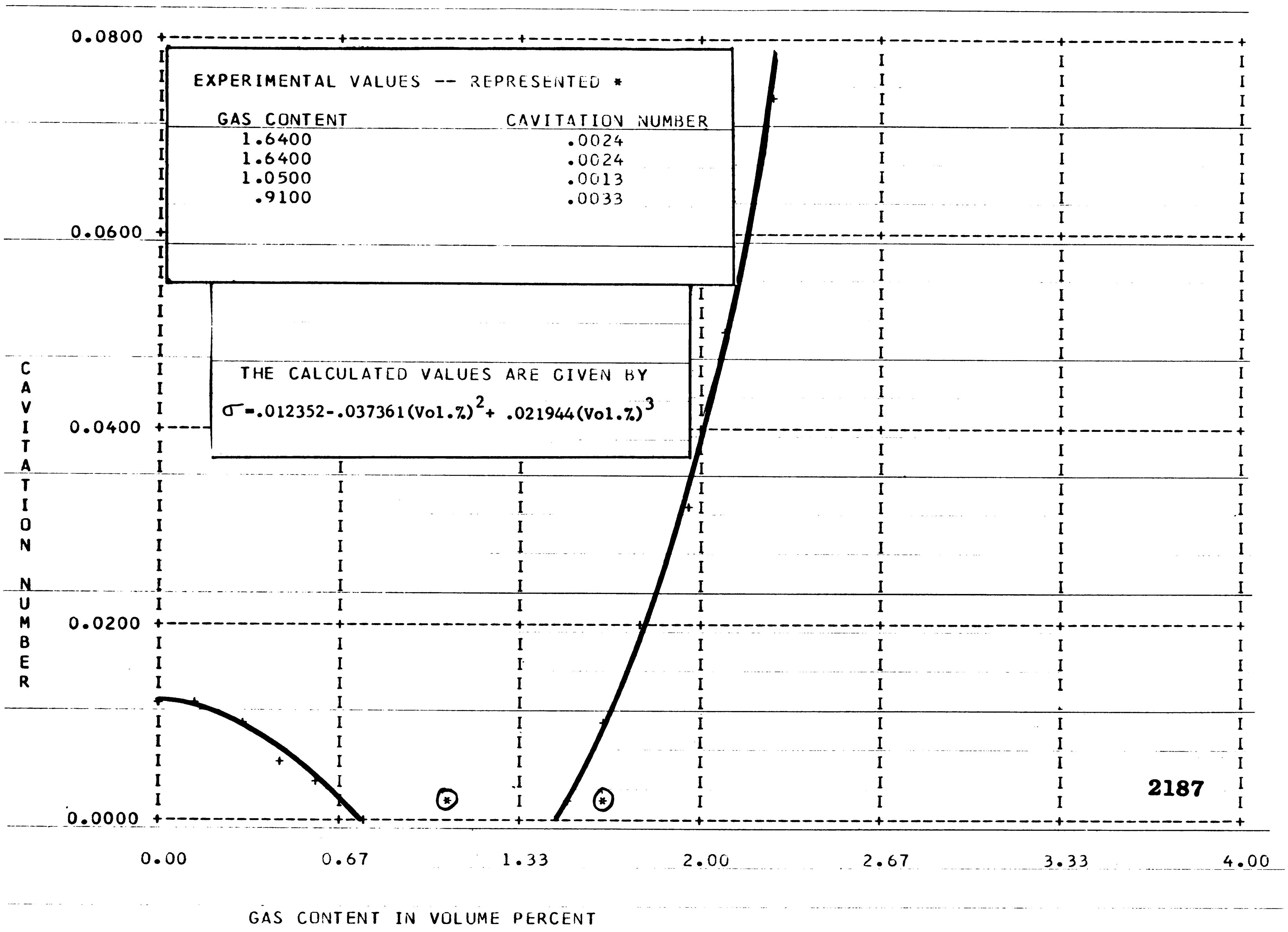

PLOTTING OF EXPERIMENTAL AND CALCULATED VALUES FOR PROBLEM NO 17

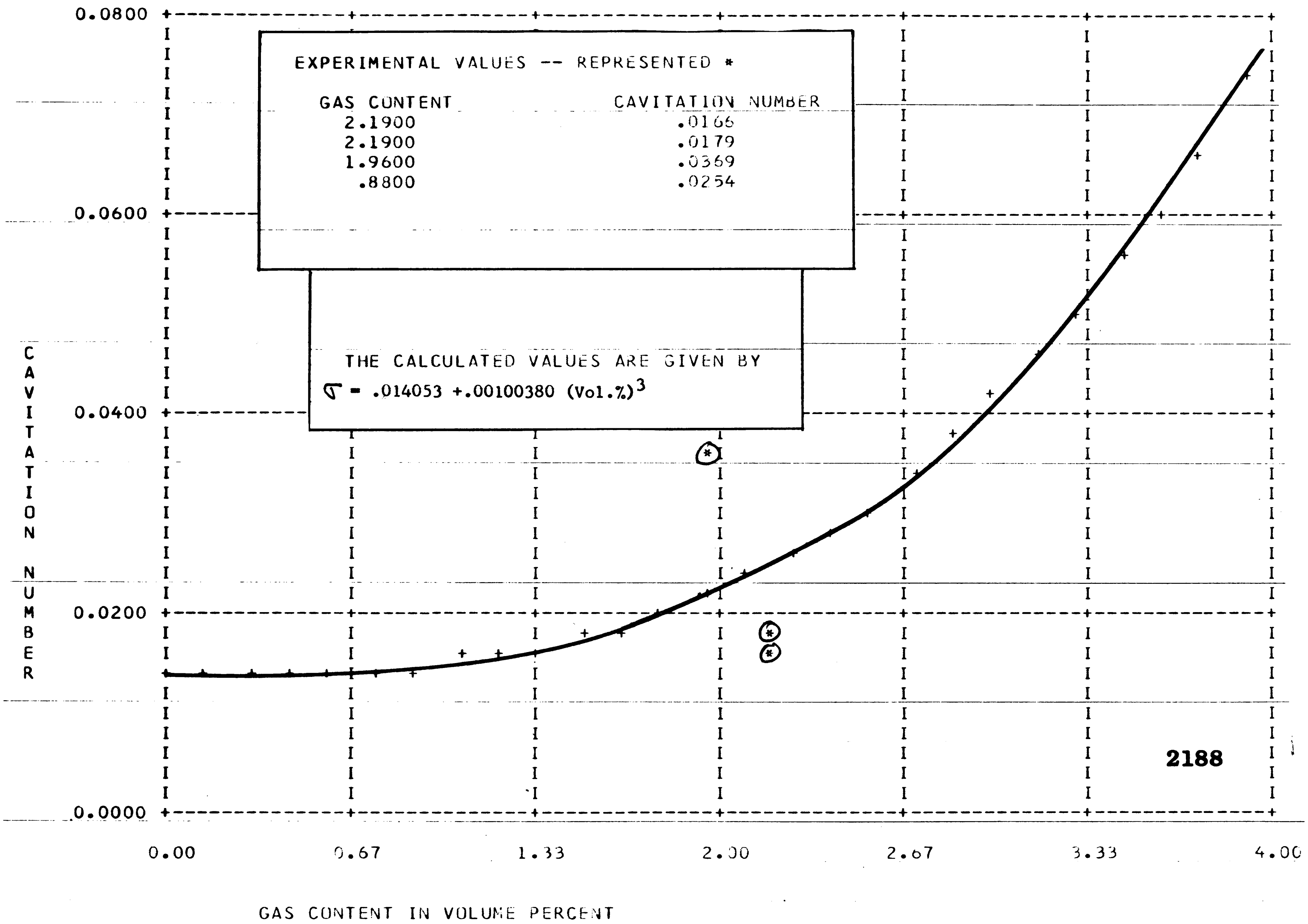

PLOTTING OF EXPERIMENTAL AND CALCULATED VALUES FOR PROBLEM NO 18

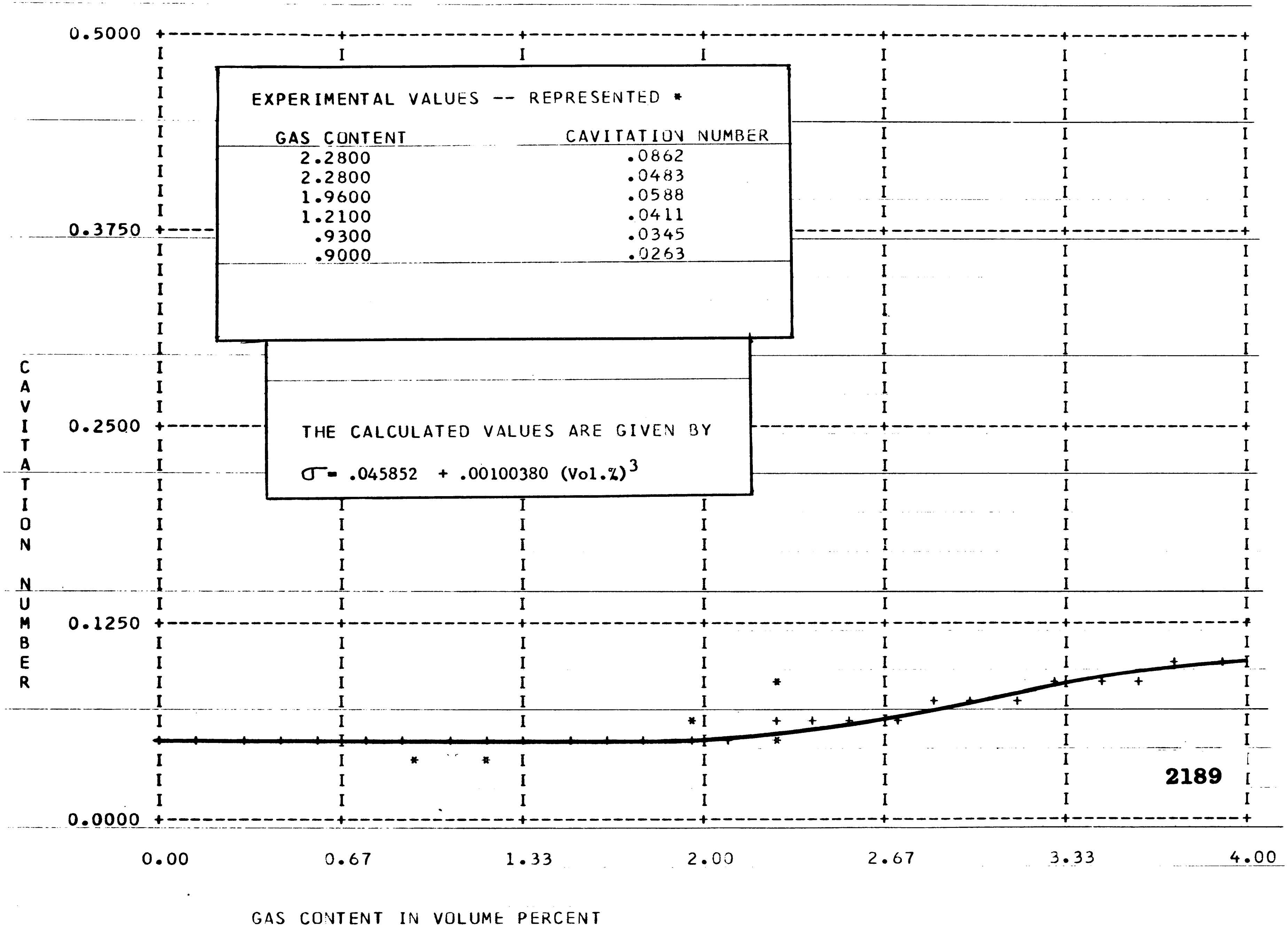

EXPERIMENTAL VALUES -- REPRESENTED *

GAS CONTENT	CAVITATION NUMBER
2.2800	.0862
2.2800	.0483
1.9600	.0588
1.2100	.0411
.9300	.0345
.9000	.0263

THE CALCULATED VALUES ARE GIVEN BY

$\sigma = .045852 + .00100380\ (\text{Vol.\%})^3$

PLOTTING OF EXPERIMENTAL AND CALCULATED VALUES FOR PROBLEM NO 19

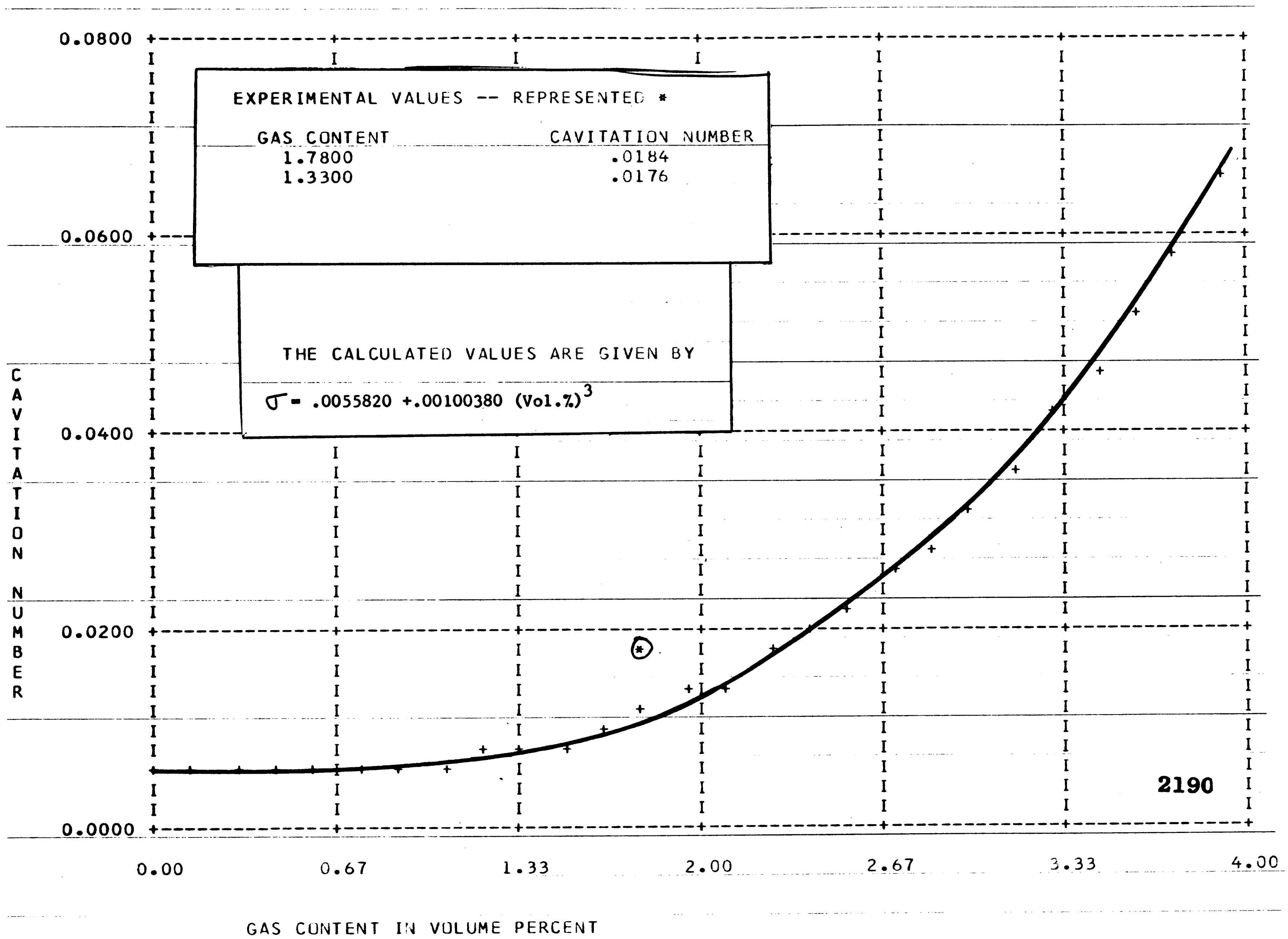

PLOTTING OF EXPERIMENTAL AND CALCULATED VALUES FOR PROBLEM NO 20

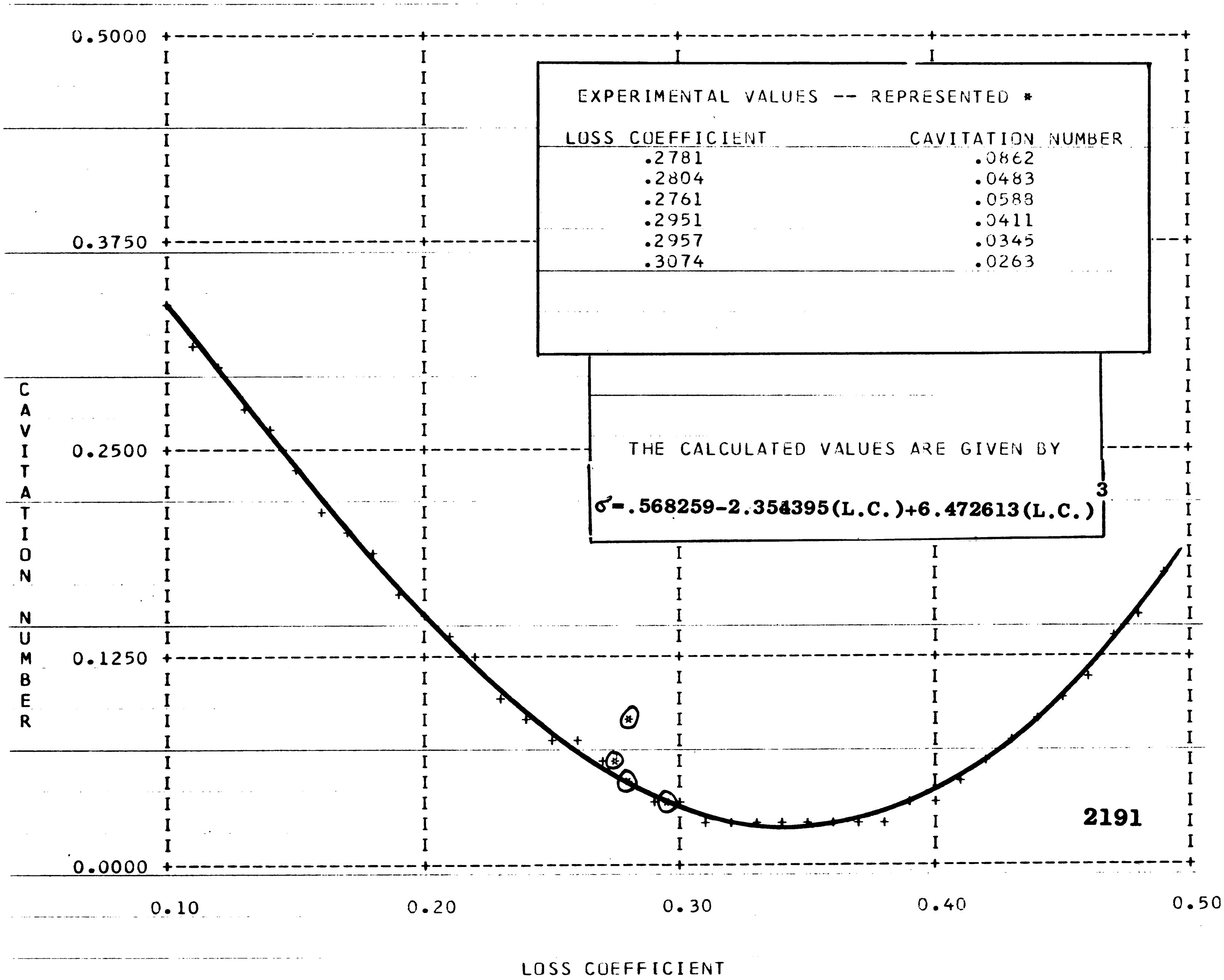

PLOTTING OF EXPERIMENTAL AND CALCULATED VALUES FOR PROBLEM NO 21

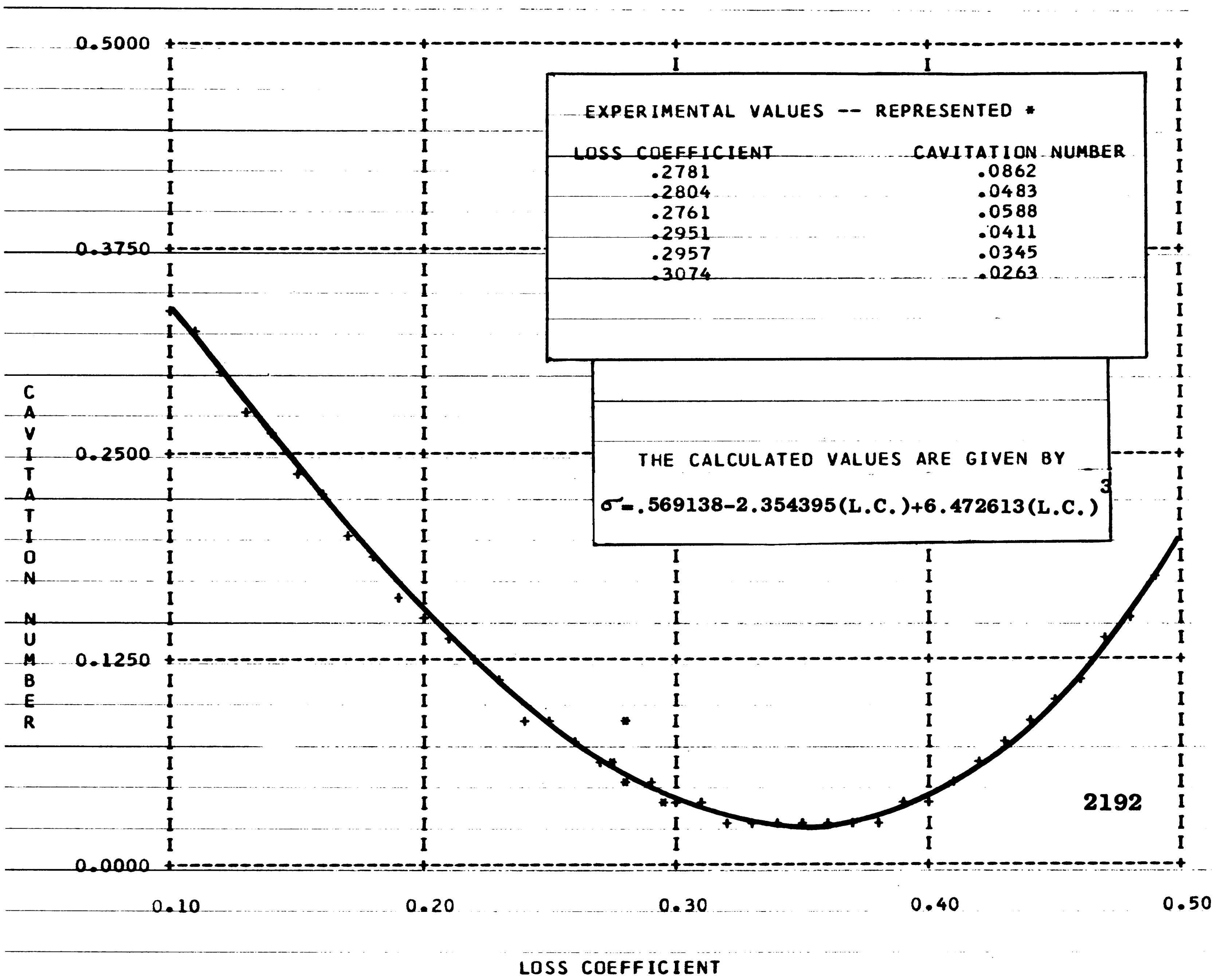

EXPERIMENTAL VALUES -- REPRESENTED *

LOSS COEFFICIENT	CAVITATION NUMBER
.2781	.0862
.2804	.0483
.2761	.0588
.2951	.0411
.2957	.0345
.3074	.0263

THE CALCULATED VALUES ARE GIVEN BY

$$\sigma = .569138 - 2.354395(L.C.) + 6.472613(L.C.)^3$$

PLOTTING OF EXPERIMENTAL AND CALCULATED VALUES FOR PROBLEM NO 22

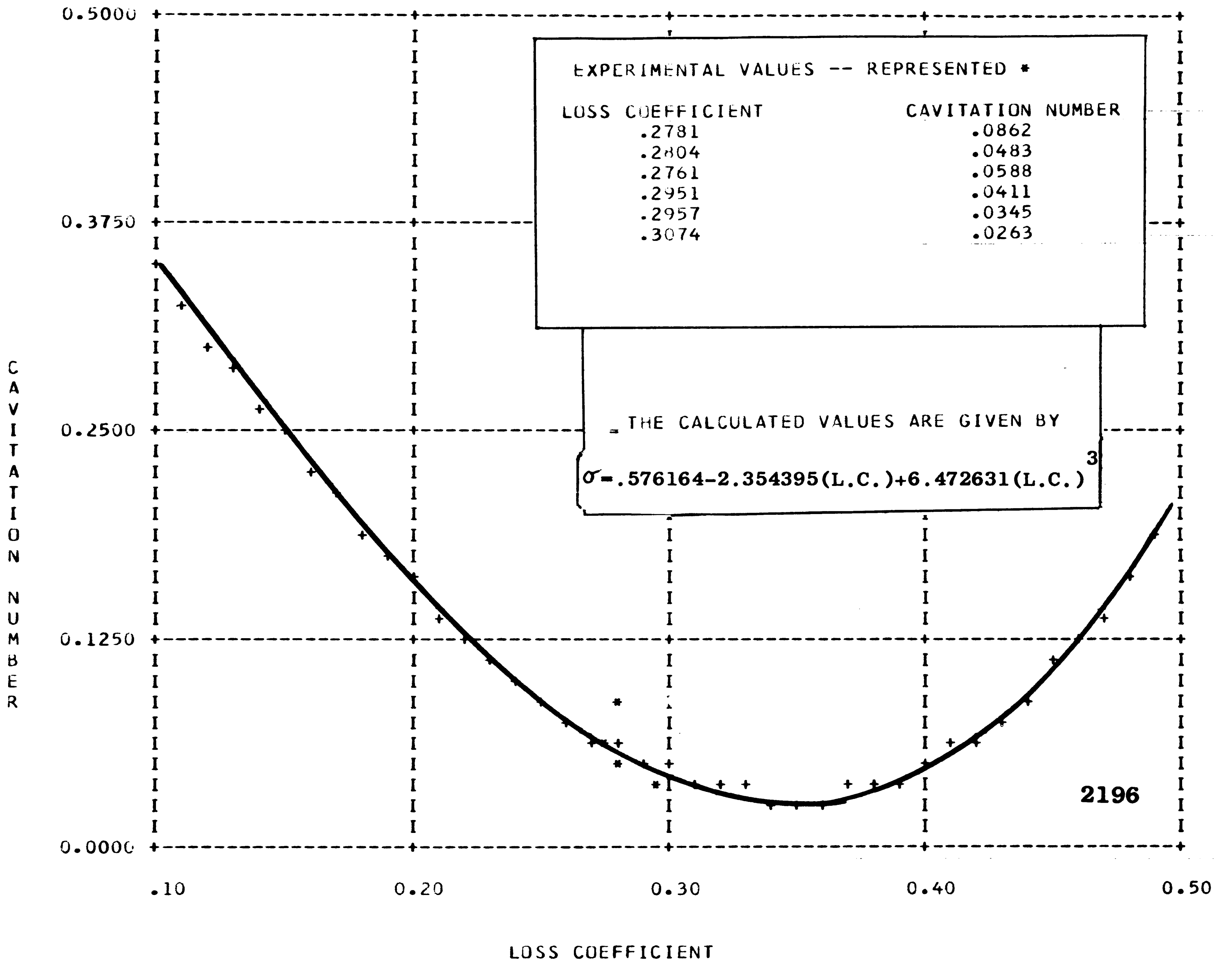

EXPERIMENTAL VALUES -- REPRESENTED *

LOSS COEFFICIENT	CAVITATION NUMBER
.2781	.0862
.2804	.0483
.2761	.0588
.2951	.0411
.2957	.0345
.3074	.0263

THE CALCULATED VALUES ARE GIVEN BY

$$\sigma = .576164 - 2.354395(L.C.) + 6.472631(L.C.)^3$$

PLOTTING OF EXPERIMENTAL AND CALCULATED VALUES FOR PROBLEM NO 23

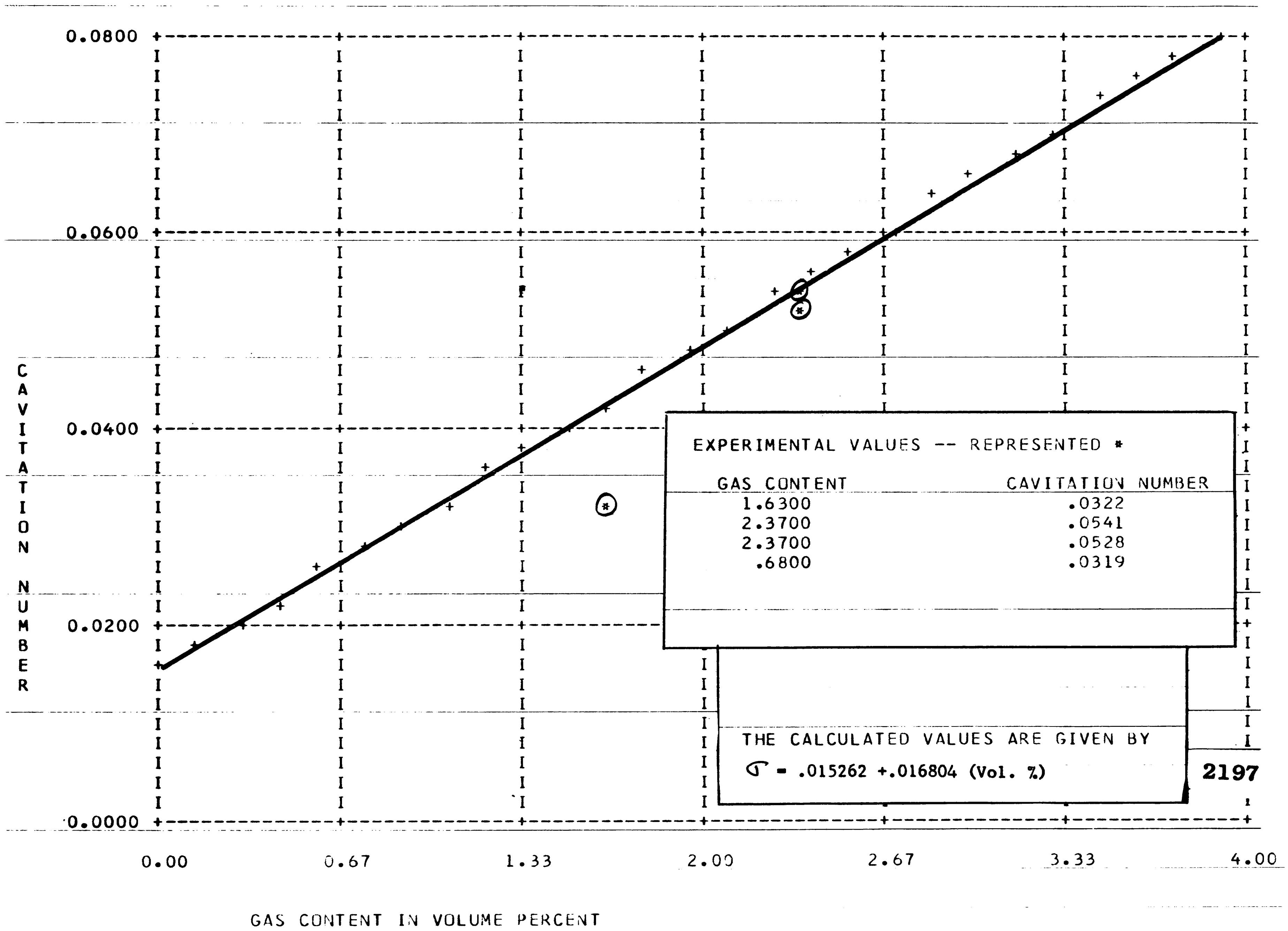

PLOTTING OF EXPERIMENTAL AND CALCULATED VALUES FOR PROBLEM NO 24

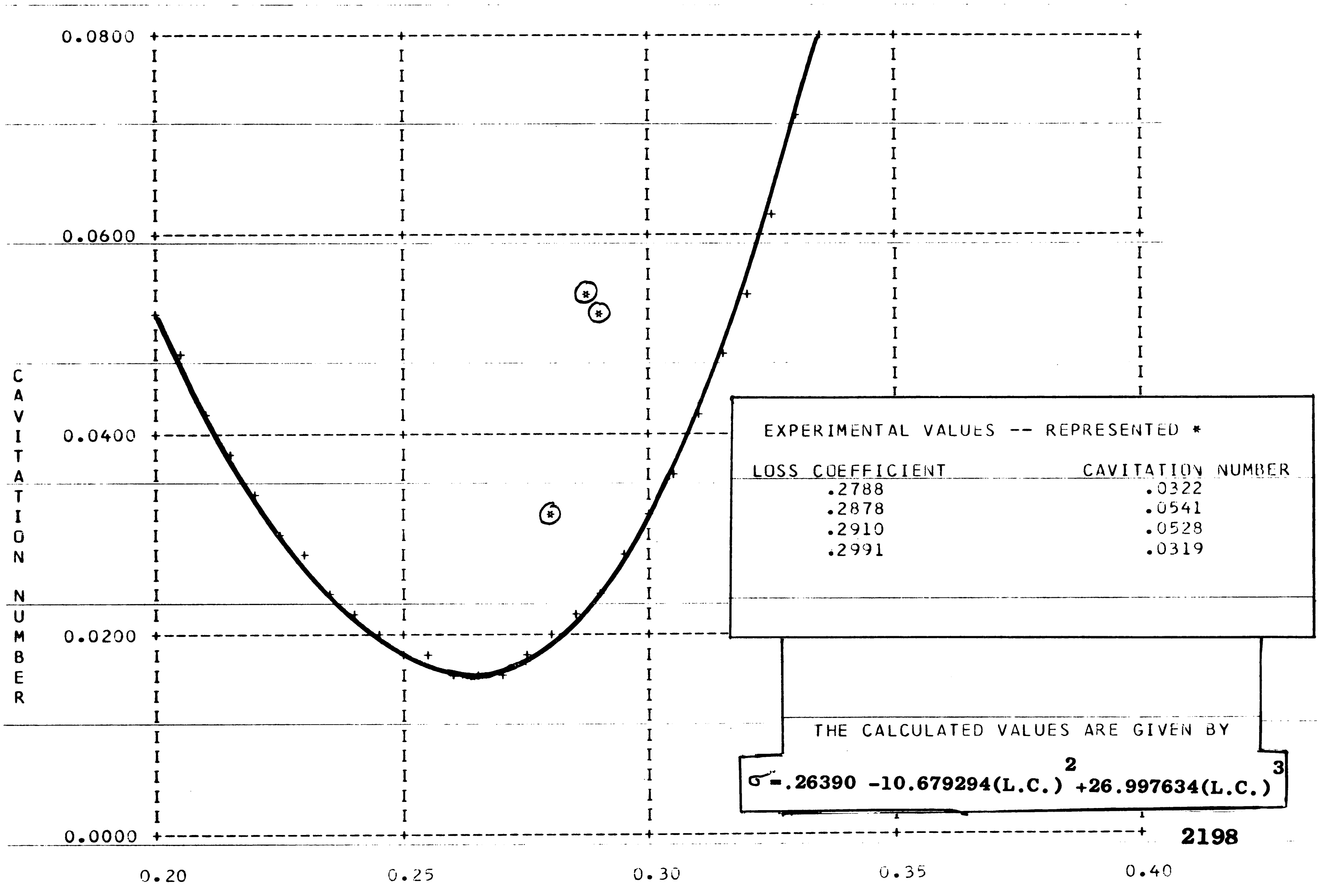

EXPERIMENTAL VALUES -- REPRESENTED *

LOSS COEFFICIENT	CAVITATION NUMBER
.2788	.0322
.2878	.0541
.2910	.0528
.2991	.0319

THE CALCULATED VALUES ARE GIVEN BY

$$\sigma = .26390 - 10.679294(L.C.)^{2} + 26.997634(L.C.)^{3}$$

2198

PLOTTING OF EXPERIMENTAL AND CALCULATED VALUES FOR PROBLEM NO 25

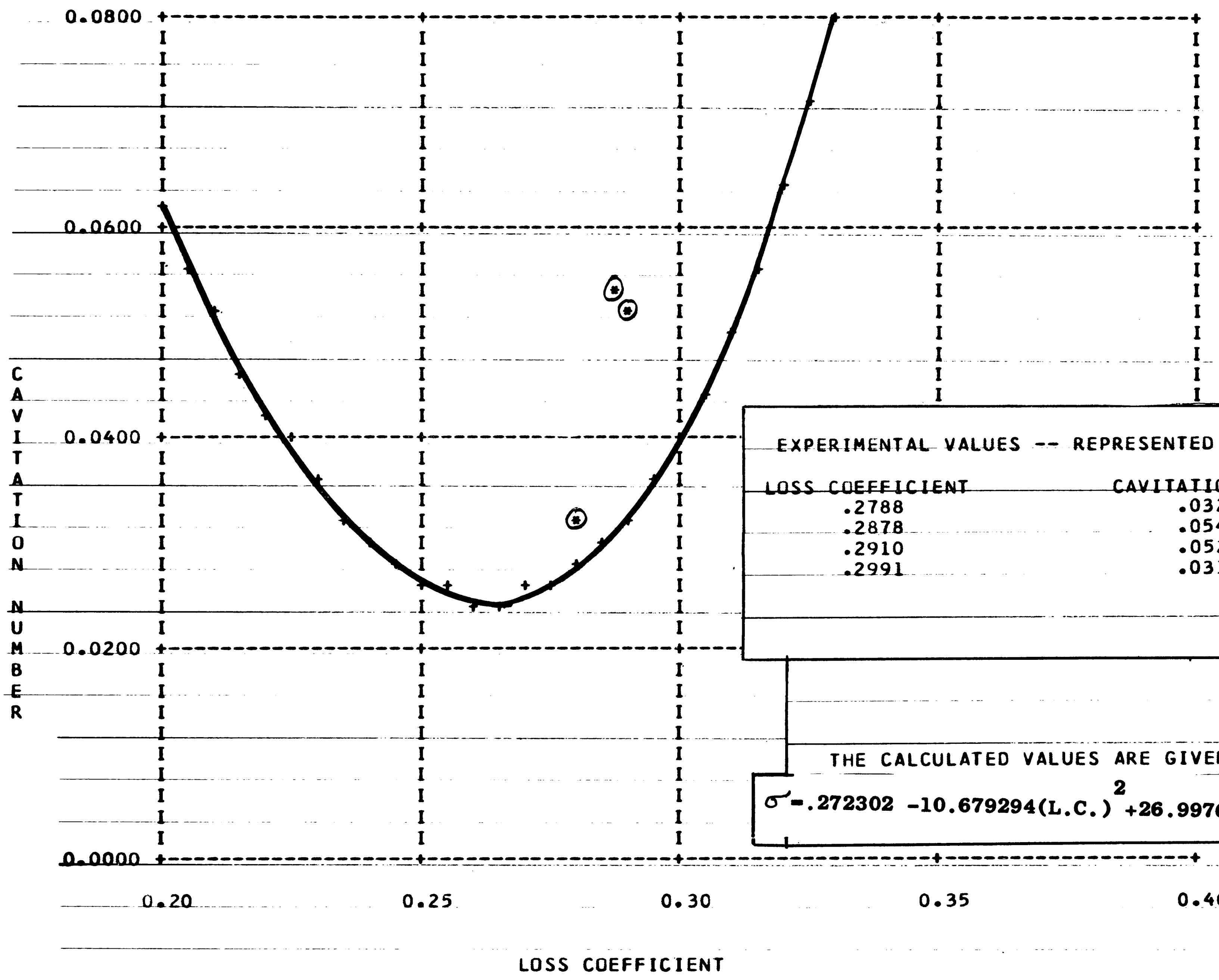

EXPERIMENTAL VALUES -- REPRESENTED *

LOSS COEFFICIENT	CAVITATION NUMBER
.2788	.0322
.2878	.0541
.2910	.0528
.2991	.0319

THE CALCULATED VALUES ARE GIVEN BY

$$\sigma = .272302 - 10.679294(L.C.)^{2} + 26.997634(L.C.)^{3}$$

2199

PLOTTING OF EXPERIMENTAL AND CALCULATED VALUES FOR PROBLEM NO 26

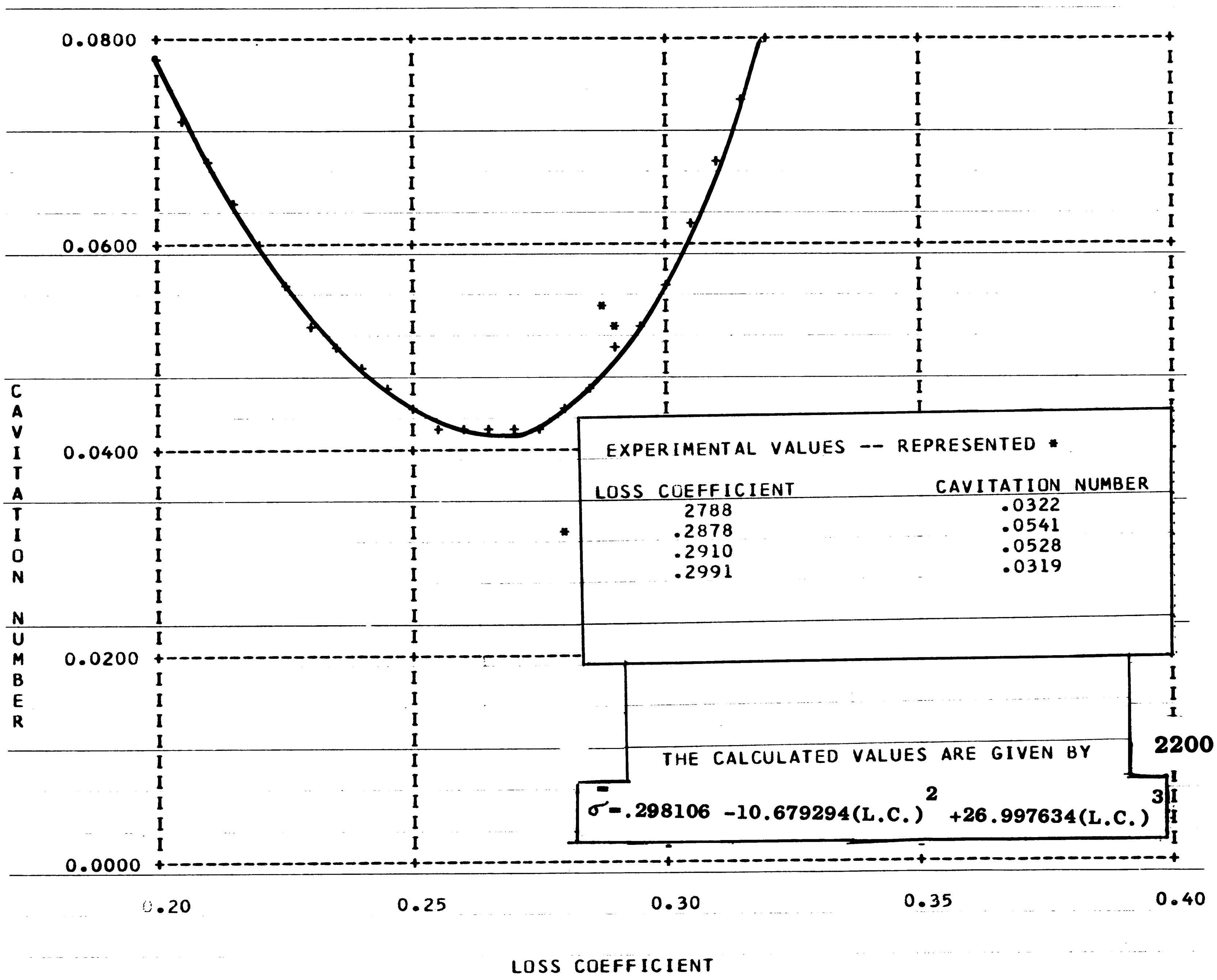

PLOTTING OF EXPERIMENTAL AND CALCULATED VALUES FOR PROBLEM NO 27

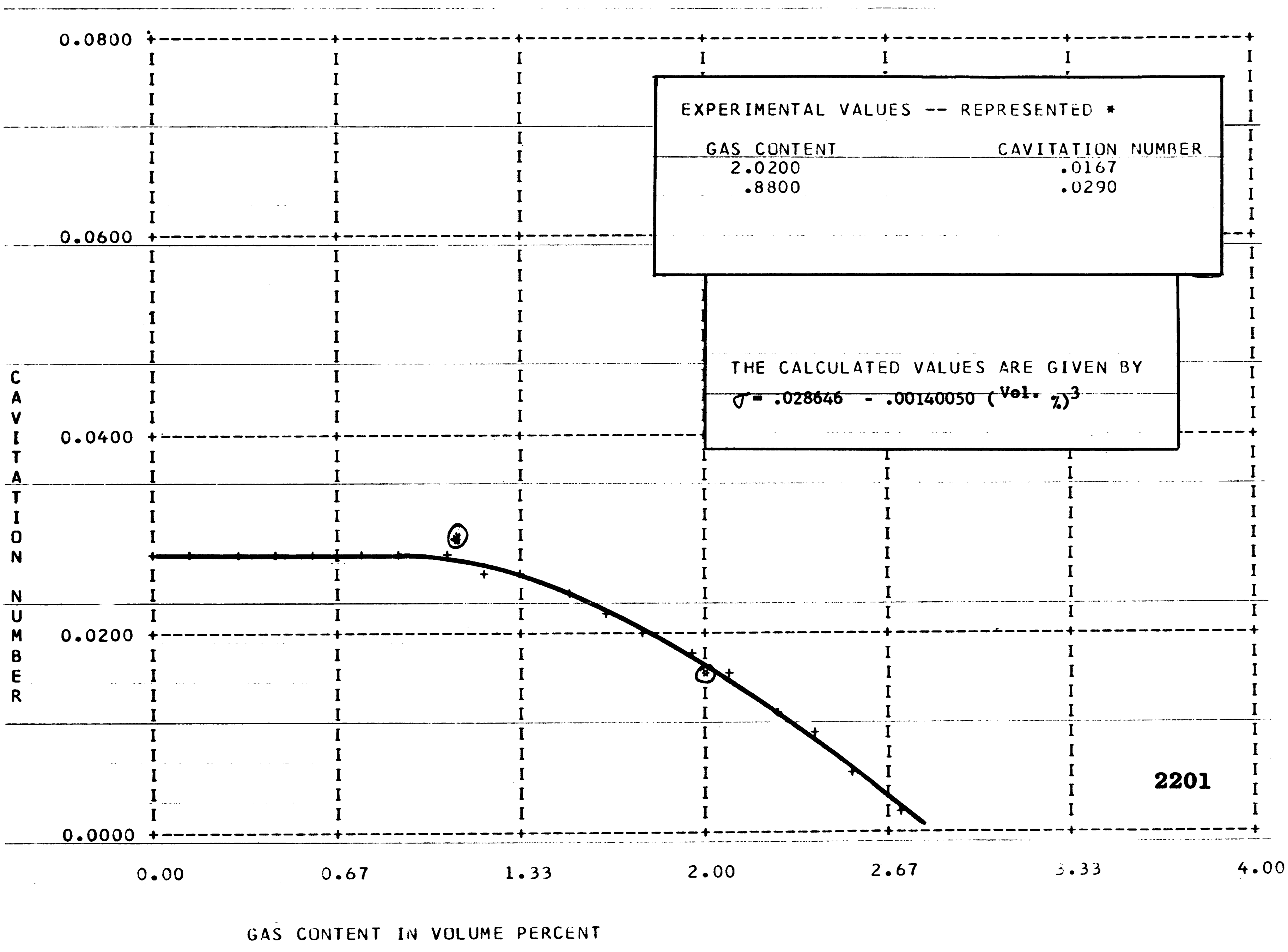

PLOTTING OF EXPERIMENTAL AND CALCULATED VALUES FOR PROBLEM NO 28

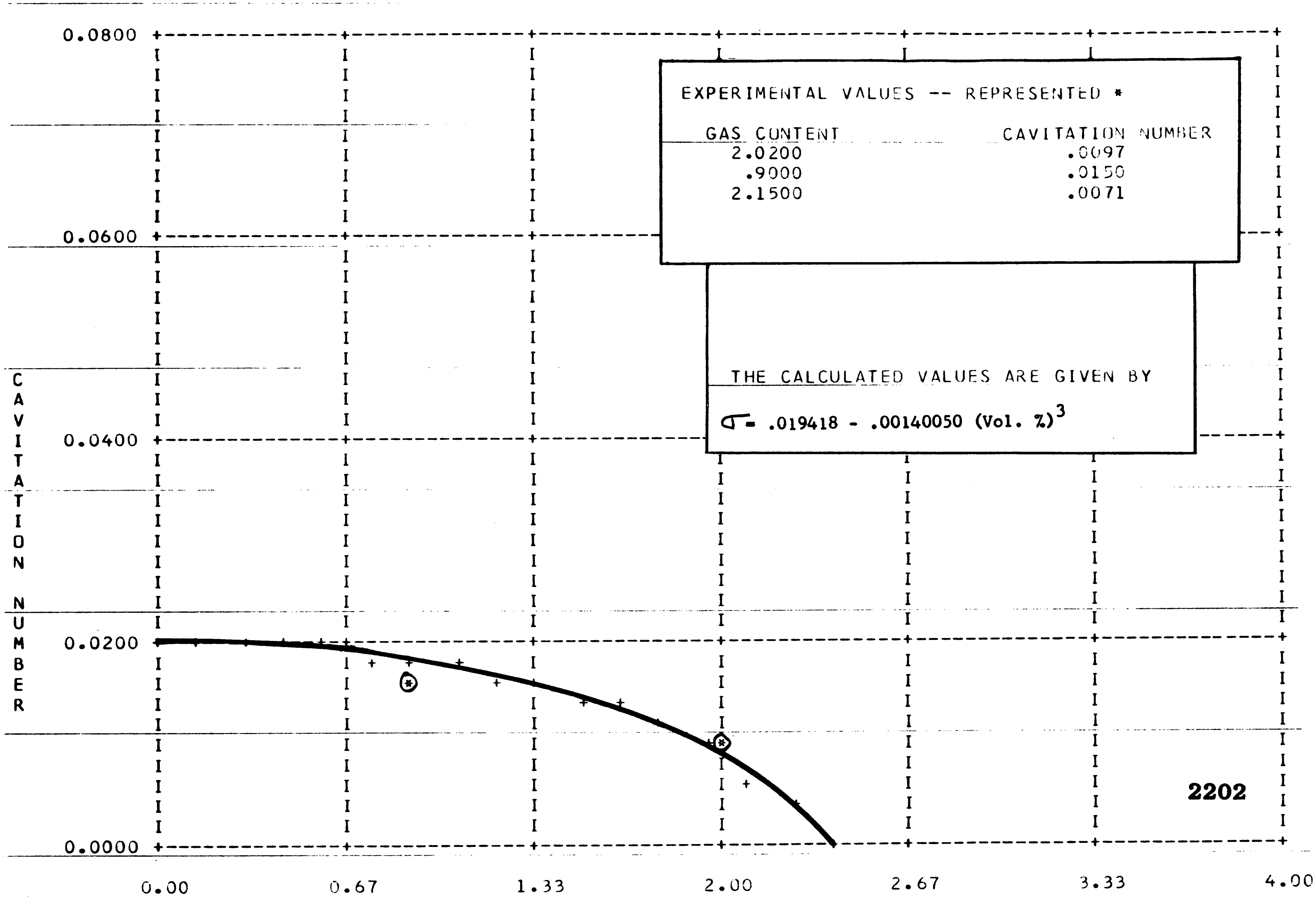

GAS CONTENT IN VOLUME PERCENT

PLOTTING OF EXPERIMENTAL AND CALCULATED VALUES FOR PROBLEM NO 29

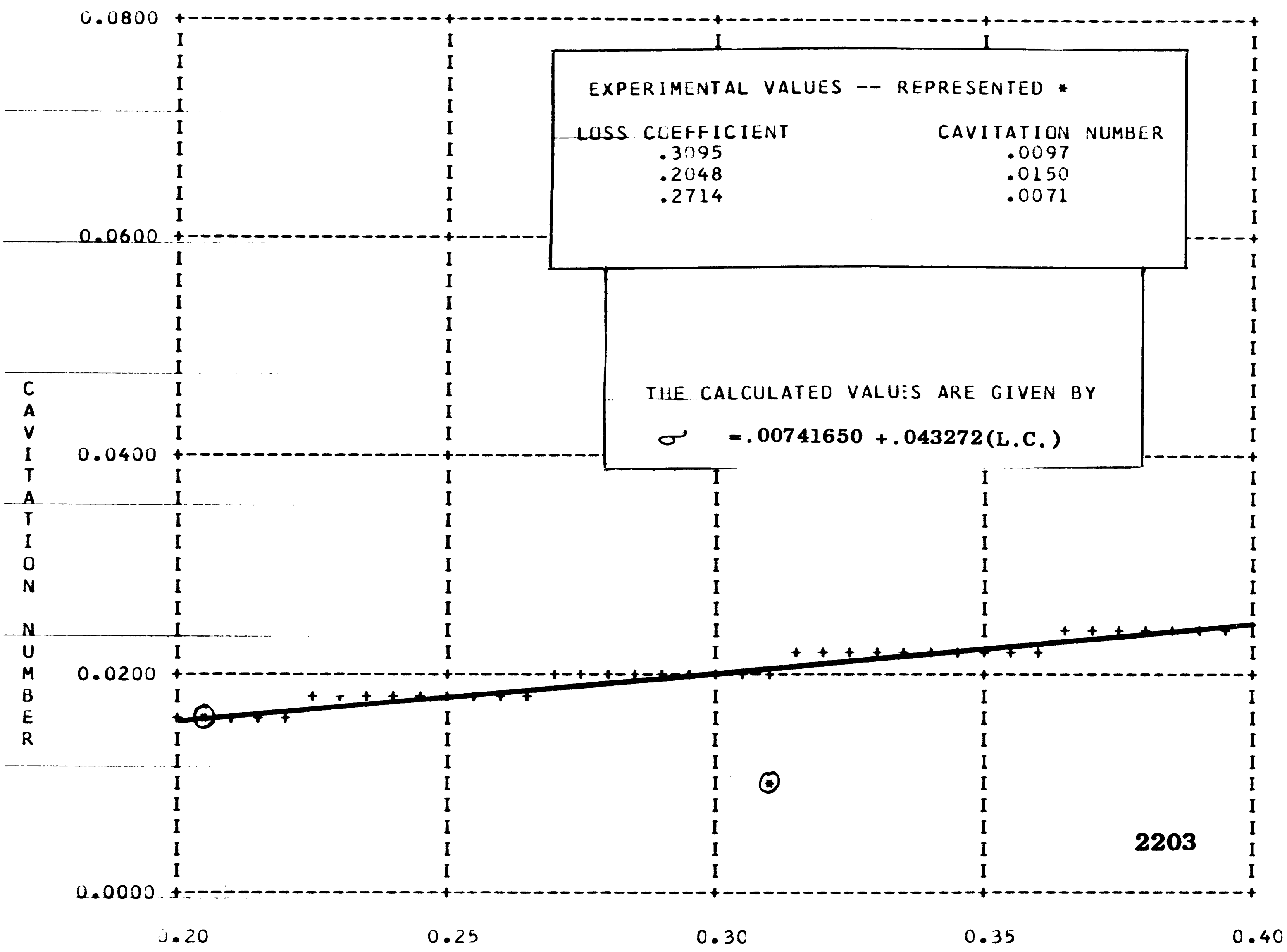

LOSS COEFFICIENT

PLOTTING OF EXPERIMENTAL AND CALCULATED VALUES FOR PROBLEM NO 30

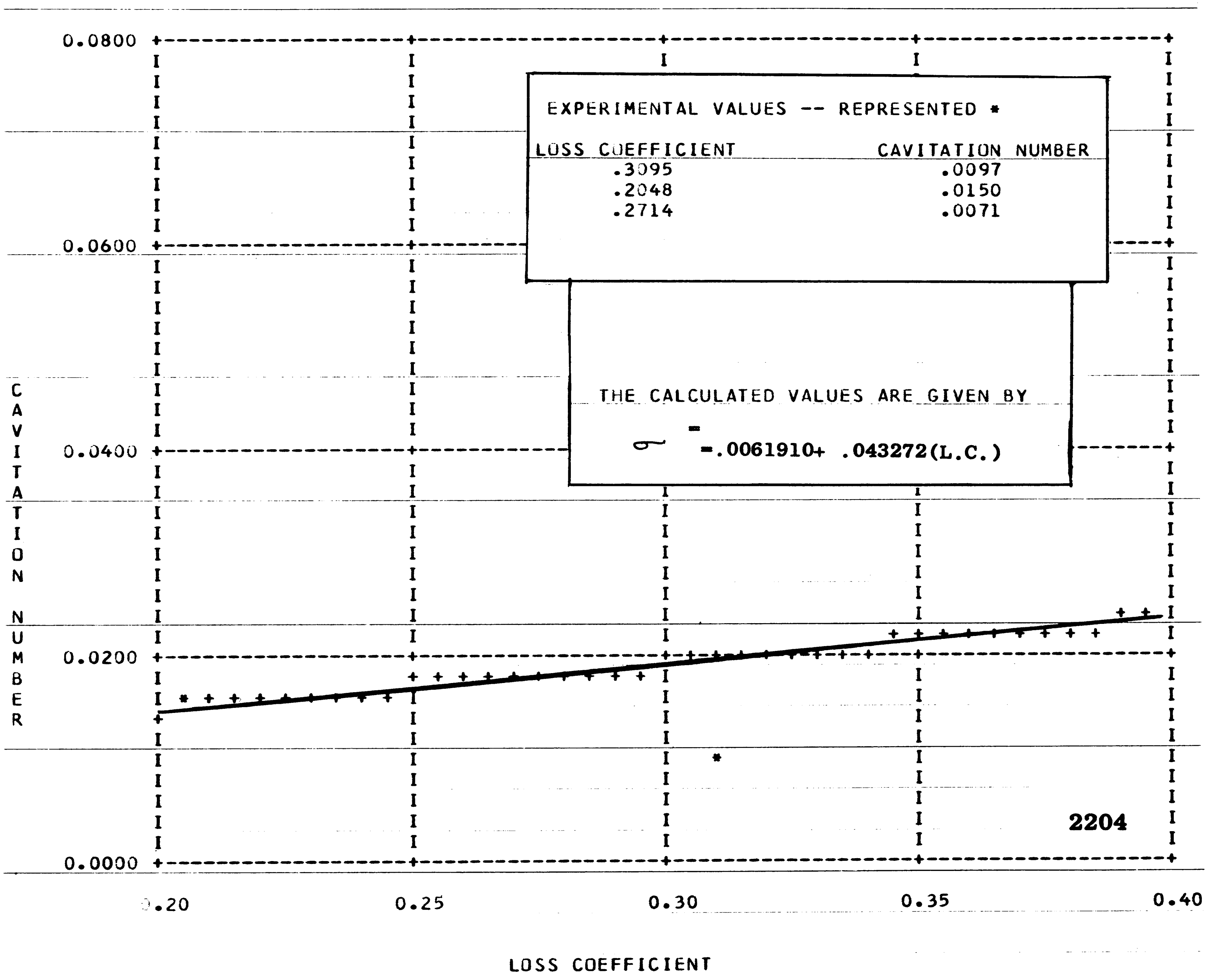

PLOTTING OF EXPERIMENTAL AND CALCULATED VALUES FOR PROBLEM NO 31

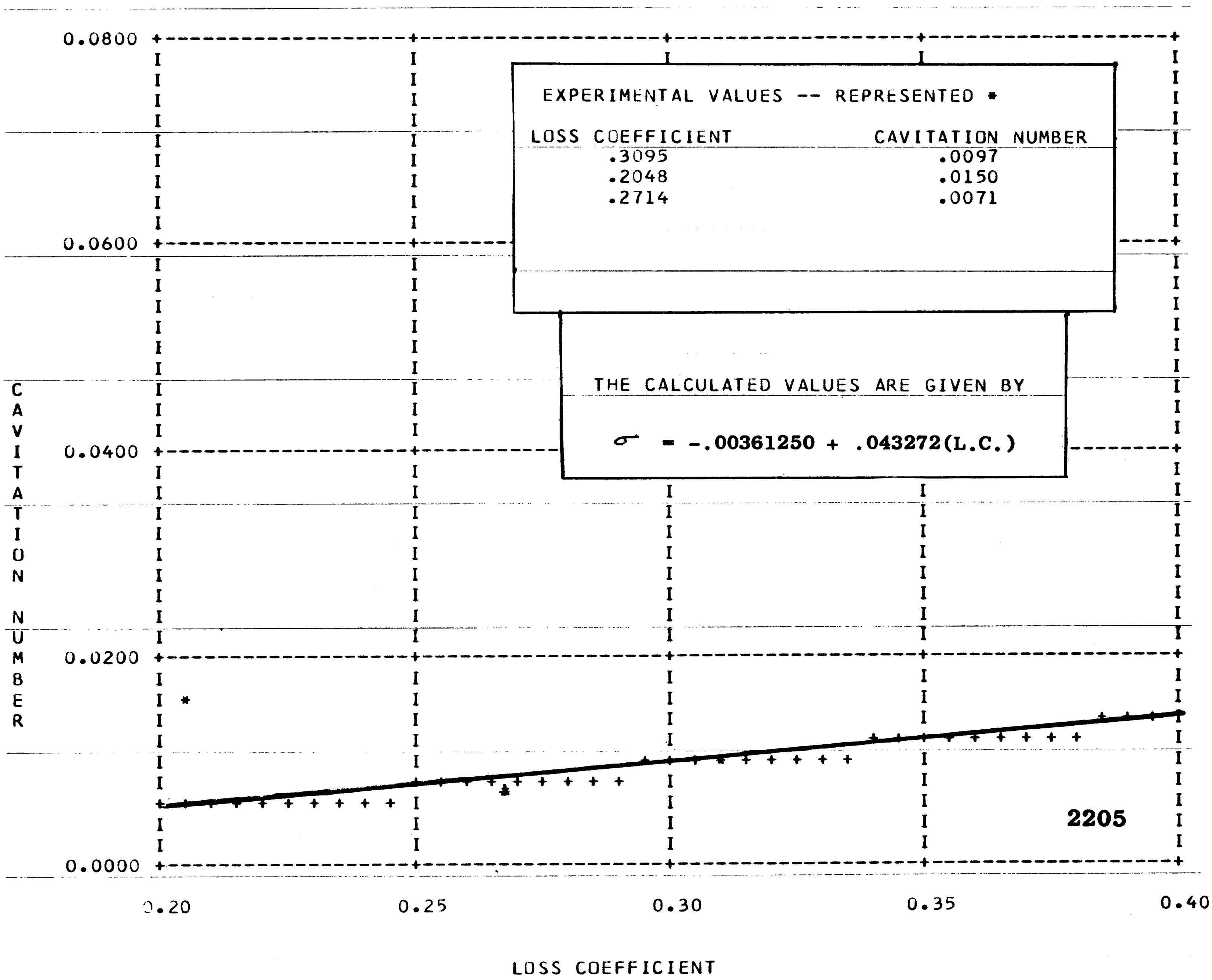

PLOTTING OF EXPERIMENTAL AND CALCULATED VALUES FOR PROBLEM NO 32

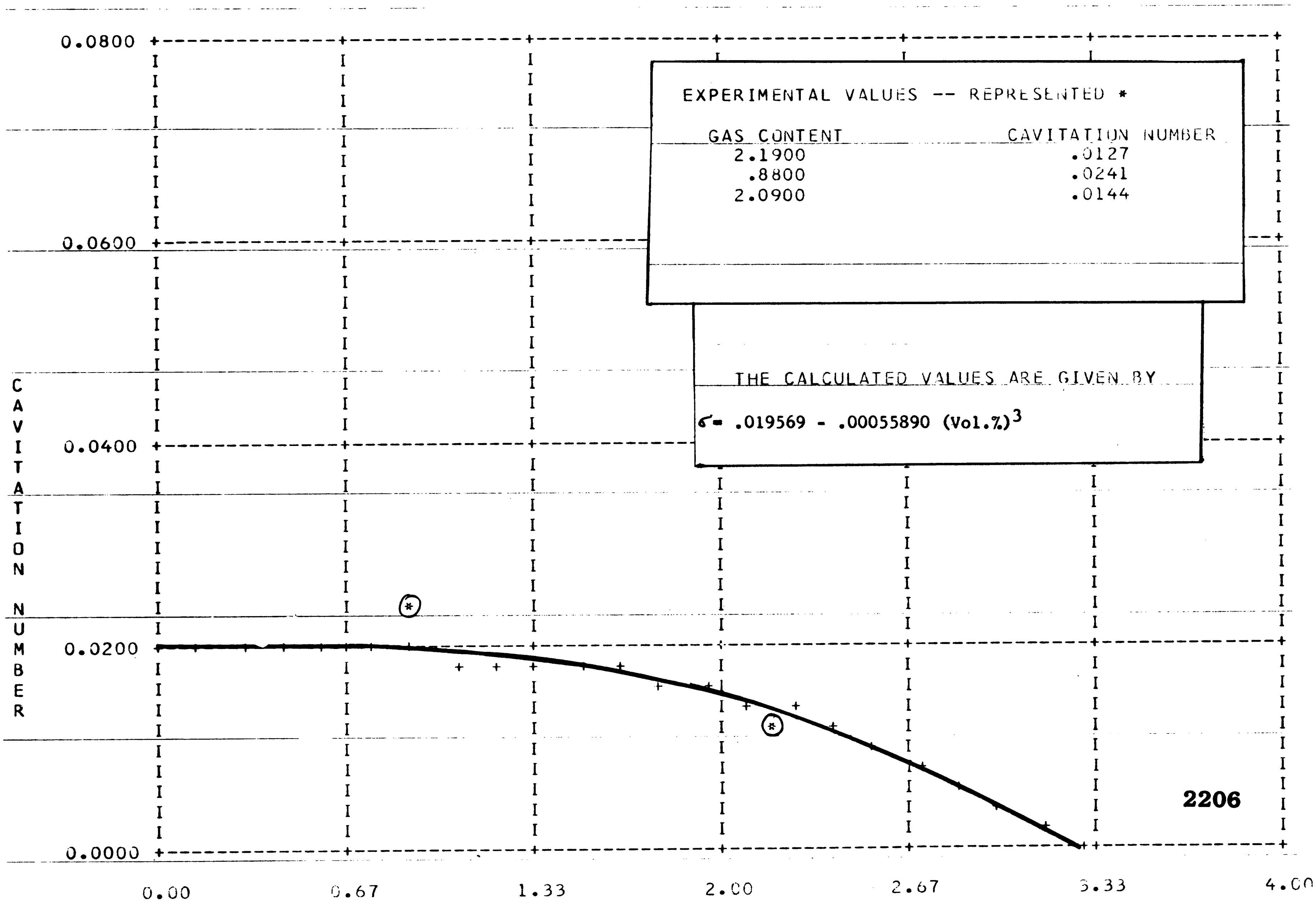

GAS CONTENT IN VOLUME PERCENT

PLOTTING OF EXPERIMENTAL AND CALCULATED VALUES FOR PROBLEM NO 33

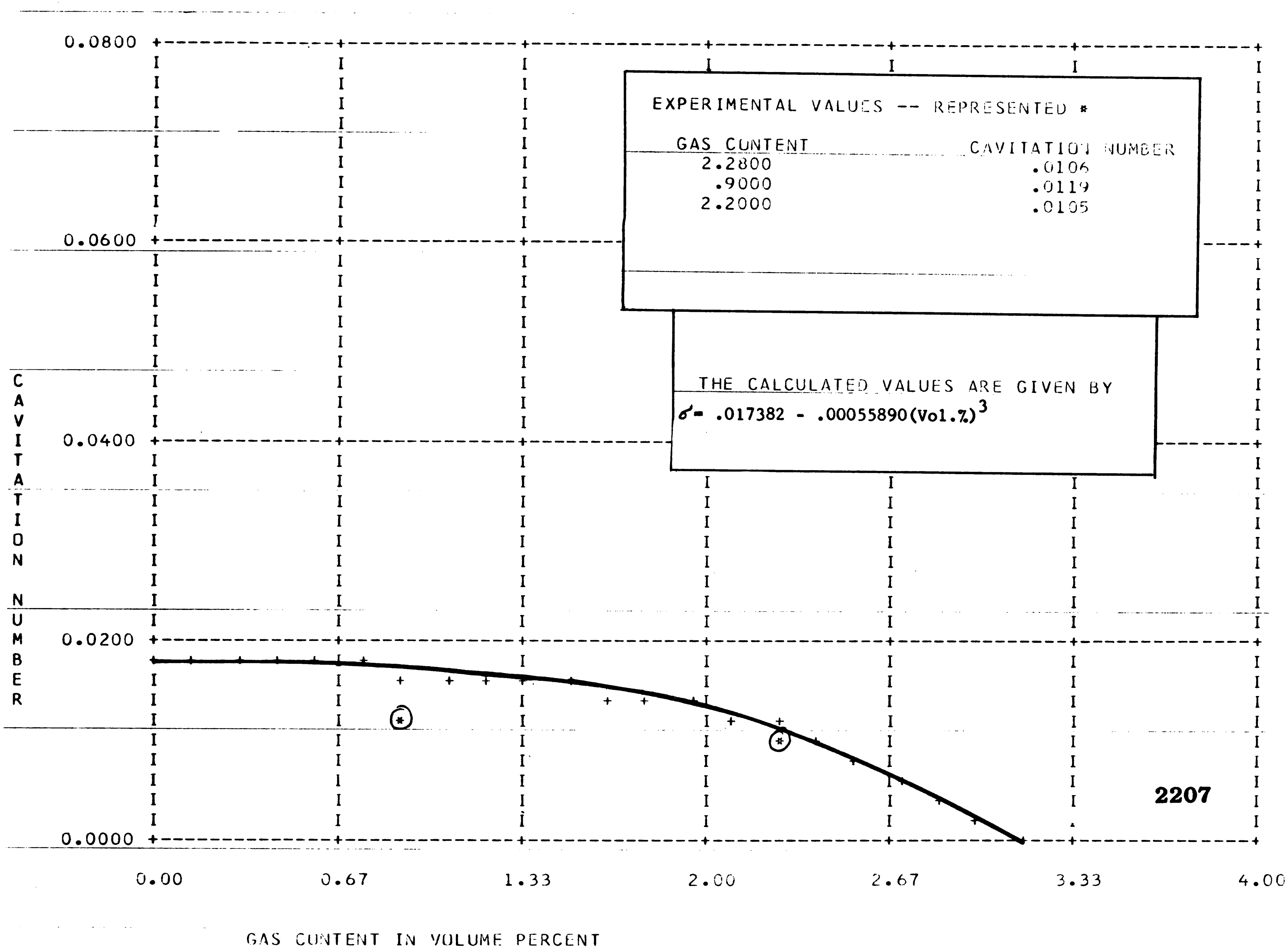

PLOTTING OF EXPERIMENTAL AND CALCULATED VALUES FOR PROBLEM NO 34

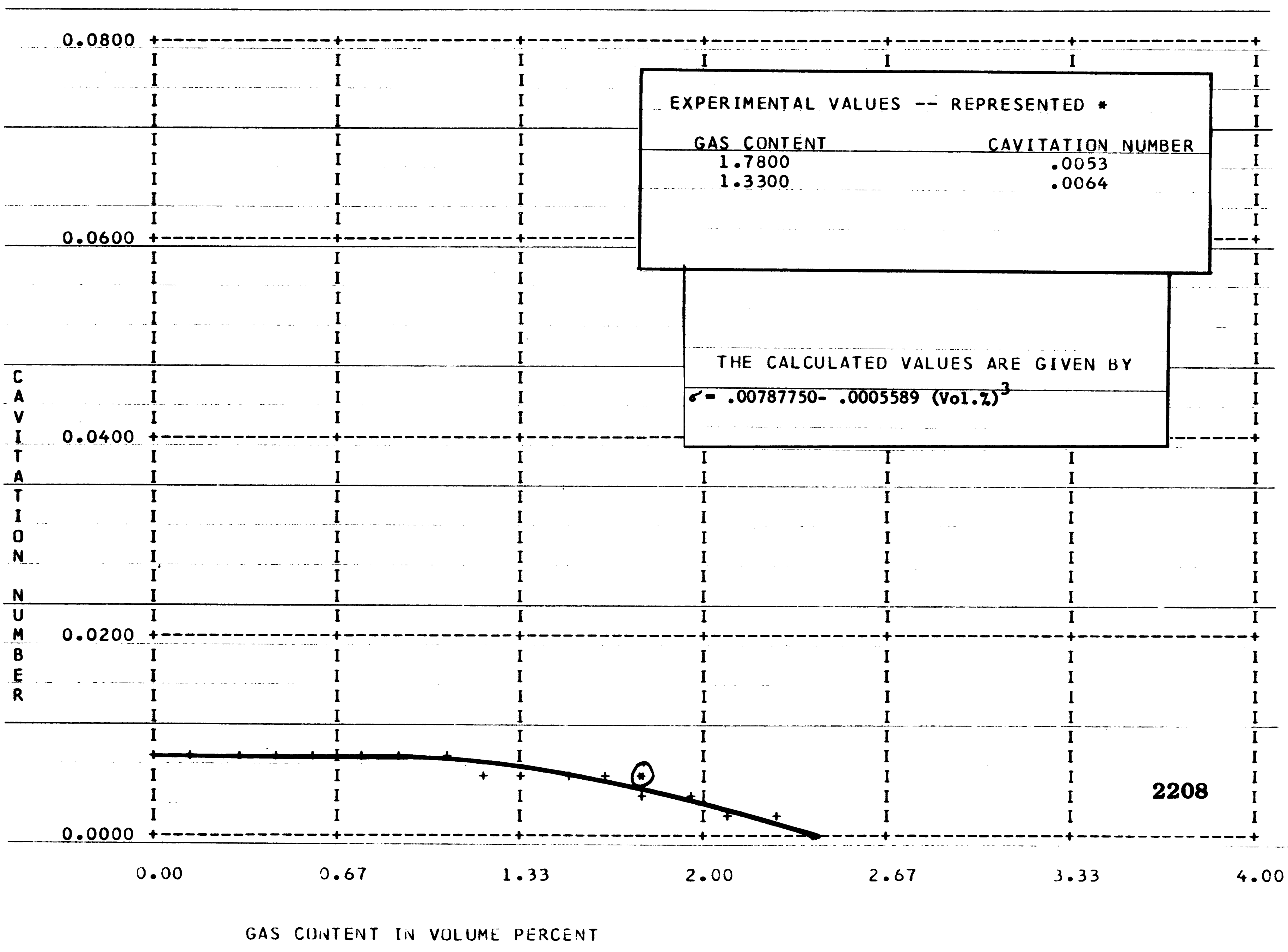

PLOTTING OF EXPERIMENTAL AND CALCULATED VALUES FOR PROBLEM NO 35

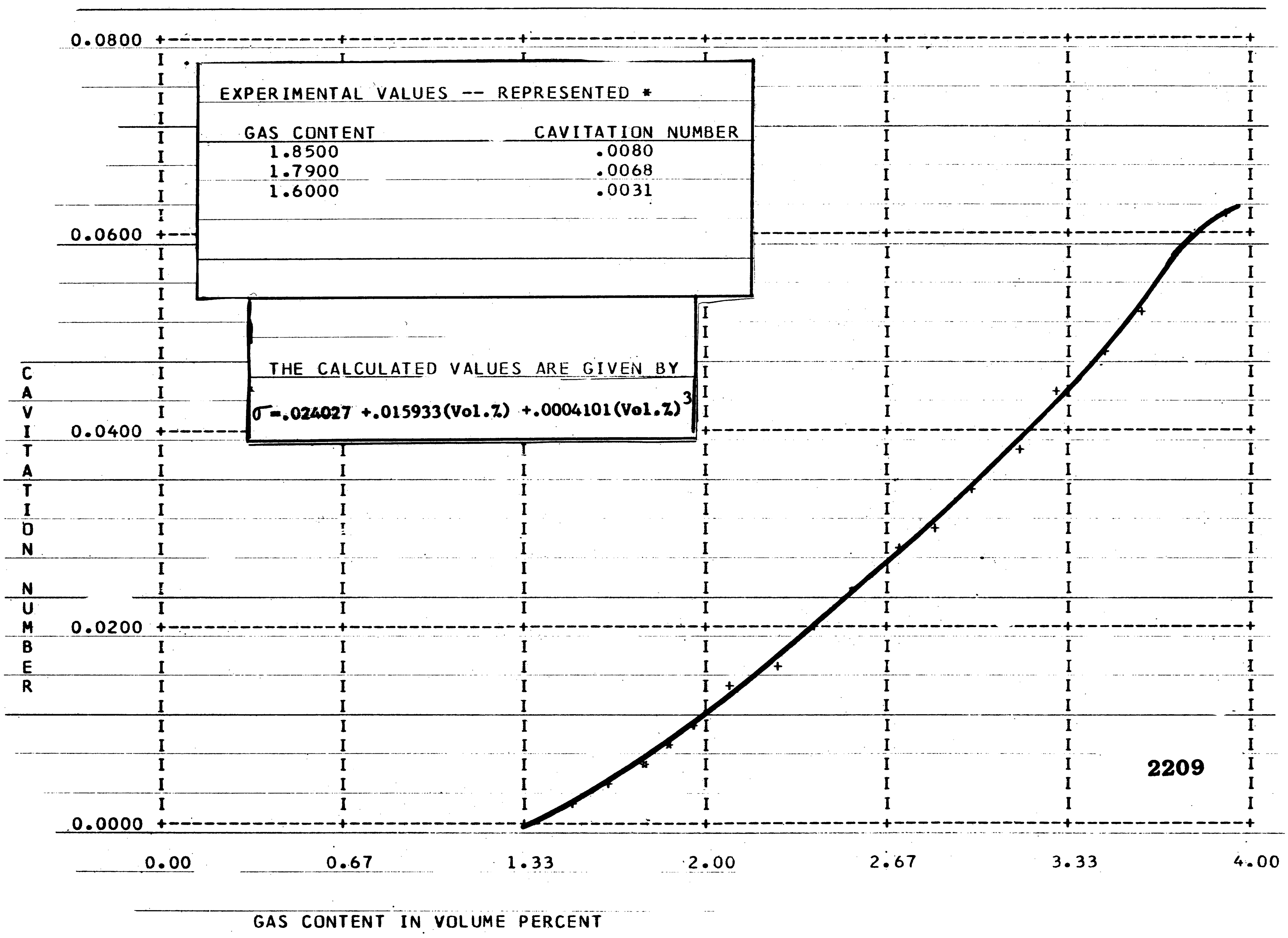

PLOTTING OF EXPERIMENTAL AND CALCULATED VALUES FOR PROBLEM NO 36

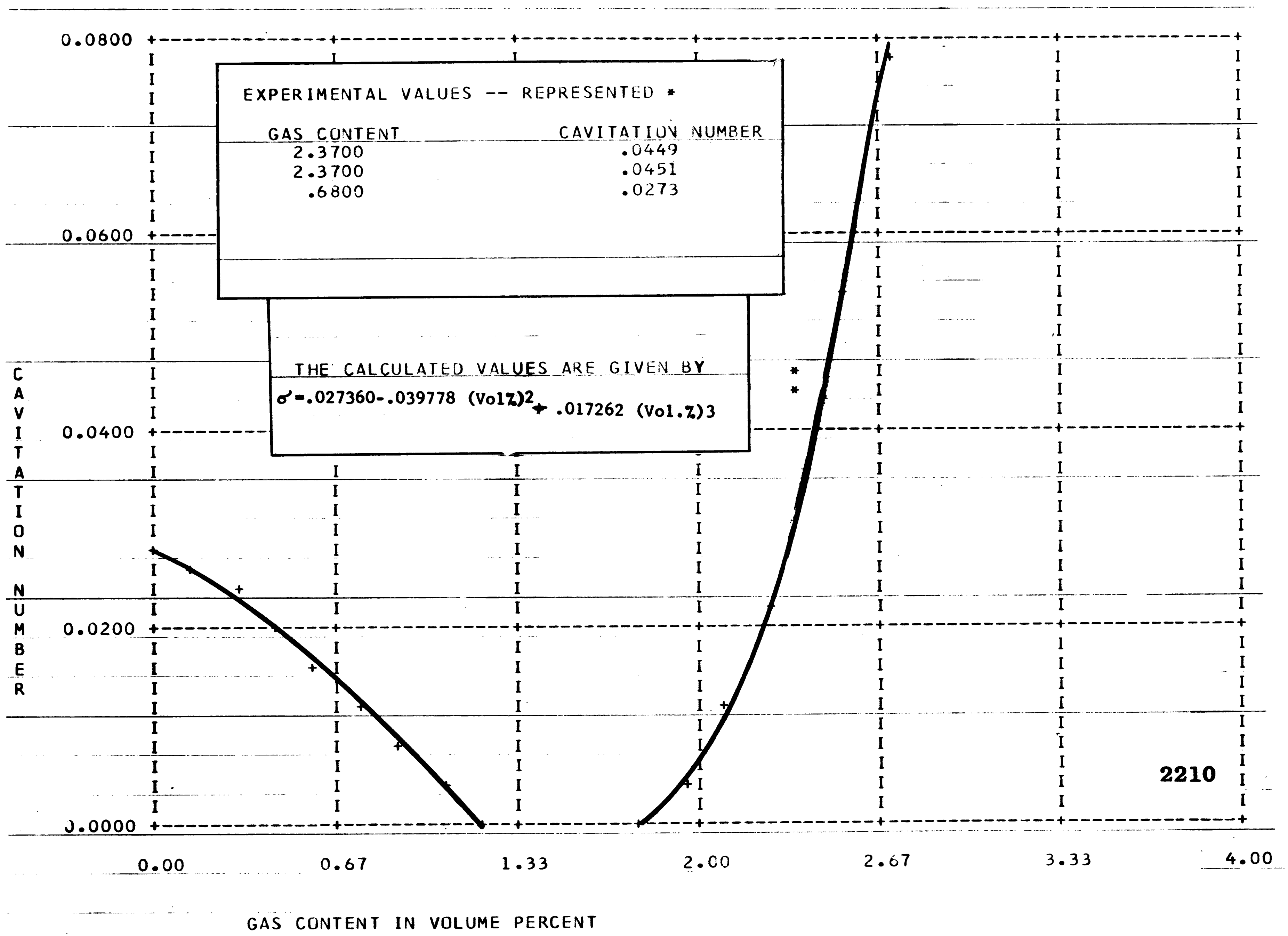

BIBLIOGRAPHY

1. Robinson, M. J., Hammitt, F. G., "Cavitation damage characteristics in water and mercury from studies in a cavitating venturi," ORA Technical Report Number 03424-17-T, Laboratory for Fluid Flow and Heat Transport Phenomena, Department of Nuclear Engineering, The University of Michigan, April, 1966.

2. Hammitt, F. G., "Observations of Cavitation Scale and Thermodynamic Effects in Stationary and Rotating Components," Trans ASME J. Basic Eng., March, 1963, p. 1-16 (Vol. 85, September, 1963, pp. 347-359).

3. Ericson, USAF Capt. D. M., Jr., Ph.D. Thesis in progress, Nuclear Engineering Department, The University of Michigan.

4. Hammitt, F. G., Robinson, M. J., Ericson, D. M., Robinson, R. A., Koopman, R. P., Ahmed, O.S.M., "An Investigation of Entrained Gas Effect on Cavitation Number in Mercury in a Venturi," ORA Technical Report No. 06110-3-T, Laboratory for Fluid Flow and Heat Transport Phenomena, Nuclear Engineering Department, The University of Michigan, February, 1966.

5. Koopman, R. P., et. al., "Computer Developed Programs and Resulting Correlations for Cavitation Number Studies in Mercury with Gas Injection," Laboratory for Fluid Flow and Heat Transfer Phenomena, Nuclear Engineering Department, University of Michigan, ORA Report No. 06110-8-I, December, 1965.

6. Private communication from A. P. Fraas, Oak Ridge National Laboratory.

7. Ripken, J. F., and Killen, J. M., "Gas Bubbles: Their Occurrance, Measurement, and Influence in Cavitation Testing," Proc. of IAHR - Symp., Sendai, Japan, 1962.

8. Hammitt, F. G., "Cavitation Damage and Performance Research Facilities," Symposium on Cavitation Research Facilities and Techniques, ASME, 1964, p. 175.

9. Lehman, A. F. and Young, Y.O., "Experimental Investigations of Incipient and Desinent Cavitation," ASME Paper 63-AHGT-20, December, 1962, to be published in J. Basic Engr.

10. Knapp, R. T., "Cavitation and Nuclei," ASME Trans.

11. Ahmed, O. S. M., PhD. Thesis in progress, Nuclear Engineering Department, The University of Michigan.

12. Robinson, M. J. and Hammitt, F. G., "Gas Bubble Entrainment in Water and Mercury Vs. Gas Content," Laboratory for Fluid Flow and Heat Transfer Phenomena, Nuclear Engineering Department, University of Michigan, ORA Report No. 06110-6-I, January, 1965.

13. Jekat, W., "A New Approach to Reduction of Pump Cavitation --Hubless Inducer," ASME paper No. 66-FE-8, to be published Trans. ASME, J. Basic Engr.

14. Holl, J. N., "The Estimation of the Effect of Surface Irregularities on the Inception of Cavitation," ASME Symp. on Cavitation in Fluid Machinery, November 7-11, 1965, pp. 3-5.